2-17-2016

CONVERTING LOW VALUE LIGNOCELLULOSIC RESIDUES INTO VALUABLE PRODUCTS USING PHOTO AND BIOELECTROCHEMICAL CATALYSIS

Wudneh Ayele Shewa
University of Windsor

CONVERTING LOW VALUE LIGNOCELLULOSIC RESIDUES INTO
VALUABLE PRODUCTS USING PHOTO AND BIOELECTROCHEMICAL
CATALYSIS

By

Wudneh Shewa

A Dissertation
Submitted to the Faculty of Graduate Studies
through the Department of Civil and Environmental Engineering
in Partial Fulfillment of the Requirements for
the Degree of Doctor of Philosophy
at the University of Windsor

Windsor, Ontario, Canada

2016

CONVERTING LOW VALUE LIGNOCELLULOSIC RESIDUES INTO
VALUABLE PRODUCTS USING PHOTO AND BIOELECTROCHEMICAL
CATALYSIS

by

Wudneh Shewa

APPROVED BY:

_____
A. Margaritis, External Examiner
Western University

_____
C. Weisener
The Great Lakes Institute for Environmental Research (GLIER)

_____
X.Xu
Civil and Environmental Engineering

_____
P. Henshaw
Civil and Environmental Engineering

_____
J. Lalman, Advisor
Civil and Environmental Engineering

January 29, 2016

DECLARATION OF CO-AUTHORSHIP / PREVIOUS

PUBLICATION

I. Co-Authorship Declaration

I hereby declare that this thesis incorporates the outcome of a joint research undertaken in collaboration with Dr. Subba Rao Chaganti under the supervision of Professor Daniel Heath. The collaboration is covered in Chapters 3, 6 and Appendix F of the thesis. In all cases, the key ideas, primary contributions, experimental designs, data analysis and interpretation, were performed by the author, and the contribution of co-authors was primarily through the provision of microbiological data.

I am aware of the University of Windsor Senate Policy on Authorship and I certify that I have properly acknowledged the contribution of other researchers to my thesis, and have obtained written permission from the co-authors to include the above material in my thesis.

I certify that, with the above qualification, this thesis, and the research to which it refers, is the product of my own work.

II. Declaration of Previous Publication

This thesis includes two original papers that have been previously published in a peer reviewed journal and in a conference proceeding, as follows:

Thesis Chapter	Publication title/full citation	Publication status
Chapter 3	*Electricity generation and biofilm formation in microbial fuel cells using plate anodes constructed from various grades of graphite.* **J. Green Eng., 2014, 4, 13-32.**	*Published*
Chapter 5	*Producing electricity using a microbial fuel cell fed with feedstock chemicals produced from the photocatalysis of a lignin model chemical.* ***Proceedings of the Water Environment Federation, 2014, 13, 2484-2503.***	*Published*

I certify that I have obtained a written permission from the copyright owner(s) to include the above published material(s) in my thesis. I certify that the above material describes work completed during my registration as graduate student at the University of Windsor.

I declare that, to the best of my knowledge, my thesis does not infringe upon anyone's copyright nor violate any proprietary rights and that any ideas, techniques,

quotations, or any other material from the work of other people included in my thesis, published or otherwise, are fully acknowledged in accordance with the standard referencing practices. Furthermore, to the extent that I have included copyrighted material that surpasses the bounds of fair dealing within the meaning of the Canada Copyright Act, I certify that I have obtained a written permission from the copyright owner(s) to include such material(s) in my thesis.

I declare that this is a true copy of my thesis, including any final revisions, as approved by my thesis committee and the Graduate Studies office, and that this thesis has not been submitted for a higher degree to any other University or Institution.

ABSTRACT

Depleting fossil fuel resources, environmental damage and energy security are key factors driving the search for renewable energy supplies. Anaerobic digestion (AD), a well-developed technology, is widely used globally to produce an energy rich biogas from degradable organic matter. An alternative technology under development which produces electricity from the degradation of organic matter is microbial fuel cells (MFCs). Lignin, an abundant renewable organic chemical, is difficult to degrade using biological methods. This dissertation is focused on generating electricity from lignin-rich organic matter using a two-step process which included producing a chemical feedstock using photocatalysis followed by a bioelectrochemical conversion in an MFC.

Studies were conducted using sodium lignosulfonate (LS), a model lignin compound, and black liquor (BL), a lignin-rich waste product from pulp and paper industries. Titanium dioxide (TiO_2) plus ultraviolet light was used in the photocataysis step. Optimization and modeling of the photocatalytic degradation process was performed using the Box-Behnken design method to achieve a maximum biological oxygen demand (BOD_5) to chemical oxygen demand (COD) ratio. The effluent from the photocatalytic degradation process was fed into a single chamber air-cathode microbial fuel cell (SCMFC) to generate electricity.

In this study, commonly available electrode materials were selected, evaluated and compared with a focus on selecting the best performing type of electrode. Cyclic voltammetry and linear sweep voltammetry were used to evaluate the performance of the electrodes. The biofilm microbial diversity and performance of SCMFCs fed pretreated

LS (PrLS) and pretreated black liquor (PrBL) were compared to SCMFCs fed glucose at the same COD loadings and operating conditions.

The energy production from PrBL using SCMFCs was also compared with the anaerobic digestion (AD) process. A total biogas production of 195 ± 30 mL CH_4 per g COD_{added} was obtained from two-stage AD of PrBL. The PrBL feed SCMFCs, generated maximum current and power densities of 8045 ± 440 mA m^{-3} and 2815 ± 120 mW m^{-3}, respectively. The SCMFCs removed $89.3\pm0.8\%$ of the COD of PrBL and achieved coulombic and potential efficiencies of $7.8\pm0.6\%$ and 65.7% respectively. This dissertation demonstrated that combining photocatalysis together with a bioelectrochemical process was useful for treating and generating electricity from lignin rich waste matter simultaneously.

DEDICATION

I dedicate this dissertation to my wife Mahder, son Daniel and daughter Grace.

ACKNOWLEDGEMENTS

TABLE OF CONTENTS

xiii

LIST OF TABLES

LIST OF FIGURES

LIST OF APPENDICES

LIST OF ABBREVIATIONS/SYMBOLS

AD	Anaerobic digestion
ADS	Anderson-Darling statistic
ANOVA	Analysis of variance
APHA	American Public Health Association
AQDS	Anthraquinone-2, 6-disufonate
AWWA	American Water Works Association
BBD	Box-Behnken design
BES	Bioelectrochemical system
BET	Brunauer–Emmett–Teller
BL	Black liquor
BOD	Biochemical oxygen demand
CE	Coulombic efficiency
CEM	Cation exchange membrane
CH_4	Methane
CHP	Combined heat and power
CO_2	Carbon dioxide
COD	Chemical oxygen demand
CV	Cyclic voltammetry
DNA	Deoxyribonucleic acid
ECE	Energy conversion efficiency
EE	Energy efficiency
EFC	Enzymatic fuel cell

EIS	Electrochemical impedance spectroscopy
emf	Electromotive force
GC	Gas chromatograph
GL	Glucose
H_2	Hydrogen
H_2O_2	Hydrogen peroxide
I.D.	Internal diameter
LCFA	Long chain fatty acids
LC-MS	Liquid chromatography-mass spectrometry
LS	Sodium lignosulfonate
LSV	Linear sweep voltammetry
m/z	Mass-to-charge ratio
MDC	Microbial desalination cell
MEC	Microbial electrolysis cell
MFC	Microbial fuel cell
MSC	Microbial solar cell
MW	Molecular weight
OCV	Open circuit voltage
•OH	Hydroxyl radical
PCA	Principal component analysis
PCR	Polymerase chain reaction
PE	Potential efficiency
PEM	Proton exchange membrane

PrBL	Pretreated black liquor
PrLS	Pretreated sodium lignosulfonate
PTFE	Polytetrafluoroethane
RPM	Revolutions per minute
RSM	Response surface methodology
RVC	Reticulated vitreous carbon
SCMFC	Single-chamber microbial fuel cell
STD	Standard deviation
TCD	Thermal conductivity detector
TiO_2	Titanium dioxide
T-RFLP	Terminal restriction fragment length polymorphism
UN	United Nations
UV	Ultraviolet
V	Voltage
VS	Volatile solids
VSS	Volatile suspended solids
WPCF	Water Pollution Control Federation
ηCOD	COD removal efficiency

CHAPTER 1

INTRODUCTION

1.1 Context

"The clear and present danger of climate change means we cannot burn our way to prosperity. We already rely too heavily on fossil fuels. We need to find a new, sustainable path to the future we want. We need a clean industrial revolution."

Ban Ki-moon (UN Secretary-General)

Today's energy is supplied from oil (34%), coal (25%), natural gas (21%), biomass (8%), nuclear energy (6.5%), hydropower (2%) and others including wind and solar energy (3.5%) (Yang et al., 2010). This indicates that 80 % of the global energy supply is derived from fossil fuels and only 8% from biomass. Rittmann (2008) pointed out that our dependence on fossil fuels poses three great risks for the survival of human society as we now know it. The first risk is that we will deplete fossil-fuel reserves, leaving human society metaphorically and perhaps literally ''cold, hungry, and in the dark.'' The second risk is that geopolitical strife from competition for dwindling resources will lead to economic and energy disruptions, political turmoil, and war. The third risk is from global climate change caused by the net increase in atmospheric CO_2 due to combustion of the fossil fuels.

According to He (2012), the only natural and renewable carbon resource that is large enough to be used sustainably as a substitute for fossil fuels is a biomass. Biomass includes forestry (woody and non-woody) and agricultural residues as well as industrial waste such as municipal solid waste and sewage waste (He, 2012). Woody biomass includes forest residues containing primarily lignocellulosics such as roots, wood, wood

1

waste from saw mills, bark, leaves as well as agricultural residues such as roots, leaves, stalks, corn cobs and bagasse (http://www.wgbn.wisc.edu/key-concepts/grassland-biomass-sources/sources-biomass). The non-woody biomass category includes agriculture crops producing carbohydrates and lipids. Biomass is a feedstock source which could be utilized for renewable energy production.

A bioelectrochemical system (BES) is a unique technology capable of converting the chemical energy stored in biodegradable biomass to direct electric current using microorganisms (Ren, 2013). Therefore, wastewater treatment employing BES is a novel and promising biotechnological approach for the production of renewable energy from wastewaters containing reduced carbon compounds (Rozendal et al., 2008). BES can be used to upgrade or replace current biological treatment units such as activated sludge because this alternative technology will result in the elimination of aeration, the reduction of biosolids generated and the production of useful products (Ren, 2013). Many useful products include direct electricity during treatment and with simple modifications, other value-added products, such as H_2, CH_4 or organic chemicals can be produced.

Depending on the biocatalyst, BESs can be classified as microbial fuel cells (MFCs) and enzymatic fuel cells (EFCs); and based on their mode of application, BESs can be also sub-divided into MFCs, microbial electrolysis cells (MECs), microbial desalination cells (MDCs) and microbial solar cells (MSCs) (Pant et al., 2012).

An MFC can be defined as a system in which microorganisms function as biocatalysts to convert chemical energy into electrical energy (Rabaey, 2010). Piccolino (1998) pointed out that the first experimental evidence of bioelectricity was observed in the late eighteenth century by Luigi Galvani, who observed electric response by

connecting frog legs to a metallic conductor. One of the earliest developments in the area of microbial fuel cell was described by Michael Cresse Potter in 1911, when he placed a platinum electrode into cultures of yeast or *E. Coli* and showed that a potential difference could be generated. Further work by Barbet Cohen at Cambridge led to development of batteries of microbial fuel cells capable of generating potentials in excess of 35 V (Davis and Higson, 2007).

The MFC technology could be highly adaptable to a sustainable pattern of wastewater treatment for the following reasons (Li et al, 2014): (1) it enables direct recovery of electric energy and value-added products; (2) good effluent quality and low environmental footprint can be achieved because of effective combination of biological and electrochemical processes; and (3) it is inherently amenable to real-time monitoring and control, which benefits good operating stability. Therefore, the main goal of this thesis is to devise a novel technology to successfully convert wastes rich in lignocellosic substances into simple, non-toxic carbon compounds and use these compounds to generate electricity using a MFC or to produce a methane rich biogas using anaerobic digestion (AD). The research in this thesis, designed to achieve this goal, are described in Chapters 3 to 7.

1.2 Hypothesis and research objectives

In this thesis, it was hypothesized that low value lignocellulosic residues can be converted into biodegradable chemicals using UV/TiO_2 photocatalysis and these chemicals can be used for energy production by means of MFCs or AD. Initial studies were conducted using a model lignin compound which was followed by studies with black liquor, a waste generated from pulp and paper manufacturing industries. Black

liquor was selected because it is an abundant renewable waste, toxic to the environment, and the treatment and recovering energy from black liquor is of increasing concern (US EPA, 2002; Font et al., 2003, Pokhrel and Viraraghavan, 2004; Oller et al., 2011; Bajpai, 2012).

1.3 Research phases

The research in this dissertation was conducted in different phases. These research phases together with their associated objectives are as follows:

Phase 1: **(Chapter 3 objectives)**

A. Evaluate electricity generation and biofilm formation in MFCs configured using three different graphite plate electrodes (HK06, G347 and POCO3) with different physical characteristics (specific resistance, grain size and specific gravity).

B. Assess the significance of cost for the different graphite plate electrodes on the performance of MFCs.

Phase 2: **(Chapter 4 objectives)**

A. Evaluate electricity generation and performance in single chamber microbial fuel cells (SCMFCs) configured with graphite fibre brush and felt anodes.

B. Compare the performance of the graphite plate anodes with that of graphite fiber brush and felt anodes and select the preferred option for SCMFCs.

Phase 3: **(Chapter 5 objectives)**

A. Assess the effect of irradiation time, catalyst particle size, catalyst concentration and oxygen purging on the photocatalytic degradation of a model lignin chemical using TiO_2.

B. Examine the generation of electricity using SCMFCs from a feedstock produced from the photocatalytic degradation of a model lignin chemical.

Phase 4: **(Chapter 6 objectives)**

A. Determine the optimum process parameters of the photocatalytic degradation of a model lignin chemical using a Box-Behnken design combined with response surface methodology (RSM).

B. Evaluate and compare the performance of SCMFCs fed a photocatalytic pretreated model lignin chemical with those fed glucose in SCMFCs at the same COD loading and operating conditions.

Phase 5: **(Chapter 7 objectives)**

A. Evaluate TiO_2 photocatalysis pretreatment of diluted black liquor

B. Examine energy production from pretreated diluted black liquor using 1) a two-stage anaerobic digestion (biogas formation) process and 2) a single chamber microbial fuel cell (SCMFC) (electricity generation).

1.4 References

Bajpai, P. (2012) Brief description of the pulp and paper making process. In *Biotechnology for Pulp and Paper Processing*. New York, NY: Springer, pp. 7–14.

Davis, F., and Higson, S.P.J. (2007) Biofuel cells–recent advances and applications. *Biosens. Bioelectron.* **22**(7): 1224–35.

Font, X., Caminal, G., Gabarrell, X., Romero, S., and Vicent, M.T. (2003) Black liquor detoxification by laccase of *Trametes versicolor* pellets. *J. Chem. Technol. Biotechnol.* **78**(5): 548–554.

He, Z. (2013) Microbial fuel cells: Now let us talk about energy. *Environ. Sci. Technol.* **47**(1): 332–333.

Li, W.W., Yu, H.Q., and He, Z. (2014) Towards sustainable wastewater treatment by using microbial fuel cells-centered technologies. *Energy Environ. Sci.* **7**(3): 911–924.

Manohar, A.K., Bretschger, O., Nealson, K.H., and Mansfeld, F. (2008) The use of electrochemical impedance spectroscopy (EIS) in the evaluation of the electrochemical properties of a microbial fuel cell. *Bioelectrochemistry* **72**(2): 149–154.

Oller, I., Malato, S., and Sánchez-Pérez, J. A. (2011) Combination of advanced oxidation processes and biological treatments for wastewater decontamination-A review. *Sci. Total Environ.* **409**(20): 4141–4166.

Pant, D., Singh, A., Van Bogaert, G., Irving Olsen, S., Singh Nigam, P., Diels, L., and Vanbroekhoven, K. (2012) Bioelectrochemical systems (BES) for sustainable energy production and product recovery from organic wastes and industrial wastewaters. *RSC Adv.* **2**(4): 1248-1263.

Piccolino, M. (1998) Animal electricity and the birth of electrophysiology: the legacy of Luigi Galvani. *Brain Res. Bull.* **46**(5): 381–407.

Pokhrel, D., and Viraraghavan, T. (2004) Treatment of pulp and paper mill wastewater - A review. *Sci. Total Environ.* **333**(1): 37–58.

Rabaey, K., Lissens, G., and Verstraete, W. (2005) Microbial fuel cells: performances and perspectives. In *Biofuels for fuel cells: Renewable energy from biomass*

fermentation. Lens, P., Westermann, P., Haberbauer, M., and Moreno, A. eds. London: IWA Publishing, pp. 377–399.

Ren, Z.J. (2013) The principle and applications of bioelectrochemical systems. In *Biofuel Technologies*: *Recent Developments*. Gupta, V.K., and Tuohy, M.G. eds. Berlin-Heidelberg: Springer, pp. 501–527.

Rittmann, B.E. (2008) Opportunities for renewable bioenergy using microorganisms. *Biotechnol. Bioeng.* **100**(2): 203–212.

Rozendal, R.A., Hamelers, H.V.M., Rabaey, K., Keller, J., and Buisman, C.J.N. (2008) Towards practical implementation of bioelectrochemical wastewater treatment. *Trends Biotechnol.* **26**(8): 450–459.

US EPA (2002) EPA office of compliance sector notebook project: profile of pulp and paper industry, 2nd edn. Washington, DC: EPA/310-R-02-002.

Yang, Z., Liu, J., Baskaran, S., Imhoff, C.H., and Holladay, J.D. (2010) Enabling renewable energy-and the future grid-with advanced electricity storage. *JOM* **62**(9): 14–23.

CHAPTER 2

LITERATURE REVIEW

2.1 Overview

Rising global energy demand coupled with declining fossil fuel reserves and increasing climate change are major factors driving our research for alternative energy supplies (Pant et al., 2012b). Global warming can be slowed, and perhaps reversed, only by replacing fossil fuels with renewable, carbon-neutral alternatives (Rittmann, 2008). Bioelectrochemical systems (BESs), such as microbial fuel cells (MFCs) and microbial electrolysis cells (MECs), are generally regarded as promising future technologies for producing energy from organic substrates (Rozendal et al, 2008). The MFC technology was used in the proposed work since it is able to produce renewable and carbon-neutral energy (Logan, 2008).

The research and development of the BES concept had been stagnant until the turn of the century, as only a limited number of articles were published before 2001. However, since 2002, the research productivity has experienced an exponential growth, with more than 2,000 published articles in the past decade (Ren, 2013). In subsequent sections of this thesis, published studies that provided the required background to accomplish the research objectives of this thesis are reviewed. The processes addressed in this literature review include photocatalysis, MFC and biomethanation.

2.2 Photocatalysis

2.2.1 Introduction

Photocatalysis (photocatalytic degradation) is an advanced oxidation process used to degrade organic chemicals in water supplies and wastewater effluents. In the photocatalytic degradation process, the destruction of recalcitrant organics is governed by the combined action of a semiconductor photocatalyst, an energetic radiation source and an oxidizing agent (Ahmed et al., 2011). Gogate and Pandit (2004) lists various chalcogenides (oxides such as TiO_2, ZnO, ZrO_2, CeO_2 etc. or sulfides such as CdS, ZnS etc.) that have been used as photocatalysts in different studies. In the last few years, a great variety of novel photoactive semiconductors which include mixed oxides of transition metals such as Nb, V or Ta, or with main group elements such as Ga, In, Sb or Bi have been developed and extensively investigated as alternative photocatalysts (Hernández-Alonso et al., 2009). A photocatalyst is able to harnesses radiation from sunlight or artificial light and uses the energy to degrade different substances including a variety of organic materials including organic acids, estrogens, pesticides, dyes, crude oil, microbes (including viruses) and chlorine resistant organisms, and inorganic molecules such as nitrous oxides (NOx) (Ibhadon and Fitzpatrick, 2013).

During photocatalysis, light absorbed by the catalyst creates an activated surface. The photoreaction can proceed via the following two mechanisms (Castellote and Bengtsson, 2011):

1) Via energy transfer (Equations 2.1 to 2.3), by forming an activated state of the reactant of interest, S, which is more easily oxidized than their ground state:

$$C \xrightarrow{hv} {}^*C \tag{2.1}$$

$$^*C + S \rightarrow {}^*S + C \tag{2.2}$$

$$^*S \rightarrow P \tag{2.3}$$

2) Via electron transfer (Equations 2.4 to 2.7), by acting either as an electron donor or acceptor.

$$C \xrightarrow{hv} {}^*C \tag{2.4}$$

$$^*C + S \rightarrow S^- + C^+ \tag{2.5}$$

$$S^- \rightarrow P^- \tag{2.6}$$

$$P^- + C^+ \rightarrow P + C \tag{2.7}$$
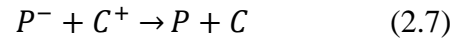
where C, S and P represent the catalyst, substrate/reactant and product respectively.

In this thesis, photocatalytic oxidation was performed using TiO_2 as a catalyst because of the following advantages (Gogate and Pandit, 2004):

- Use of natural resources, i.e. sunlight, which should result in considerable economic savings as discussed earlier.

- Chemical stability of TiO_2 in aqueous media and in larger range of pH ($0 \leq$ pH ≤ 14).

- Low cost.

- System applicable at low concentrations and no additives required.

- Capacity for noble metal recovery.

- Total mineralization achieved for many organic pollutants.

- Efficiency of photocatalysis with halogenated compounds sometimes very toxic for bacteria in biological water treatment.

2.2.2 Working principle of UV/TiO₂ photocatalysis

The photocatalytic process can be carried out by simply using a slurry of nano-size photocatalysts dispersed in an aqueous phase and placed in a reactor irradiated with UV light. An alternative to using a catalyst in suspension is to attach the photocatalyst on a solid support (Gogate and Pandit, 2004). As far as the mechanism of photocatalysis is concerned, UV radiation is used to excite the solid-state metal catalyst creating a positive and negative charge (electron-hole, e^- h^+ pairs) on the catalyst's surface (Kim et al., 2004). These positive and negative charges promote redox reactions in the solution by the photogenerated positive charges and reduction of metal ions or oxygen by the photogenerated negative charges. The overall photocatalysis process and the reactions involved are described in Chapters 5 and 6.

2.2.3 Factors affecting photocatalysis

Factors affecting the photocatalytic process include amount and type of catalyst, reactor design, wave length of irradiation, initial concentration of the reactant, temperature, radiant flux, medium pH, aeration and presence of ionic species (Gogate and Pandit, 2004). The catalyst particle size (Almquist and Biswas, 2002) and irradiation/reaction time (Kaneco et al., 2006; Chin et al., 2013) are the other factors which have significant influence on the photocatalytic processes.

A number of studies have investigated the effect of different factors on the TiO₂ photocatalytic process efficiency (Almquist and Biswas, 2002; Kaneco et al., 2006; Akpan and Hameed, 2009; Ray et al., 2009; Verma et al., 2012, Choquette-Labbé et al., 2014). In this thesis, the selected factors include catalyst particle size, concentration,

irradiation time, pH, aeration (oxygen purging) and mixing. In addition, the impact of photocatalysis on biodegradability was examined.

2.2.4 Application of photocatalysis

Photocatalysis potentially can aid in providing solutions to many environmental challenges because it provides a simple method of using sunlight and artifical light to induce chemical transformations of organics to CO_2 (Hernández-Alonso et al., 2009). There are several possible applications of photocatalysis in addition to the removal of organic contaminants from water and wastewater. Many industrial applications of this technology are commercially available. These technologies on the market include air and water cleaning devices, self-cleaning surfaces, solar cells, and even solar fuel generators (Schneider et al., 2014). Fujishima et al. (2000) has summarized selected applications of photocatalysis (Table 2.1).

Table 2.1 Selected applications of photocatalytic technology (Fujishima et al. (2000)).

Property	Category	Application
Self-cleaning	Materials for residential and office buildings	Exterior tiles, kitchen and bathroom components, interior furnishings, plastic surfaces, aluminium siding, building stone and curtains, paper window blinds
	Indoor and outdoor lamps and related systems	Translucent paper for indoor lamp covers, coatings on fluorescent lamps and highway tunnel lamp cover glass
	Materials for roads	Tunnel wall, soundproofed wall, traffic signs and reflectors
	Others	Tent material, cloth for hospital garments and uniforms and spray coatings for cars
Air cleaning	Indoor air cleaners	Room air cleaner, photocatalyst-equipped air conditioners and interior air cleaner for factories

Property	Category	Application
	Outdoor air purifiers	Concrete for highways, roadways and footpaths, tunnel walls, soundproof walls and building walls
Water purification	Drinking water	River water, ground water, lakes and water-storage tanks
	Others	Fish feeding tanks, drainage water and industrial wastewater
Antitumor activity	Cancer therapy	Endoscopic-like instruments
Self-sterilizing	Hospital	Tiles to cover the floor and walls of operating rooms, silicone rubber for medical catheters and hospital garments and uniforms
	Others	Public rest rooms, bathrooms and rat breeding rooms

The photocatalytic process can remove a wide range of contaminants, ranging from pesticides, herbicides and detergents to pathogens, viruses, coliforms and bacterial spores (Chong et al., 2010). The photocatalytic process can also be used to improve the biodegradability and reduce toxicity of organic compounds (Velegraki et al., 2006; Pekakis et al., 2006). Yurdakal and Augugliaro (2012) reported the oxidation of aromatic alcohols to aldehydes. Inertness to the environment and long-term photostability has made TiO_2 an important material in many practical applications and in commercial products ranging from drugs to foods, cosmetics to catalysts, paints to pharmaceuticals, and sunscreens to solar cells in which TiO_2 is used as a desiccant, brightener, or reactive mediator (Kamat, 2012). In this thesis, a controlled/partial photocatalytic process is developed to convert lignin and black liquor into degradable organic compounds using TiO_2.

2.3 Microbial fuel cells

2.3.1 Introduction

MFCs can be divided into the following two categories: a) mediator assisted MFCs and b) mediator-less MFCs. In the mediator assisted configuration, electron transfer from bacteria (microbial cells) to the electrode is facilitated by mediators such as potassium ferric cyanide, thionine, methyl viologen, humic acid, neutral red, anthraquinone-2,6-disufonate (AQDS) (Rajalakshmi and Dhathathreyan, 2008). In the alternate, mediator-less configuration, electrochemically active bacteria transfer electrons to the electrode. In this thesis, the MFCs used are mediator-less.

2.3.2 Working principles of MFCs

The working components of MFCs are depicted in Figure 2.1. The main components are electrochemically-active microorganisms on an anode and a cathode. During oxidation, the electrons travel to the cathode where water is produced from the reduction of oxygen. In its most basic form, a MFC is a device which uses microorganisms to generate an electrical current via the oxidation of organic matter in a fashion similar to a chemical fuel cell. (Franks and Nevin, 2010).

(a)

(b)
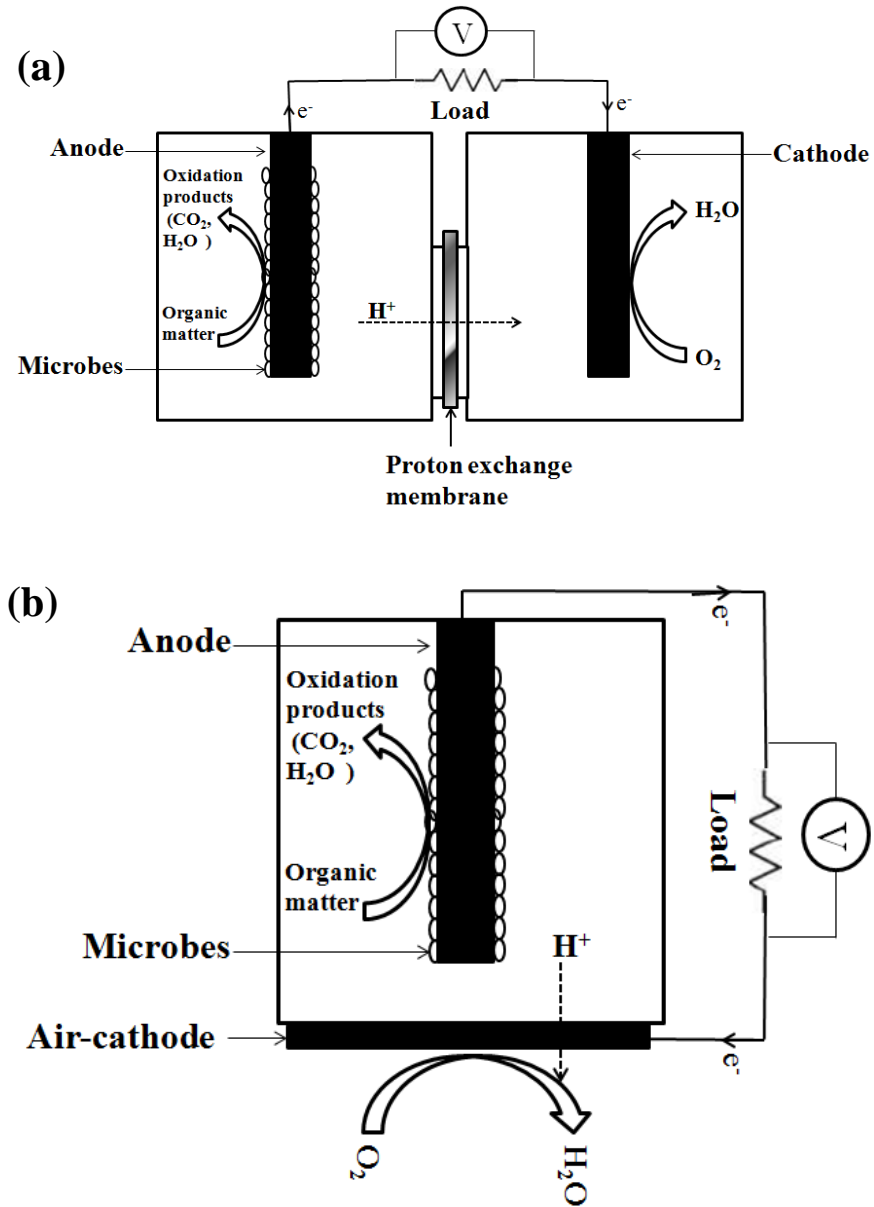
Figure 2.1 Schematic showing the working principle of microbial fuel cells: a) Two chamber MFC and b) Single chamber MFC.

The diagrams in Figure 2.1 showing the working principles of MFCs in two configurations include a) a two chamber system (Figure 2.1a) which consists of anode and cathode chambers that are separated by a proton exchange membrane (He and Angenent, 2006) and b) a single chamber MFC (Figure 2.1b) consisting of only one

15

chamber (anode chamber) and an air-cathode. Other MFC configurations are described in section 2.3.3. The main reactions taking place when glucose is used as a substrate are shown as Equation 2.8 (at the anode) and Equation 2.9 (at the cathode). Numerous different microorganisms are involved in mediating the oxidation reaction. In some cases, microbes which are not electrochemically active, such as methanogens, also degrade a fraction of the organic matter and hence, reduce the amount of electrons available for electricity production. Electrochemically active microbes are able to utilize intermediate organic compounds produced by other microbes.

$$C_6H_{12}O_6 + 6H_2O \quad \rightarrow \quad 6CO_2 + 24H^+ + 24e^- \qquad (2.8)$$

$$6O_2 + 24H^+ + 24e^- \rightarrow 12H_2O \qquad (2.9)$$
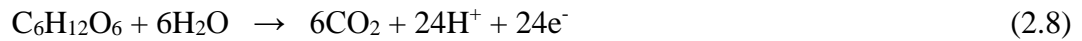
To fully understand the principles on which MFCs operate, expertise is required in electrochemistry, microbiology, materials science and engineering, molecular biology and environmental engineering (Zhao et al., 2009). Apart from the technical design aspects such as the anode or fuel cell design, the metabolic pathways and mechanisms of the bioelectrochemical energy conversion process determine the MFC power and energy output (Schroder, 2007). The path that the electrons trace out onroute to the electrode remains a matter of debate and ongoing research (Oh et al., 2010). However, various researchers reported the possible electron transfer mechanism from the bacteria to the anode electrode (Zhang and Halme, 1995; Rabaey and Verstraete, 2005; Gorby et al., 2006; Schroder, 2007, Du et al., 2007; Mohan et al., 2013).

Oh et al. (2010) has summarised a proposed electron transport mechanisms (Figure 2.2) in MFCs as involving (a) redox mediators, (b) electron shuttling and diffusion, (c)

conductive nanowire or bacteria pilli and (d) outer membrane cytochrome or conductive extracellular polymeric substances. Regardless of the mechanism, the electron transfer outside of the cell must lead to redox active species which are capable of electronically linking the bacterial cell to the electrode (Schroder, 2007).

According to Schroder (2007), for efficient electron transfer, the mediator must fulfill the following requirements:

(i) Able to physically contact the electrode surface.

(ii) Electrochemically active, i.e., it must possess low oxidation potential at given electrode surfaces, and

(iii) The standard potential of the mediators should be as close to the redox potential of the primary substrate, as possible, or it must at least be significantly negative to that of the oxidant (usually oxygen).
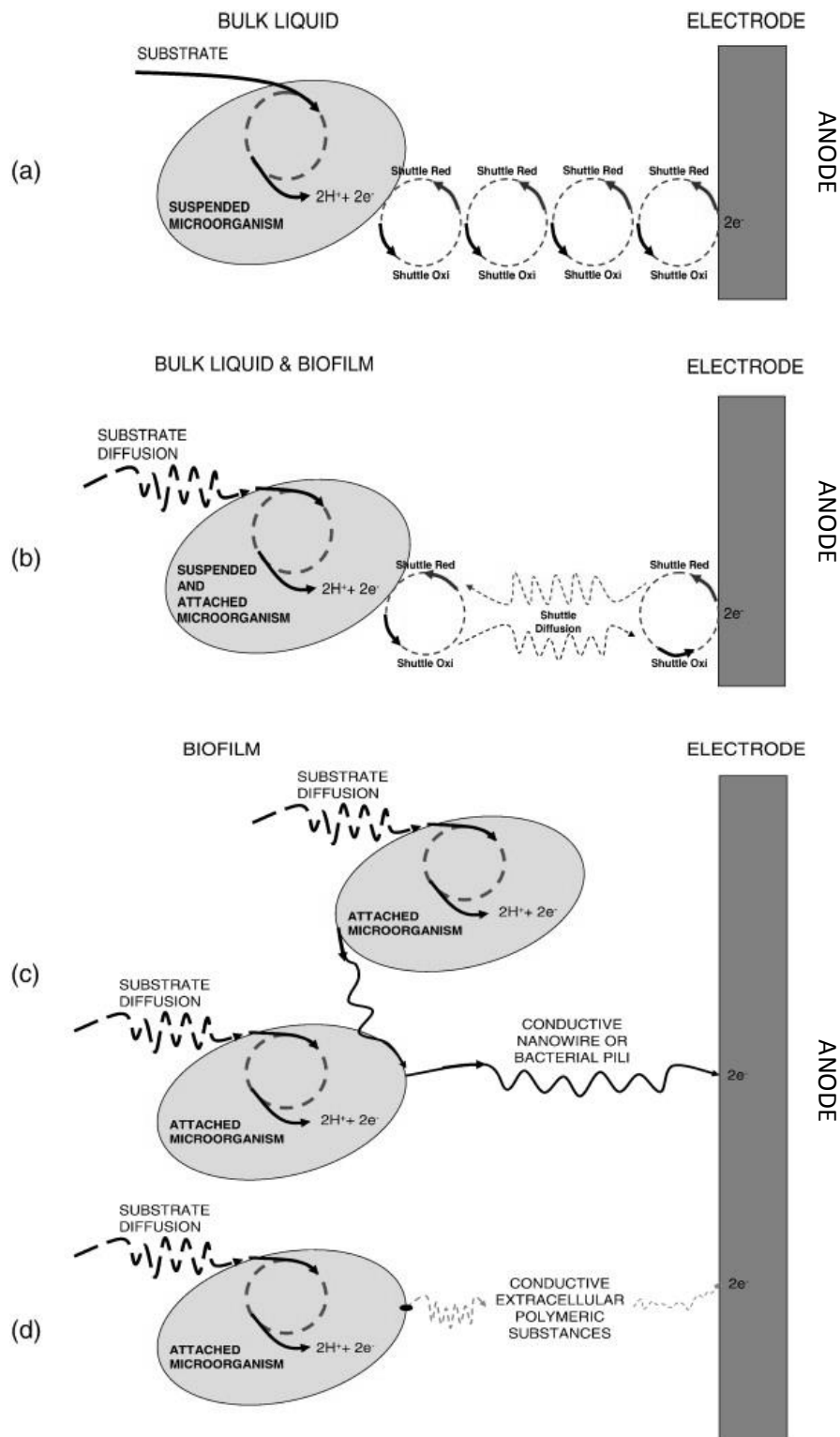
Figure 2.2 Schematic diagrams of electron transport in microbial fuel cells (Oh et al., 2010).

2.3.3 MFC architecture and configuration

MFC have rapidly advanced from low-power laboratory designs constructed with bottles and expensive materials to higher power densities and designs that appear to be more cost effective (Logan, 2010). The different designs are listed in Table 2.2 (Zhou et al., 2013).

Table 2.2 Classification of MFCs (Zhou et al., 2013).

MFC classification criteria	Type of MFC
MFC configuration	• Single-chamber • Dual- chamber • Multi-Chamber • Roll type
Reactor structure	• Flat plate • Disc • Tubular • Concentric cylinders
Separator	• Salt-bridge • Membrane-less • Anion-exchange membrane • Cation-exchange membrane
Flow type	• Batch • Continuous flow
Cathode type	• Air-cathode • Biocathode • Chemical cathode

SCMFCs have low internal resistance and rapid mass transfer from the anode to cathode (Liu et al., 2005; Kim et al., 2007). Therefore, it is preferable to use this MFC

configuration in an attempt to achieve more efficient electricity generation yields. In this study, SCMFCs were used in all the investigations carried out except in Chapter 3 where double chamber MFCs were used in studies involving the comparison of electrode performances.

The MFCs working volumes used in various studies are variable and range from 2 mL (Ieropoulos et al., 2003) to larger volumes such as 100 mL (Jiang et al., 2010), 150 mL and 250 mL (Jiang and Li, 2009) and 2.5 L (Kalathil et al., 2012). Studies conducted at Foster's brewery in Yatala, Queensland (Australia), by the Advanced Water Management Center at the University of Queensland, used an MFC with a working volume of 1000 L and configured with a 3 m tall reactor with 12 modules (Logan, 2010). Comparing the performance of MFCs used by researchers based on the volume/size is difficult because the designs are variable from two-chambered to single chamber, using mediator or without mediator and using a membrane or membrane-less (Pant et al., 2012a). In addition, using different types of electrode material and design makes the comparison difficult. In this thesis, the SCMFCs were constructed with a 130 mL working volume and the double chamber MFCs were designed with a 2 L volume.

2.3.4 Electrode materials

The electrode material of construction must consider the following properties: conduction, chemical stability, mechanical strength, and cost (Wei et al, 2011). The most-widely used carbon materials for MFC applications include (Wei et al, 2011): 1) carbon paper, 2) graphite plate, 3) carbon cloth, 4) carbon mesh 5) granular graphite, 6) granular activated carbon, 7) carbon felt, 8) reticulated vitrified carbon, 9) carbon brush and 10) stainless steel mesh. In this thesis, graphite plate, carbon cloth, carbon felt and carbon

brush electrodes were evaluated. Selecting the best performing and most cost effective electrode was also conducted.

2.3.5 Substrates used in MFCs

In recent years, there has been an increasing amount of work on the generation of electricity from various substrates using MFCs. These substrates can range from simple organic compounds such as glucose (Rabaey et al., 2003), monosaccharides (Catal et al., 2008), alcohols (Kim et al., 2007) to complex substrates which include cattle dung (Zhao et al., 2012), dye wastewater (Kalathil et al., 2012), steroidal drug industrial effluent (Li et al., 2012), synthesis gas (Hussain et al., 2012), corncob pellets (Gregoire and Becker, 2012), starch processing wastewater (Lu et al., 2009), potato-processing wastewater (Durruty et al., 2012), landfill leachate (Oxakya et al., 2013) and artificial urine (Ieropoulos et al., 2003). In this thesis, the three substrates under consideration included glucose, lignin and black liquor. Lignin and black liquor were pretreated with UV/TiO$_2$ photocatlaysis prior to use as a feed to the MFCs.

2.3.5.1 Glucose

Glucose, an easily biodegradable chemical, was used to initiate microbial film on the anode surface. In this work reported herein, when a stable power was observed with glucose, the MFC feed was replaced with other substrates (pretreated lignin or black liquor). The current produced with glucose was compared to the current produced with other substrates while maintaining the same reactor configuration and operating conditions.

2.3.5.2 Lignin

Lignin (from the Latin word *lignum*, wood) is a highly branched polymer of henylpropanoid compounds, and a component of the plant cell wall. After cellulose, lignin is the second most abundant organic compound in plants, representing approximately 30% of the organic carbon in the biosphere (Boerjan et al., 2003). Lignin is an amorphous, cross-linked, and three dimensional phenolic polymer. Lignin typically contains three phenylpropane units denoted as guaiacyl (G) as well as syringyl (S) and phydroxyphenyl (H) units plus their respective precursors which include three aromatic alcohols (monolignols). These chemicals include coniferyl, sinapyl, and p-coumaryl alcohols (Hu and Ragauskas, 2012). The three structures are depicted in Figure 2.3 (Pu et al., 2008).

Coniferyl alcohol/guaiacyl: $R_1 = OMe$, $R_2 = H$
Sinapyl alcohol/ syringyl: $R_1 = R_2 = OMe$
p-Coumaryl alcohol: $R_1 = R_2 = H$
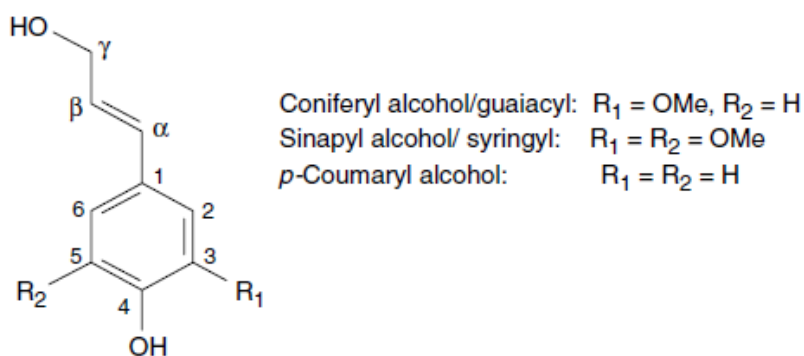
Figure 2.3 Three building blocks of lignin.

The global production of lignin as a by-product of the pulping process is approximately 30 million tonnes per year (Hatakeyama and Hatakeyama, 2010). The chemical structure and stability of lignin makes biological degradation difficult hence, the treatment of wastewater from paper and pulp industries and other facilities that generate

lignin-rich wastewater is potentially challenging. Therefore, one objective of this thesis is to convert lignin compounds into biodegradable organic chemicals.

2.3.5.3 Black liquor

Black liquor, a lignin rich waste, is generated from wood pulping processes. Black liquor is characterized by high alkalinity and high dissolved solids content, mainly dissolved alkali–lignin and polysaccharide degradation by-products (Lara et al., 2003). Pulping can be performed mechanically (mechanical pulping) or chemically (chemical pulping). The process descriptions are shown in Figure 2.4 (adopted from Viraraghavan and Pokhrel, 2004).
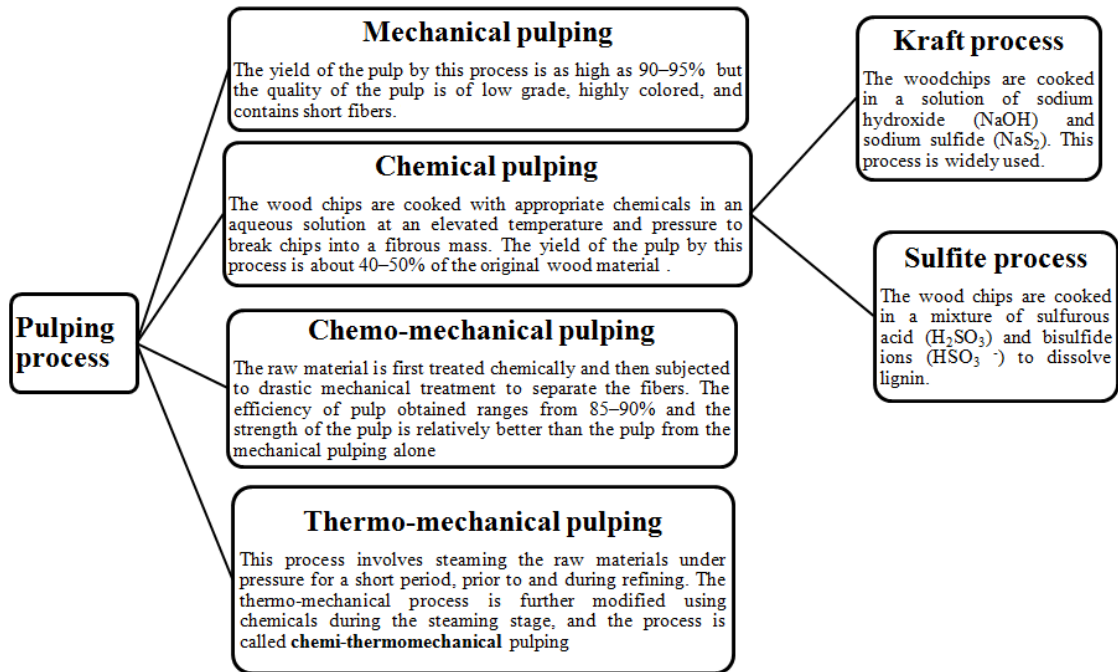
Figure 2.4 The pulping making process.

For every tonne of pulp produced, the kraft pulping process produces approximately 10 tonnes of weak black liquor or about 1.5 tonnes of black liquor dry solids (Tran and Vakkilainen, 2007). The black liquor chemical composition depends on the type of the

raw material processed, i.e. softwoods (such as pine), hardwoods (such as eucalyptus) or fibrous plants (such as bamboo), as well as, on the operational conditions of the pulping process (Cardoso et al., 2009).

2.3.6 MFC operating temperatures

Several studies have demonstrated and evaluated the application and performance of MFCs at ambient, mesophilic and thermophilic temperatures. For example Hussain et al. (2012) operated MFCs at moderately thermophilic temperature of 50 °C. Jiang et al. (2010) started and operated a series of MFCs at 15 °C for 2 cycles and then changed the operational conditions to 30 °C to determine the effects of temperature. The work conducted by Jiang et al. (2010) verified that higher temperatures increased the bacterial activity, which in return enhanced the power output and lowered internal resistance. Yang et al. (2013) and Sun et al. (2012) operated MFCs in fed-batch mode at a constant temperature of 30 °C. Electricity was also successfully produced using a carbon source mixture of D-glucose, D-galactose, D-xylose, D-glucuronic acid and sodium acetate with a mixed bacterial culture in single chamber air-cathode mediator-less MFCs at sub-ambient temperatures (<20 °C, down to 4 °C) (Catal et al., 2011).

Oh et al. (2010) has pointed out that some researchers believe additional heating is required to maintain temperature which may not be necessary for the energy recovery, or wastewater treatment using the MFC technology. Oh et al. (2010) noted that it is suitable to maintain optimum temperature conditions by some energy; however, such a strategy ultimately leads to reducing the energy efficiency. In this thesis, the MFCs were operated at ambient (21±1 °C) and mesophilic temperatures (37±1 °C).

2.3.7 Resistors

Several studies investigating MFC performances have reported using a fixed external resistance of 1000 Ω (Jiang et al., 2010; Wang et al., 2008, Yang et al., 2013). However, fixed external resistance of 100 ohms (Lee et al., 2008), 500 ohms (Sun et al., 2012), 2.2 kΩ (Ledezma et al., 2012) were also used. In most MFC studies reported, it appears that optimization of external resistance is not always done (Rabaey et al., 2005). In this thesis, unless and otherwise mentioned a fixed external resistance of 1000 Ω was used for start-up and operating the MFCs.

2.3.8 Inocula

Bacterial species which have reported to be elecrochemicaly active include *Shewanella oneidensis, Geobacter sulfurreducens, Pseudomonas aeruginos,* and *Clostridium butyricum* (Watanabe, 2008). Du et al. (2007) has provided a list of microorganisms possessing the ability to transfer electrons derived from the metabolism of organic matters to the anode and indicated that marine sediment, soil, wastewater, fresh water sediment and activated sludge are rich sources for these microorganisms.

Due to the high cost, pure cultures are impractical for full-scale operation. Mixed cultures (i.e., soil, wastewater) containing significant amounts of electrogenic bacteria can be used as the cost-effective inocula for MFCs (Jiang et al., 2010). To date, attempts to simplify the study of complex communities with representative pure cultures have been disappointing because pure cultures have generally produced substantially lower power densities than mixed cultures (Nevin et al., 2008). According to Wang et al. (2008), pure cultures grow slowly, having a high risk of microbiological contamination and

generally a high substrate specificity compared to mixed-culture systems. Aside from availability at close to no cost, mixed-culture systems have diverse microbial populations which are more resilient to changes when compared to pure cultures (Patra et al., 2008). Therefore, based on the previous justifications mixed anaerobic cultures were used as inocula in all the MFCs. However, using mixed anaerobic cultures are affiliated with several technical issues when compared to pure cultures. When compared with pure-culture MFCs, mixed-culture MFCs generally need longer time to obtain a stable power (Wang et al., 2008). Nevin et al., (2008) argues that (i) it would be difficult to replicate mixed culture communities and maintain a stable community composition and (ii) functional analysis with approaches, such as genetic manipulation and gene expression studies, which are readily tractable with pure cultures growing on anodes would be substantially more technically difficult with mixed cultures.

2.3.9 Evaluation of MFC performance

Several factors affecting MFC performance include the microbial inoculum, chemical substrate (fuel), type of proton exchange material (and the absence of this material), cell internal and external resistance, solution ionic strength, electrode materials, and electrode spacing (Cheng et al., 2006). Evaluating the performance of MFCs can be conducted by assessing the amount of power or current generated. The power or current density of MFCs could be expressed as power or current generated per unit area of the anode surface or the cathode surface. Alternatively, the power or current generated per unit of the working volume of the MFC can be used as an evaluation parameter. Logan (2012) suggested that an appropriate procedure is to normalize the power per unit area of the membrane or separator placed between the electrodes (two chamber MFCs), or the

cathode (single chamber MFCs) because it is known that the membrane or cathode usually limit maximum power densities. In this thesis, the power and current densities are expressed as per unit area of cathode surface and volume unless and otherwise specified.

In this study, the open circuit voltage (OCV) was measured to evaluate the voltage efficiency of the MFCs. OCV is the cell voltage that can be measured after some time in the absence of current and the cell electromotive force (emf) is a thermodynamic value that does not take into account internal losses (Logan et al., 2006). According to Logan et al. (2006), theoretically, the OCV should approach the cell emf; however, in practice, the OCV is substantially lower than the cell emf. This difference is due to various potential losses such as activation, bacterial metabolism and mass transport losses.

In addition to power and current density (per volume), power and current density (per area), OCV, efficiency based performance indicators used for evaluating MFCs included coulombic efficiency (CE), energy efficiency (EE) and COD removal efficiency (η_{COD}) (Rabaey, 2010). These parameters are described in subsequent chapters.

In evaluating the performance of MFCs, electrochemical/analytical techniques are vitally important in analysing the limiting performances of MFC components, to optimise operation and to allow for continued innovation (Zhao et al., 2009). In a detailed review of the techniques employed in recent studies, Zhao et al. (2009) discussed their principles, experimental implementation, data processing requirements, capabilities and weaknesses. In this thesis, the main electrochemical techniques used are linear swipe voltammetry and cyclic voltammetry. These methods are described in the following sections:

1) Linear sweep voltammetry (LSV): LSV is a method where the current is recorded as a function of potential. This is equivalent to recording current versus time

27

profiles (Bard and Faulkner, 2001). In LSV, the voltage is scanned from a lower limit to an upper limit. In addition to electrochemical characteristics, the linear sweep voltammogram depends on the scan rate. In this thesis, LSV tests were conducted at a scan rate of 0.1 mV s^{-1} unless and otherwise mentioned (Velasquez-Orta et al., 2009; Logan, 2012).

2) Cyclic voltammetry (CV): CV has been used as a principal diagnostic method in protein film voltammetry study (Marsili et al., 2008). The shape, height, steepness and potential of the cyclic voltammograms are functions of mass transport, interfacial electron-transfer rate, kinetics and thermodynamics (Heering et al., 1998). According to Fricke et al. (2008), CV is a standard tool in electrochemistry and has regularly been exploited to study and to characterize the electron transfer interactions between microorganisms or microbial biofilms and microbial fuel cell anodes. Cyclic voltammetry is used to measure current as a function of a cyclic applied potential. In this technique, the potential is ramped linearly at selected scan rates with reversal of the ramp after a given time (potential) and the resulting current (I) is monitored as a function of applied potential (E) to give the I-E curve which is denoted as the cyclic voltammogram. A redox system can be characterized from the potentials of the peaks (redox couple) on the cyclic voltammogram and from changes caused by variations in scan rate. By recording cyclic voltammograms during different stages of biofilm formation and substrate availability (different stages of current generation), valuable information on the electron transfer mechanism can be gained (Fricke et al., 2008). Data from the CV study was combined with the data obtained from molecular biology analysis to better understand and characterize the microbial biofilm responsible for the electricity generation.

2.3.10 Application of MFCs

MFCs have a number of uses which include the following (Rajalakshmi and Dhathathreyan, 2008):

- The first and most obvious is for wastewater treatment while simultaneously generation electricity

- MFCs could be implanted in the body to be employed as power sources for a pacemaker, a micro sensor or a micro actuator. The MFC would consume glucose samples from the blood stream or possibly use substrates contained in the body and use it to generate electricity to power these devices, and

- MFCs can be used in EcoBots, Gastrobots and biosensors

Logan (2005) estimated that electricity accounts for roughly 25% of the total operating costs of a wastewater treatment plant. Assuming a BOD concentration of 300 mg/L, a population of 100,000 individuals and a total flow of $1.64*10^7$ L/yr, the maximum electricity production using MFCs can reach 2.3 MW. He (2012) argues that it may be unrealistic to convert a wastewater treatment plant into a "power plant". He (2012) evaluated the energy balances and showed that an MFC does not consume much energy. According to He (2013) the energy consumed by MFCs of <0.04 kWh/m^3, or <0.07 kWh/kg COD is much less than that consumed in an aerobic process such as activated sludge (0.3 kWh/m^3 or 0.6 kWh/kg COD).

The first large-scale test of MFCs was conducted at Foster's brewery in Yatala, Queensland (Australia), by the Advanced Water Management Center at the University of Queensland (Logan, 2010). The reactor consisted of 12 modules, each 3 m high, with a total volume of approximately 1 m^3.

The electricity yield from MFCs is less than that theoretical expected. The causes for lower generation of electricity have been widely investigated. Physical, chemical and biochemical factors which determine the electricity yield in MFCs are as follows (Kim et al., 2006):

(1) The microbial activity to oxidize carbon substrates,

(2) Electron transfer to the electrode from the microbial population,

(3) Circuit resistance,

(4) Proton transfer from the anode compartment to the cathode compartment,

(5) Oxygen supply and reduction at the cathode, and

(6) Oxygen diffusion into the anode compartment through the membrane.

According to studies conducted by Liu et al. (2005), factors responsible for low electron and energy recoveries in MFCs could be due to an increase in oxygen transfer into the anode chamber, substrate loss due to methanogenesis, use of substrate for bacterial growth and production of biomass, and the presence of alternate electron acceptors, such as sulfate. Lee et al. (2008) established a complete electron-equivalent balance in microbial fuel cells (MFCs) fed acetate and glucose electron donors by experimentally quantifying current, biomass, residual organic compounds, H_2, and CH_4 gas. In the electron balance analysis, Lee et al. (2008) identified that the electrical current, the most significant electron sink, in both glucose and acetate fed MFCs, were 71% and 49%, respectively. The second largest electron sink was biomass (acetate 15%, glucose 26%), and the third was the residual organic compounds (acetate 11%, glucose 18%).

The power densities produced by MFCs are less when compared to other fuel cells such as those utilizing hydrogen. According to Logan and Rabaey (2012), this difference

is due to high internal resistances, the limited temperature and solution conditions tolerated by microorganisms, substrate degradability and biofilm kinetics. However, the MFC technology, although still at its infancy, might bring in new opportunities because of its many unique features listed in Table 2.3 (Li et al., 2014).

Table 2.3 Potential benefits of MFCs for energy, environmental, operational and economic sustainability (Adopted from Li et al. (2014).

S. No.	Potential benefit	Description
1	Energy benefit	• Direct electricity generation • Need no aeration • Low sludge yield • Adaptable to decentralized treatment
2	Operating stability	• Self-regeneration of microorganisms • Good resistance to environmental stress • Amenable to real- time monitoring and control
3	Environmental impact	• Water reclamation • Low carbon foot print • Less sludge disposal
4	Economics	• Energy recovery • Valuable products recovery • Ease burden of subsequent treatment

2.4 Biomethanation

Biomethanation (biogas formation) represents one of the most versatile types of bio-energy and can be produced from organic solid wastes and organic wastewaters (Plugge et al., 2010). Anaerobic methanogenic treatment of organic solid waste and wastewaters is able to reduce our dependency on fossil fuels. Anaerobic processing provides an efficient waste treatment with low energy requirement; meanwhile bio-energy is produced in the form of methane (Plugge et al., 2010).

Anaerobic wastewater treatment processes are advantageous when compared to aerobic processes. According to van Lier (2008), anaerobic wastewater treatment has the following advantages over conventional aerobic treatment systems:

1. Reduction of up to 90% of the sludge produced.

2. Up to 90% reduction in space requirement when using expanded sludge bed systems.

3. High applicable COD loading rates reaching up to 20–35 kg COD m^{-3} reactor volume. day^{-1}, leads to smaller reactor volumes.

4. No use of fossil fuels for treatment leads to savings of approximately 1 kWh/kg COD removed.

5. Production of approximately 13.5 MJ CH_4 energy/kg COD removed.

6. Rapid start-up (< 1 week), using seed granular anaerobic sludge.

7. No or very little use of chemicals.

8. High COD treatment efficiencies, and

9. High-rate systems facilitate water recycling.

The main biochemical processes in the anaerobic degradation of complex substrates under methanogenic conditions are depicted in Table 2.4 (Costa et al., 2013). Methanogenesis is the final step in the anaerobic degradation process and the substrates/compounds used by the methanogenic organisms include hydrogen, formic acid, carbon monoxide, methanol, methylamine and acetate (George et al., 2003). The typical conversion reactions involving these compounds are given in Equations 2.10 to 2.15.

Table 2.4 Biochemical process description of biomethanation (Costa et al. (2013)).

Step	Name of process	Process Description
1	Hydrolysis	• Carbohydrates are converted into soluble sugars (saccharides) by cellulases, amylases, xylanases and other hydrolytic enzymes; • Proteins are degraded via peptides and amino acids by proteases and peptidases; and • Lipids are transformed into long chain fatty acids (LCFA) and glycerol by lipases.
2	Acidogenesis	• Main substrates for acidogenesis include soluble saccharides, amino acids and glycerol and results in the formation of acetate, propionate, butyrate, carbon dioxide, hydrogen and other organic products, such as lactate and alcohols • Soluble sugars are largely converted into acetate and hydrogen
3	Acetogenesis	• Fermentation products (short chain fatty acids and alcohols) and LCFA (resulting from lipid hydrolysis) can be further oxidized to acetate by obligate hydrogen producing acetogens • Fatty acids oxidation is coupled to the reduction of hydrogen ions or bicarbonate, functioning as external electron acceptors, to form hydrogen and formate, respectively.
4	Methanogenesis	• Methanogenesis is carried out by methanogenic archaea, which metabolize the end products of the previous reactions (mainly hydrogen, carbon dioxide, formate, methanol, methylamines, and acetate) to form methane. • This process mainly occurs through two pathways: (1) carbon dioxide reduction (hydrogenotrophic methanogenesis), and (2) acetate dissimilation (acetoclastic methanogenesis).

$$4H_2 + CO_2 \rightarrow CH_4 + 2H_2O \qquad\qquad (2.10)$$

$$4HCOOH \rightarrow CH_4 + 3CO_2 + 2H_2O \qquad\qquad (2.11)$$

$$4CO + 2H_2O \rightarrow CH_4 + 3CO_2 \qquad\qquad (2.12)$$

$$4CH_3OH \rightarrow 3CH_4 + CO_2 + 2H_2O \qquad\qquad (2.13)$$

33

$$4(CH_3)_3N + 6H_2O \rightarrow 9CH_4 + 3CO_2 + 4NH_3 \tag{2.14}$$

$$CH_3COOH \rightarrow CH_4 + CO_2 \tag{2.15}$$
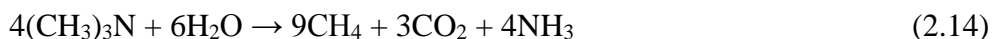
George et al. (2003) has determined the COD equivalent of methane by stoichiometry and depicted that the theoretical amount of CH_4 that can be produced under anaerobic conditions is 0.35 L CH_4 per g COD. In this study, biomethanation of pre-treated lignin and black liquor was investigated and compared with the theoretical COD yield.

2.5 Summary of research objectives

This thesis is organized in manuscript format. Two published manuscripts are included in Chapters 3 and 5. The work reported in Chapter 3 is focused on evaluating electricity generation and biofilm formation in MFCs configured with three different graphite plate electrodes. The three graphite plate electrodes have different electrical properties. A logical follow up to the work in Chapter 3 is the evaluation of electrodes with different surface areas. Chapter 4 describes the performance and comparison of graphite fibre brush and felt anodes with plate electrodes. The work in Chapter 5 used the best performing electrode based on the work in Chapter 4.

The work in Chapter 5 outlines a scheme which demonstrates utilizing photocatalysis of recalcitrant chemicals to produce biodegradable chemicals for electricity production using a microbial fuel cell. The effects of different parameters on the photocatalytic degradation of a model lignin chemical are articulated in this chapter.

Chapter 6 reports on optimizing the photocatalytic degradation of a model lignin chemical using the Box-Behnken design and converting the degradation byproducts into

electricity. Based on data gathered in Chapter 6, the work in Chapter 7 describes using two-stage anaerobic digestion and bioelectrochemical processes to treat black liquor and recovering energy simultaneously. This revised process configuration is designed to increase electricity production from black liquor. Black liquor is lignin rich waste which is produced from pulp and paper mills.

2.6 References

Ahmed, S., Rasul, M.G., Martens, W.N., Brown, R., and Hashib, M.A. (2011) Advances in heterogeneous photocatalytic degradation of phenols and dyes in wastewater: A review. *Water Air Soil Pollut.* **215**(1-4): 3–29.

Akpan, U.G., and Hameed, B.H. (2009) Parameters affecting the photocatalytic degradation of dyes using TiO_2-based photocatalysts: A review. *J. Hazard. Mater*. **170**(2-3): 520–529.

Almquist, C.B., and Biswas, P. (2002) Role of synthesis method and particle size of nanostructured TiO_2 on its photoactivity. *J. Catal.* **212**(2): 145–156.

Bard, A.J., and Faulkner, L.R. (2001) Electrochemical methods: fundamentals and applications. New York, NY: John Wiley and Sons.

Boerjan, W., Ralph, J., and Baucher, M. (2003) Lignin biosynthesis. *Annu. Rev. Plant Biol.* **54**(1): 519–546.

Cardoso, M., de Oliveira, É.D., and Passos, M.L. (2009) Chemical composition and physical properties of black liquors and their effects on liquor recovery operation in Brazilian pulp mills. *Fuel* **88**(4): 756–763.

Castellote, M., and Bengtsson, N. (2011) Principles of TiO_2 photocatalysis. In *Applications of titanium dioxide photocatalysis to construction materials*. Ohama, Y., and Van Gemert, D. eds. Dordrecht: Springer, pp. 5-10.

Catal, T., Kavanagh, P., O'Flaherty, V., and Leech, D. (2011) Generation of electricity in microbial fuel cells at sub-ambient temperatures. *J. Power Sources* **196**(5): 2676–2681.

Catal, T., Li, K., Bermek, H., and Liu, H. (2008) Electricity production from twelve monosaccharides using microbial fuel cells. *J. Power Sources* **175**(1): 196–200.

Chen, C.Y., Kuo, J.T., Yang, H.A., and Chung, Y.C. (2013) A coupled biological and photocatalysis pretreatment system for the removal of crystal violet from wastewater. *Chemosphere* 92: 695–701.

Cheng, S., Liu, H., and Logan, B.E. (2006) Increased performance of single-chamber microbial fuel cells using an improved cathode structure. *Electrochem. Commun.* **8**(3): 489–494.

Chong, M.N., Jin, B., Chow, C.W.K., and Saint, C. (2010) Recent developments in photocatalytic water treatment technology: A review. *Water Res.* **44**(10): 2997–3027.

Choquette-Labbé, M., Shewa, W.A., Lalman, J.A., and Shanmugam, S.R. (2014) Photocatalytic degradation of phenol and phenol derivatives using a nano-TiO_2 catalyst: integrating quantitative and qualitative factors using response surface methodology. *Water*, **6**(6), 1785–1806.

Costa, J.C., Sousa, D.Z., Pereira, M.A., Stams, A.J.M., and Alves, M.M. (2013) Biomethanation potential of biological and other wastes. In *Biofuel technologies*: *recent developments*. Gupta, V.K., and Tuohy, M.G. eds. Berlin-Heidelberg: Springer, pp. 369-396.

Du, Z., Li, H., and Gu, T. (2007) A state of the art review on microbial fuel cells: A promising technology for wastewater treatment and bioenergy. *Biotechnol. Adv.* **25**(5): 464–482.

Durruty, I., Bonanni, P.S., González, J.F., and Busalmen, J.P. (2012) Evaluation of potato-processing wastewater treatment in a microbial fuel cell. *Bioresour. Technol.* **105**: 81–87.

Franks, A., and Nevin, K. (2010) Microbial fuel cells, a current review. *Energies* **3**(5): 899–919.

Fricke, K., Harnisch, F., and Schröder, U. (2008) On the use of cyclic voltammetry for the study of anodic electron transfer in microbial fuel cells. *Energy Environ. Sci.,* **1**(1), 144-147.

Fujishima, A., Rao, T.N., and Tryk, D.A. (2000) Titanium dioxide photocatalysis. *J. Photochem. Photobiol. C Photochem. Rev.* **1**(1): 1–21.

George, T., Franklin, L.B., and Stensel, H.D. (2003) Wastewater engineering treatment and reuse, Metcalf and Eddy, Inc., 4th edn. New York, NY: McGraw-Hill.

Gogate, P.R., and Pandit, A.B. (2004) A review of imperative technologies for wastewater treatment I: Oxidation technologies at ambient conditions. *Adv. Environ. Res.* **8**(3): 501–551.

Gorby, Y.A., Yanina, S., McLean, J.S., Rosso, K.M., Moyles, D., Dohnalkova, A., et al. (2006) Electrically conductive bacterial nanowires produced by *Shewanella oneidensis* strain MR-1 and other microorganisms. *Proc. Natl. Acad. Sci. U.S.A.* **103**(30): 11358–11363.

Gregoire, K.P., and Becker, J.G. (2012) Design and characterization of a microbial fuel cell for the conversion of a lignocellulosic crop residue to electricity. *Bioresour. Technol.* **119**: 208–215.

Hatakeyama, H., and Hatakeyama, T. (2010) Lignin structure, properties, and applications. *Adv. Polym. Sci.* **232**(1): 1–63.

He, Z. (2012) Microbial fuel cells: Now let us talk about energy. *Environ. Sci. Technol.* **47**(1): 332–333.

He, Z., and Angenent, L.T. (2006) Application of bacterial biocathodes in microbial fuel cells. *Electroanalysis* **18**(19–20): 2009–2015.

Heering, H.A, Hirst, J., and Armstrong, F.A. (1998) Interpreting the catalytic voltammetry of electroactive enzymes adsorbed on electrodes. *J. Phys. Chem. B* **102**(35): 6889–6902.

Hernández-Alonso, M.D., Fresno, F., Suárez, S., and Coronado, J.M. (2009) Development of alternative photocatalysts to TiO_2: Challenges and opportunities. *Energy Environ. Sci.* **2**(12): 1231–1257.

Hu, F., and Ragauskas, A. (2012) Pretreatment and lignocellulosic chemistry. *Bioenergy Res.* **5**(4): 1043–1066.

Hussain, A., Mehta, P., Raghavan, V., Wang, H., Guiot, S.R., and Tartakovsky, B. (2012) The performance of a thermophilic microbial fuel cell fed with synthesis gas. *Enzyme Microb. Technol.* **51**(3): 163–170.

Ibhadon, A., and Fitzpatrick, P. (2013) Heterogeneous photocatalysis: Recent advances and applications. *Catalysts* **3**(1): 189–218.

Ieropoulos, I., Greenman, J., Lewis, D., and Knoop, O. (2013) Energy production and sanitation improvement using microbial fuel cells. *J. Water Sanit. Hyg. Dev.* **3**(3): 383–391.

Jiang, D., and Li, B. (2009) Granular activated carbon single-chamber microbial fuel cells (GAC-SCMFCs): a design suitable for large-scale wastewater treatment processes. *Biochem. Eng. J.* **47**(1), 31-37.

Jiang, D., Li, B., Jia, W., and Lei, Y. (2010) Effect of inoculum types on bacterial adhesion and power production in microbial fuel cells. *Appl. Biochem. Biotechnol.* **160**(1): 182–196.

Kalathil, S., Lee, J., and Cho, M.H. (2012) Efficient decolorization of real dye wastewater and bioelectricity generation using a novel single chamber biocathode-microbial fuel cell. *Bioresour. Technol.* **119**: 22–27.

Kamat, P. V. (2012) TiO_2 nanostructures: Recent physical chemistry advances. *J. Phys. Chem. C* **116**(22): 11849–11851.

Kaneco, S., Katsumata, H., Suzuki, T., and Ohta, K. (2006) Titanium dioxide mediated photocatalytic degradation of dibutyl phthalate in aqueous solution-kinetics, mineralization and reaction mechanism. *Chem. Eng. J.* **125**(1): 59–66.

Kim, B.H., Chang, I.S., and Moon, H. (2006) Microbial fuel cell-type biochemical oxygen demand sensor. *Encycl. Sensors* **10**: 1–12.

Kim, J.R., Jung, S.H., Regan, J.M., and Logan, B.E. (2007) Electricity generation and microbial community analysis of alcohol powered microbial fuel cells. *Bioresour. Technol.* **98**(13): 2568–2577.

Lara, M.A., Rodríguez-Malaver, A.J., Rojas, O.J., Holmquist, O., González, A.M., Bullón, J., et al. (2003) Black liquor lignin biodegradation by *Trametes elegans*. *Int. Biodeterior. Biodegrad.* **52**(3): 167–173.

Ledezma, P., Greenman, J., and Ieropoulos, I. (2012) Maximising electricity production by controlling the biofilm specific growth rate in microbial fuel cells. *Bioresour. Technol.* **118**: 615–618.

Lee, H.S., Parameswaran, P., Kato-Marcus, A., Torres, C.I., and Rittmann, B.E. (2008) Evaluation of energy-conversion efficiencies in microbial fuel cells (MFCs) utilizing fermentable and non-fermentable substrates. *Water Res.* **42**(6): 1501–1510.

Li, W.W., Yu, H.Q., and He, Z. (2014) Towards sustainable wastewater treatment by using microbial fuel cells-centered technologies. *Energy Environ. Sci.* **7**(3): 911-924.

Liu, H., Cheng, S., and Logan, B.E. (2005) Production of electricity from acetate or butyrate using a single-chamber microbial fuel cell. *Environ. Sci. Technol.* **39**(2): 658–662.

Liu, R., Gao, C., Zhao, Y.G., Wang, A., Lu, S., Wang, M. Maqbool, F., and Huang, Q. (2012). Biological treatment of steroidal drug industrial effluent and electricity generation in the microbial fuel cells. *Bioresour. Technol.*, **123**: 86-91.

Logan, B.E. (2005) Simultaneous wastewater treatment and biological electricity generation. *Water Sci. Technol.* **52**(1): 31–37.

Logan, B.E. (2010) Scaling up microbial fuel cells and other bioelectrochemical systems. *Appl. Microbiol. Biotechnol.* **85**(6): 1665–1671.

Logan, B.E. (2012) Essential data and techniques for conducting microbial fuel cell and other types of bioelectrochemical system experiments. *ChemSusChem* **5**(6): 988–994.

Logan, B.E., and Rabaey, K. (2012) Conversion of wastes into bioelectricity and chemicals by using microbial electrochemical technologies. *Science* **337**(6095): 686–690.

Logan, B.E., Hamelers, B., Rozendal, R., Schröder, U., Keller, J., Freguia, S., et al. (2006) Microbial fuel cells: Methodology and technology. *Environ. Sci. Technol.* **40**(17): 5181–5192.

Lu, N., Zhou, S., Zhuang, L., Zhang, J., and Ni, J. (2009) Electricity generation from starch processing wastewater using microbial fuel cell technology. *Biochem. Eng. J.* **43**(3): 246–251.

Marsili, E., Rollefson, J.B., Baron, D.B., Hozalski, R.M., and Bond, D.R. (2008) Microbial biofilm voltammetry: Direct electrochemical characterization of catalytic electrode-attached biofilms. *Appl. Environ. Microbiol.* **74**(23): 7329–7337.

Mohan, S.V., Srikanth, S., Velvizhi, G., and Babu, M.L. (2013) Microbial fuel cells for sustainable bioenergy generation: Principles and perspective applications. In *Biofuel Technologies*: *Recent Developments*. Gupta, V.K., and Tuohy, M.G. eds. Berlin-Heidelberg: Springer, pp. 335–368.

Nevin, K.P., Richter, H., Covalla, S.F., Johnson, J.P., Woodard, T.L., Orloff, A.L., et al. (2008) Power output and columbic efficiencies from biofilms of *Geobacter sulfurreducens* comparable to mixed community microbial fuel cells. *Environ. Microbiol.* **10**(10): 2505–2514.

Oh, S.T., Kim, J.R., Premier, G.C., Lee, T.H., Kim, C., and Sloan, W.T. (2010) Sustainable wastewater treatment: How might microbial fuel cells contribute. *Biotechnol. Adv.* **28**(6): 871–881.

Özkaya, B., Cetinkaya, A.Y., Cakmakci, M., Karadağ, D., and Sahinkaya, E. (2013) Electricity generation from young landfill leachate in a microbial fuel cell with a new electrode material. *Bioprocess Biosyst. Eng.* **36**(4): 399–405.

Pant, D., Singh, A., Van Bogaert, G., Irving Olsen, S., Singh Nigam, P., Diels, L., and Vanbroekhoven, K. (2012a) Bioelectrochemical systems (BES) for sustainable energy production and product recovery from organic wastes and industrial wastewaters. *RSC Adv.* **2**(4): 1248-1263.

Pant, D., Van Bogaert, G., Diels, L., and Vanbroekhoven, K. (2012b) A comparative assessment of bioelectrochemical systems and enzymatic fuel cells. In *Microbial Biotechnology: Energy and Environment*. Arora, R. ed. Wallingford, Oxfordshire: CAB International, pp 39-57.

Patra, A. (2008) Low-cost, single-chambered microbial fuel cells for harvesting energy and cleansing wastewater. *J. US, SJWP* **3**(1): 72–85.

Pekakis, P.A., Xekoukoulotakis, N.P., and Mantzavinos, D. (2006) Treatment of textile dyehouse wastewater by TiO_2 photocatalysis. *Water Res.* **40**(6): 1276–1286.

Plugge, C.M., Van Lier, J.B., Stams, A.J.M., and Jeison, D. (2009) Microbial energy production from biomass. In *Bioelectrochemical systems: from extracellular electron transfer to biotechnological application*. Reaby K., Angenet L., Schroder U., and Keller J. eds. London: IWA Publishing, pp. 17-38.

Pokhrel, D., and Viraraghavan, T. (2004) Treatment of pulp and paper mill wastewater - a review. *Sci. Total Environ.* **333**(1): 37–58.

Pu, Y., Zhang, D., Singh, P.M., and Ragauskas, A.J. (2008) The new forestry biofuels sector. *Biofuels, Bioprod. Biorefining* **2**(1): 58–73.

Rabaey, K., and Verstraete, W. (2005) Microbial fuel cells: novel biotechnology for energy generation. *Trends Biotechnol.* **23**(6): 291–298.

Rabaey, K., Lissens, G., and Verstraete, W. (2005) Microbial fuel cells: performances and perspectives. In *Biofuels for fuel cells: Renewable energy from biomass fermentation*. Lens, P., Westermann, P., Haberbauer, M., and Moreno, A. eds. IWA Publishing, London, pp. 377–399.

Rabaey, K., Lissens, G., Siciliano, S.D., and Verstraete, W. (2003) A microbial fuel cell capable of converting glucose to electricity at high rate and efficiency. *Biotechnol. Lett.* **25**(18): 1531–1535.

Rajalakshmi, N., and Dhathathreyan, K.S. (2008) Present trends in fuel cell technology development. New York, NY: Nova Science Publishers.

Ray, S., Lalman, J.A., and Biswas, N. (2009) Using the Box-Behnken technique to statistically model phenol photocatalytic degradation by titanium dioxide nanoparticles. *Chem. Eng. J.* **150**(1): 15–24.

Ren, Z.J. (2013) The principle and applications of bioelectrochemical systems. In *Biofuel technologies*: *Recent developments*. Gupta, V.K., and Tuohy, M.G. eds. Berlin-Heidelberg: Springer, pp. 501–527.

Rittmann, B.E. (2008) Opportunities for renewable bioenergy using microorganisms. *Biotechnol. Bioeng.* **100**(2): 203–212.

Rozendal, R.A., Hamelers, H.V.M., Rabaey, K., Keller, J., and Buisman, C.J.N. (2008) Towards practical implementation of bioelectrochemical wastewater treatment. *Trends Biotechnol.* **26**(8): 450–459.

Schneider, J., Matsuoka, M., Takeuchi, M., Zhang, J., Horiuchi, Y., Anpo, M., and Bahnemann, D.W. (2014) Understanding TiO$_2$ photocatalysis: mechanisms and materials. *Chem. Rev.* **114**(19): 9919-9986.

Schröder, U. (2007) Anodic electron transfer mechanisms in microbial fuel cells and their energy efficiency. *Phys. Chem. Chem. Phys.* **9**(21): 2619–2629.

Sun, J., Li, Y., Hu, Y., Hou, B., Xu, Q., Zhang, Y., and Li, S. (2012) Enlargement of anode for enhanced simultaneous azo dye decolorization and power output in air-cathode microbial fuel cell. *Biotechnol. Lett.* **34**(11): 2023–2029.

Tran, H., and Vakkilainen, E.K. (2007) Advances in the Kraft chemical recovery process. In *Source 3rd ICEP international colloquium on eucalyptus pulp*. Belo Horizonte, Brazil, pp. 4–7.

Van Lier, J.B. (2008) High-rate anaerobic wastewater treatment: Diversifying from end-of-the-pipe treatment to resource-oriented conversion techniques. *Water Sci. Technol.* **57**(8): 1137–1148.

Velasquez-Orta, S.B., Curtis, T.P., and Logan, B.E. (2009) Energy from algae using microbial fuel cells. *Biotechnol. Bioeng.* **103**(6): 1068–1076.

Velegraki, T., Poulios, I., Charalabaki, M., Kalogerakis, N., Samaras, P., and Mantzavinos, D. (2006) Photocatalytic and sonolytic oxidation of acid orange 7 in aqueous solution. *Appl. Catal. B Environ.* **62**(1): 159–168.

Verma, A., and Dixit, D. (2012) Photocatalytic degradability of insecticide Chlorpyrifos over UV irradiated titanium dioxide in aqueous phase. *Int. J. Environ. Sci.* **3**(2): 743–755.

Vogelpohl, A., and Kim, S.M. (2004) Advanced oxidation processes (AOPs) in wastewater treatment. *J. Ind. Eng. Chem. (Seoul, Repub. Korea),* **10**(1): 33–40.

Wang, X., Feng, Y., Ren, N., Wang, H., Lee, H., Li, N., and Zhao, Q. (2009) Accelerated start-up of two-chambered microbial fuel cells: Effect of anodic positive poised potential. *Electrochim. Acta* **54**(3): 1109–1114.

Watanabe, K. (2008) Recent developments in microbial fuel cell technologies for sustainable bioenergy. *J. Biosci. Bioeng.* **106**(6): 528–536.

Wei, J., Liang, P., and Huang, X. (2011) Recent progress in electrodes for microbial fuel cells. *Bioresour. Technol.* **102**(20): 9335–9344.

Yang, F., Ren, L., Pu, Y., and Logan, B.E. (2013) Electricity generation from fermented primary sludge using single-chamber air-cathode microbial fuel cells. *Bioresour. Technol.* **128**: 784–787.

Yurdakal, S., and Augugliaro, V. (2012) Partial oxidation of aromatic alcohols via TiO_2 photocatalysis: the influence of substituent groups on the activity and selectivity. *RSC Adv.* **2**:(22), 8375–8380.

Zhang, X.C., and Halme, A. (1995) Modelling of a microbial fuel cell process. *Biotechnol. Lett.* **17**(8): 809–814.

Zhao, F., Slade, R.C.T., and Varcoe, J.R. (2009) Techniques for the study and development of microbial fuel cells: an electrochemical perspective. *Chem. Soc. Rev.* **38**(7): 1926–1939.

Zhao, G., Ma, F., Wei, L., Chua, H., Chang, C.C., and Zhang, X.J. (2012) Electricity generation from cattle dung using microbial fuel cell technology during anaerobic acidogenesis and the development of microbial populations. *Waste Manage.* **32**(9): 1651–1658.

Zhou, M., Wang, H., Hassett, D.J., and Gu, T. (2013) Recent advances in microbial fuel cells (MFCs) and microbial electrolysis cells (MECs) for wastewater treatment, bioenergy and bioproducts. *J. Chem. Technol. Biotechnol.* **88**(4): 508–518.

CHAPTER 3

ELECTRICITY GENERATION AND BIOFILM FORMATION IN MICROBIAL FUEL CELLS USING PLATE ANODES CONSTRUCTED FROM VARIOUS GRADES OF GRAPHITE

3.1 Introduction

Depleting fossil fuel resources, environmental damage and energy security are key factors driving the search for renewable energy supplies. Microbial fuel cells (MFCs) are a promising alternative to produce renewable energy from organic matter. MFCs have many operational and functional advantages over technologies currently used for generating energy from organic matter (Rabaey and Verstraete, 2005). According to Rabaey and Verstraete (2005), these advantages include the following: high conversion efficiency is achieved by the conversion of substrate energy to electricity, efficient operation at ambient and at low temperatures distinguishes them from current bio-energy processes, gas treatment is not required because the off-gases from MFCs are enriched in carbon dioxide, energy input is not required for aeration provided the cathode is passively aerated and potential application in area lacking electrical infrastructure.

MFCs represent a potential alternative approach when compared to conventional activated sludge wastewater treatment systems because energy is produced in the form of electricity or hydrogen gas rather than using energy for aeration or for other treatment processes (Logan, 2008). The application of MFCs for wastewater treatment has been documented in many reports (Aelterman et al., 2006; Ahn and Logan, 2010; Cha et al., 2009; Kargi and Eker, 2007; Vidris et al., 2008).

In its most simple configuration, an MFC is a device which uses microorganisms to produce an electrical current. The oxidation of organic chemicals by microorganisms liberates both electrons and protons. Electrons are then transferred from microorganisms to the anode and then subsequently to the cathode through an electrical network. Simultaneously, protons migrating to the cathode combine with electrons and an electron acceptor such as oxygen to produce water. The electrical current generated is similar to that in chemical fuel cells; however, in MFCs microbial catalysts are attached to the anode surface (Franks and Nevin, 2010).

MFCs are configured in a variety of configurations. Single chamber MFCs are designed with an anodic compartment without the requirement for an aerated compartment containing the cathode. In a typical configuration, the anode contained in a compartment is coupled with an air-cathode (Liu et al., 2005). In a two chamber MFC configuration, the oxidation of the electron donors on an anode is physically separated from the reduction of an electron acceptor on the cathode. Microorganisms are cultivated on the anode where electron donors are oxidized. Electrons are transferred to the anode and subsequently to oxygen or other electron acceptors. Typically, the anode compartment is separated from the cathode compartment by a proton exchange membrane (PEM) or cation exchange membrane (CEM).

The performance and cost of electrodes are important factors affecting the design of MFCs (Wei et al., 2011). A wide range of electrode materials and configurations have been examined in recent years to improve the performance and reduce cost. A suitable electrode must be a good conductor, chemically stable, mechanically strong and not expensive (Wei et al., 2011).

Identifying materials and architectures which maximize power generation and coulombic efficiency is a major challenge in designing MFCs (Logan, 2008). Another challenge is to reduce cost and develop configurations which can be constructed from a practical point-of-view (Logan, 2008). According to Logan and Regan (2006), the most significant impediment in achieving high power densities in MFCs is the system configurations and not the composition of the bacterial community.

Utilizing electrodes with improved properties will enhance the performance of MFCs because different anode materials result in different activation polarization losses (Du et al. 2007). Because the power output of MFCs is low relative to other type of fuel cells, reducing their cost is essential if power generation using this technology is to be an economical method of energy production (Liu and Logan, 2004). Many studies have focused on maximizing the power generation in MFCs; however, work on cost minimization studies is limited. Practical applications of MFCs will require developing designs that will not only produce high power outputs and coulombic efficiencies but also will be economical to manufacture in large quantities (Logan, 2008). In this study, the cost of the material was also considered in the evaluation of different electrode materials. An improved understanding of the type together with the selection of cost effective electrodes for MFC is important. In spite of many published studies which have focused on power generation and coulombic efficiency of MFCs; no study has considered electrode cost when evaluating their performance. Hence, the objective of this study was to assess the significance of cost for different graphite plate electrodes on the performance of MFCs.

3. 2 Material and methods

3.2.1 Microbial fuel cell set-up and operation

The air-cathode single chamber microbial fuel cell (SCMFC) used in this study is depicted in Figure 3.1. The air-cathode was constructed as previously described by Cheng et al. (2006). The air-cathode was constructed with 2.5 mg/cm^2 platinum on the inner surface facing the media solution. The outer surface of cathode was coated with four layers of polytetrafluoroethane (PTFE®) to prevent water loss and substrate oxidation by oxygen. The anodes used were graphite plate electrodes with a surface area of 25.6 cm^2. The fuel cell working volume was 130 mL. The SCMFCs were operated in batch mode and fed with fresh medium (described in section 2.2) after 6 to 7 days or when the voltage decreased to below 20±5 mV. All the experiments were conducted in triplicate.
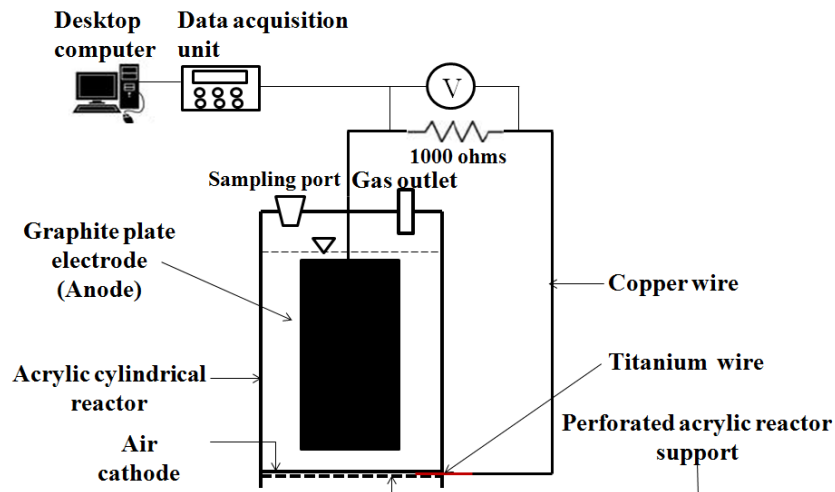
Figure 3.1 Schematic of a single chamber MFC.

Two chamber MFCs (Figure 3.2) were constructed with two cylindrical chambers connected by a polyethylene tube. The flanged tubes were fitted with porous inserts to

accommodate a proton exchange membrane (PEM) (Nafion 117, Fuel Cell Earth LLC). The total volume of each chamber was 2 litres. The PEM was pre-treated to remove impurities before placing it between the flanges. The pre-treatment process was as follows: dipped in a boiling 30% H_2O_2 solution, washed with deionized water, dipped in 0.5M H_2SO_4, and washed with deionized water (60 mins for each step). All the MFCs were operated at $21\pm1^\circ C$ with the same mixed anaerobic culture, substrate concentration and external load (1,000 ohm).
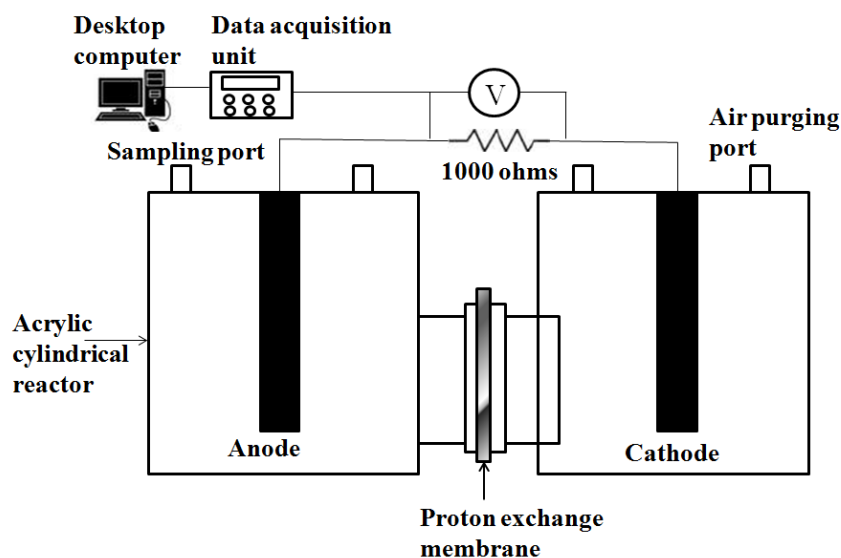
Figure 3.2 Schematic of a two chamber MFC.

3.2.2 Mixed anaerobic cultures source and medium

In this study, the SCMFCs and the two chamber MFCs were seeded with a mixed anaerobic culture which was obtained from a municipal wastewater treatment facility (Chatham, ON). The medium added to the SCMFCs and the anodic chamber of the two chamber MFCs contained the following: 500 mg L^{-1} glucose, 310 mg L^{-1} NH_4Cl, 130 mg L^{-1} KCl, 4225 mg L^{-1} $NaH_2PO_4.H_2O$, 7400 mg L^{-1} $Na_2HPO_4.12H_2O$, 10 mg L^{-1} yeast extract and 1 mL L^{-1} of a mineral solution. The mineral solution was prepared in

accordance with the procedure described by Wiegant and Lettinga (1985). The solution for the cathode chamber of the two chamber MFCs contains all the constituents mentioned above except glucose and yeast extract. The cathodic chambers of the two camber MFCs were continuously purged with air to provide oxygen in solution.

3.2.3 Electrodes

In this study, the configuration of the three graphite plate electrodes (POCO3, HK06 and G347) (MWI Inc, Rochester, NY) are shown in Figure 3.3. Specifications for the electrodes are shown in Table 3.1. The electrodes were washed with deionized water before placing them in the MFCs.
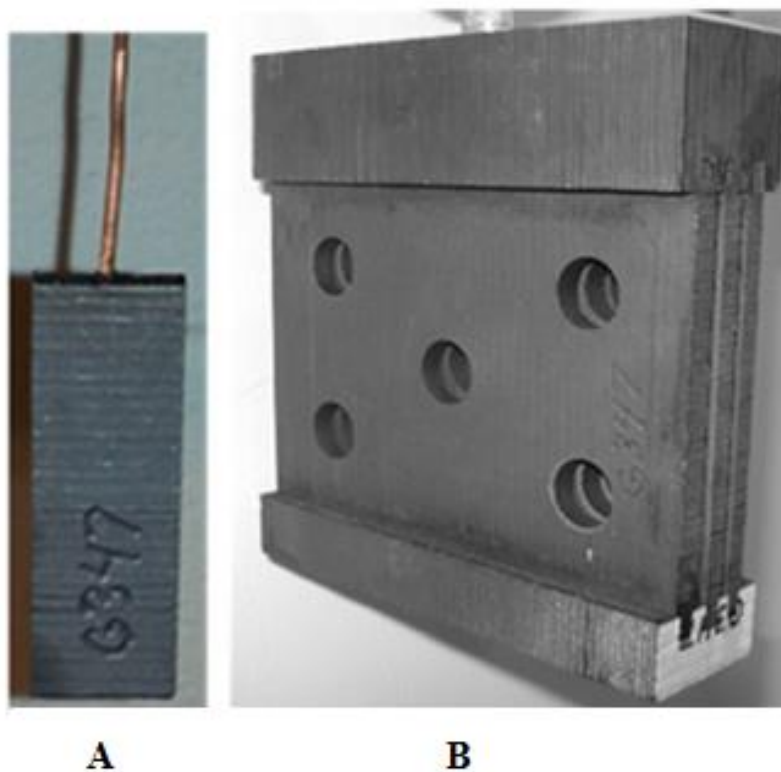
Figure 3.3 Electrode design used in the MFC experiments A) Single chamber electrode; B) Two chamber electrode.

Table 3. 1 Properties of graphite plate electrodes.

Description	Unit	Grade of electrode		
		POCO3	HK06	G347
Specific Gravity	-	1.81	1.86	1.85
Specific Resistance	μΩm	14	12	11
Flexural Strength	MPa	93	85	49
Shore Hardness	Shore	76	68	58
Average grain size	μm	<5	3	NA

3.2.4 Data acquisition and analysis

Cell voltages (V) of each MFC were sampled every 5 min using an Agilent 34970A data acquisition unit connected to a computer. A full channel scan was performed for all MFCs and the data were stored for analysis. The potential of the anode and cathode electrodes were measured versus an Ag/AgCl reference electrode (CH instruments Inc., Austin, TX) with the anode or the cathode as the working electrode.

Cyclic voltammetry was employed to acquire qualitative data related to electrochemical reactions and to locate redox potentials of the electroactive species. Electrochemical impedance spectroscopy (EIS) was used to determine the internal resisitance of the SCMFCs. The polarization and power density curves for SCMFCs were obtained using linear swipe voltammetry (LSV). Two chamber MFCs were characterised using different external resistances (1,000,000, 10,000, 5,600, 1,000, 680, 470, 330, 220, 100, 47, 8.2 and 1.5 Ω), with each resistance being connected for 15 min. The potential (V) was used to calculate the current (I). The power density, P (mW/m^2), was calculated

using the surface area (A) of the anode ($P = I \times V/A$). The power was also normalized based on working volume to express the power density in mW/m^3.

The coulombic efficiency (C_E) and the energy efficiency (η_{MFC}) were calculated using Equations 3.1 and 3.2 (Logan, 2008).

$$C_E = \frac{M_s \int_0^{t_b} I dt}{F b_{es} v_{An} \Delta c} \tag{3.1}$$

M_s is the molecular weight of the substrate, t_b is time for one feeding cycle, F is Faraday's constant, b_{es} is number of moles of electrons per mole of substrate, v_{An} is the volume of liquid in the anode compartment and Δc is the substrate concentration change over a feeding cycle.

$$\eta_{MFC} = \frac{\int_0^{t_b} E_{MFC} I dt}{\Delta H n_s} \tag{3.2}$$

where E_{MFC} is the voltage, ΔH is the molar heat of combustion and n_s is the amount (mol) of substrate added.

A principal component analysis (PCA) was employed to correlate the material characteristics and the electrode efficiencies (Appendix E2).

3.2.5 Analytical methods

Liquid samples (5 mL) were withdrawn from the MFCs after initiation of the experiment and at the end of every feeding cycle. These samples were filtered using a

0.45 µm polypropylene membrane (GE Osmonics, MN) and a 100 to 200 mesh ion exchange resin (Chelex 100, Bio-Rad, CA) to remove heavy metals and suspended solids. The filtered samples were analyzed for COD according to *Standard Methods* (APHA et al, 2005).

Microbial samples were removed from the liquid suspension in the anodic chamber and from the anode surface upon completing the last feeding cycle. DNA isolation, polymerase chain reaction (PCR) and terminal restriction fragment length polymorphism (T-RFLP) profiling of the microbial community samples were performed in accordance with methods described by Chaganti et al. (2012).

3.3 Results and discussions

3.3.1 Comparative power production

The MFCs were operated under batch conditions with each feeding cycle 6 to 7 days and the number of batch feeding cycles was 10. The feeding period was variable depending on the voltage reduction to a low value of 20 ± 5 mV. After seeding the MFCs, steady-state voltages were observed at the end of 6 feeding cycles (approximately 6 weeks). Variation in the cell potential with time in the two chamber MFCs configured with three different grades of graphite is shown in Figure 3.4. Variation in the voltage pattern was observed as follows: POCO3 > G347 > HK06. The cell potential under different loads is shown in Figure 3.5 and a distinct difference is observed in this case. A similar trend (POCO3 > G347 > HK06) was also observed for the SCMFCs voltage generation (data not shown).
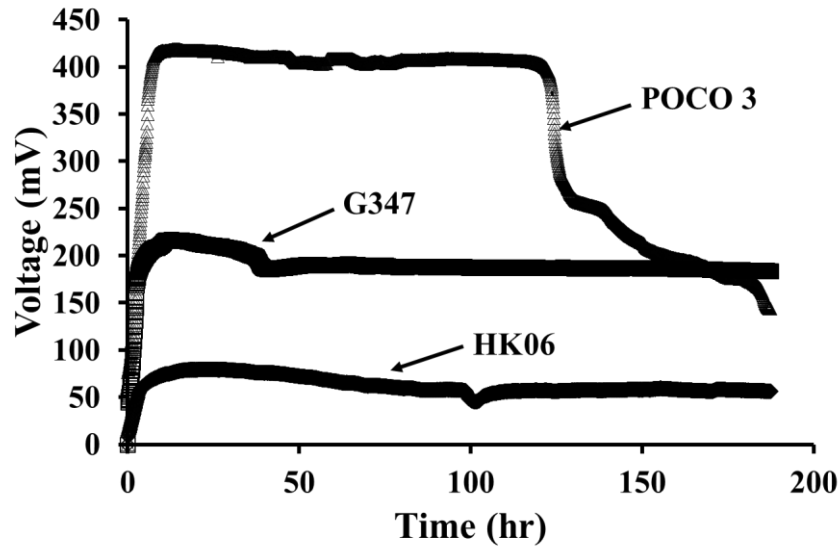
Figure 3.4 Representative single batch feeding cycle voltage generation in the two chamber MFCs configured with three different graphite electrodes.

Note: The MFCs were operated under a constant external load of 1000 ohms
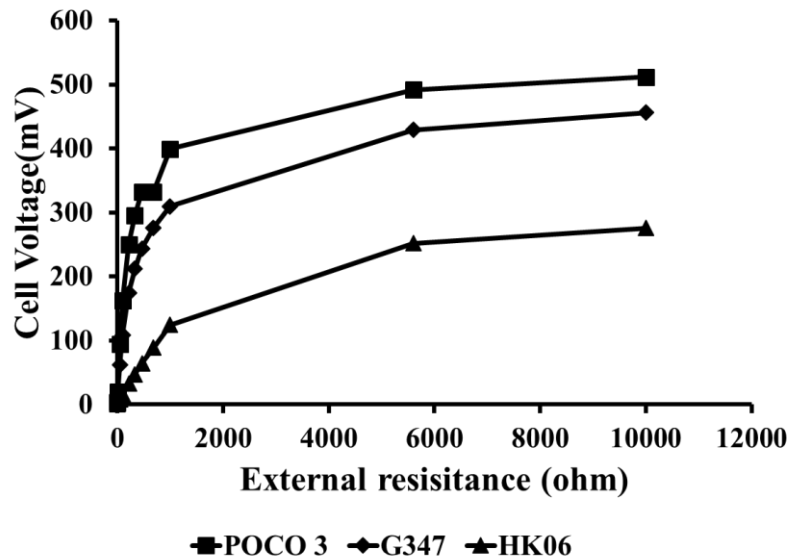
Figure 3. 5 Cell potential in the two chamber MFCs configured with three different graphite electrodes and under varying external loads.

3.3.2 Current – power profile

3.3.2.1 Single chamber MFCs

Many researchers use different units to denote the performance of an MFC. Current density, a common term, is either represented as the current generated per unit area of the anode surface area (mA/cm^2) or current generated per unit volume of the cell (mA/m^3) (Pant et al., 2010). According to Logan (2012), it is appropriate to normalize power to the membrane or cathode surface area. In this study, the current and power densities are reported as per unit area of the anode surface area, per unit of area of the air-cathode and per unit volume of the cell (Table 3.2).

Table 3.2 Maximum current and power density of SCMFCs provided with different plate electrodes.

Grade of electrode	Normalized to working volume		Normalized to cathode surface area		Normalized to anode surface area	
	I (mA/m^3)	P (mW/m^3)	I (mA/m^2)	P (mW/m^2)	I (mA/m^2)	P (mW/m^2)
POCO3	8144	2682	1078	355	414	136
HK06	769	282	102	37	39	14
G347	3929	1473	520	195	200	75

The maximum power density for the MFCs using the linear swipe voltammetry (Figure 3.6) was obtained by varying the potential of the working electrode at a scan rate of 1 mV s^{-1}. This data show that the POCO3 material produced 1078 mW/m^2 (2682 mW/m^3) which is approximately twice larger than that of the G347 material (520 mW/m^2; 1473 mW/m^3) and 10 times larger than that of the HK06 material (102 mW/m^2; 282

mW/m^3) (Table 3.2). This indicates that POCO3 has the highest current density followed by G347 and HK06.
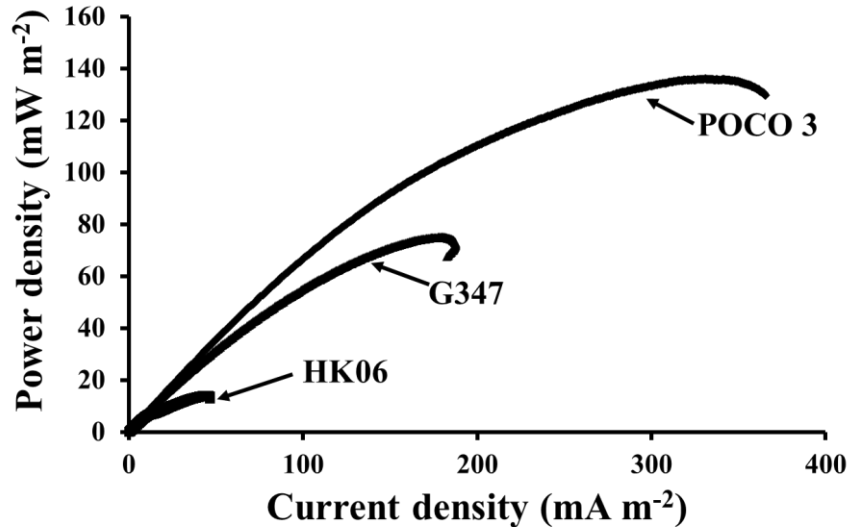
Figure 3.6 Power density curves normalized to anode surface area as a function of current density for SCMFCs.

3.3.2.2 Two chamber MFCs

The current and power densities trend for the two chamber system was similar as that observed for the single chamber MFC configuration (POCO3 > G347 > HK06). The current and power profiles for the three electrodes are depicted in Figure 3.7. The low power density observed is attributed to the large distance between the cathode and anode electrodes, membrane resistance and the solution conductivity. Another reason is low surface area of the anode compared to the volume of the anolyte (Ringeisen et al., 2006). The two chamber MFC was also not operated under strict anaerobic conditions because the sampling port (which was also used as a vent) was open throughout the entire operation of the MFCs. Therefore, the operating condition was facultative and this may

be another reason for the lower power density production. However, note the lower power production would likely have no effect in comparing the electrodes performance since, the operating conditions for the MFCs are the same. The results show differences in the electricity generation of the different electrodes (Figure 3.7).
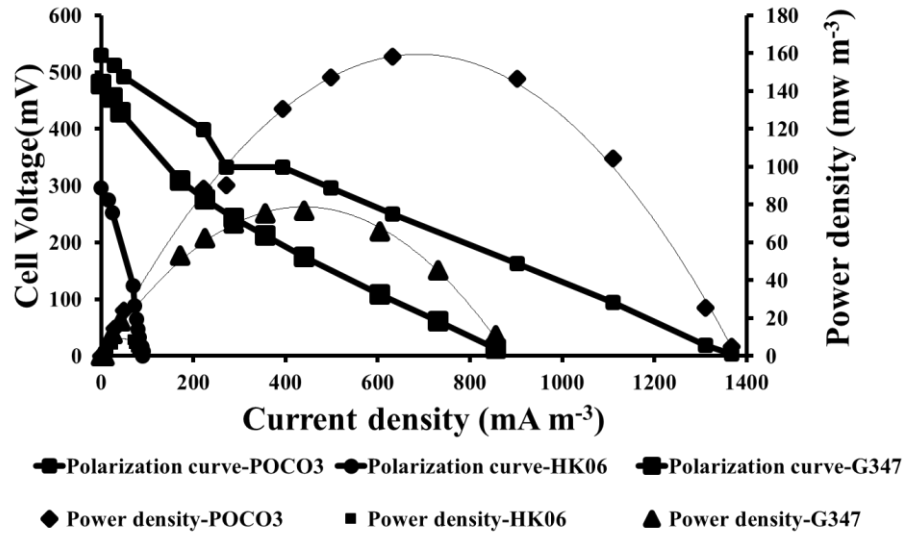
Figure 3.7 Polarization and power density curves normalized to the electrode surface area as a function of current density for the two-chamber MFC.

3.3.3 Comparison of MFC efficiencies

The coulombic efficiency, energy efficiency and COD removal efficiency for SCMFCs configured with different anode materials are shown in Table 3.3. Notice the HK06 efficiency is very low when compared to POCO 3 and G347. The POCO 3 and G347 materials did not shown significant variation in efficiency. The low (< 12%) coulombic and energy efficiencies for the three electrodes were likely due to the conversion of glucose into volatile fatty acids such as acetate, butyrate, and propionate. Rahimnejad et al. (2011) reported similar results and according to Logan (2008) the

energy efficiency values for MFCs range from 2% to 50% for easily biodegradable substrates.

Table 3.3 Efficiency of SCMFCs configured with different electrodes.

Grade of Electrode	Coulombic efficiency (%)	Energy efficiency (%)	COD removal (%)
POCO3	10.95±3.10	2.10±0.60	91.50±2.90
HK06	2.55±0.20	0.10±0.00	25.95±11.00
G347	11.80±1.45	1.70±0.20	84.65±13.30

3.3.4 Cost effectiveness

MFCs with POCO3 electrodes had the highest electricity generating capacity compared to G347 and HK06. However, when comparing the price of the electrode (anode only) per reactor, the G347 material cost was less. Based on the two chamber MFC configuration (Figure 3.2) and electrode design (Figure 3.3B), the cost of electrode (anode) is $ 9.45 per reactor where as the costs for the other two electrodes POCO3 and HK06 are approximately $125 and $40, respectively. The cost includes not only cost of material but also cost of cutting and fixing the electrodes as per the design indicated in Figure 3.3B.

To identify the most cost effective electrode, the cost of the electrode per reactor was divided by the maximum power density. The results show that the lowest cost of $0.12 for a power output of 1 mW m^{-3} per one feeding cycle was obtained for G347 while the cost for POCO3 and HK06 were, approximately $1.25 and $4.30, respectively.

Therefore, among the different graphite plate electrodes, G347 was the most cost effective electrode followed by POCO3 and HK06. The G347 electrode also had the lowest specific resistance (Table 3.1) when compared to that of POCO3 and HK06 electrodes. The lowest cost and the lower specific resistance can be attributed to the cost effectiveness of the G347 material. This indicates that the costs of the two electrodes POCO3 and HK06 are high for practical applications. Therefore, G347 is the best material for MFCs based on large scale applications. Among the different electrode materials, POCO3 is the best candidate for MFCs if the choice is based only on current or power production. However, when electrode cost is considered in addition, to the electricity production capacity, the G347 material is the most cost effective option.

3.3.5 Microbial growth and electricity generation

The physico-chemical characteristics of different electrode materials can affect the microbial colonization of surfaces (Sun et al., 2011). Variation in microbial populations was observed in the three electrodes under examination. The POCO3 electrode was more suitable for the growth of electrochemically active bacteria when compared to the G347 and HK06 materials. In addition to the power density results, the microbial analysis revealed that different microbial populations were detected in the biofilms developed on the surface of the different materials (Figure 3.8). On the POCO3 and G347 materials, similar band patterns were detected irrespective of the band intensities. However, in case of the HK06 material, the band pattern was different when compared to the POCO3 and G347 materials. The T-RFs data was further analysed for the identification of the different organisms (Chaganti et al., 2012). The results showed that *Geobacter* sp.,

Brucella sp., and *Fusobacterium* sp., were dominant on the POCO3 and G347 surfaces, whereas the relative abundance of the same bands was low in the case of HK06.

Generally, the power generation capacity is related to the biofilm formed on anodes as microbes adhere to their surface (Rabaey and Rozendal, 2010). Previous studies have reported detecting *Geobacter* sp. in MFC biofilms (Lovley et al., 2011; Bond and Lovley 2003). *Brucella* sp. and *Fusobacterium* sp. are also capable of biofilm formation; however, these microorganisms have not been reported to participate in bioelectricity production (Almiron et al., 2013; Chew et al., 2012). The abundance of *Geobacter* sp. in POCO3 is associated with greater power generation curves. In case of the HK06 material, the dominant band was uncultured bacteria. The results from this study clearly indicate that biofilm formation is dependent on the quality of the graphite material composition.
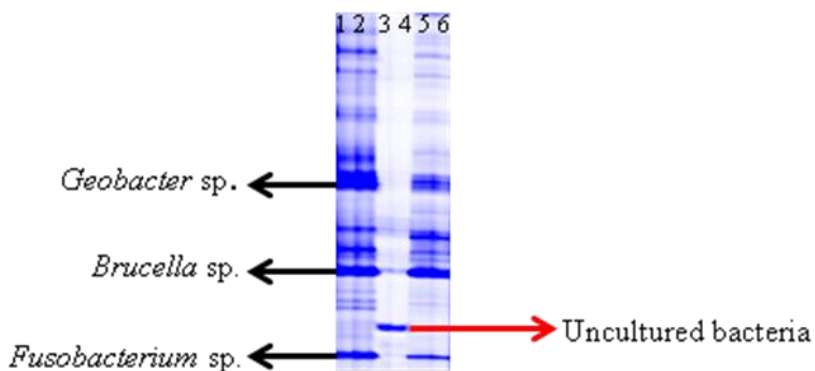
Figure 3.8 Microbial characterization of biofilms on different graphite anodes. Lane 1 and 2 = POCO3; lane 3 and 4 = HK06; lane 5 and 6 = G347.

3.3.6 Cyclic voltammograms

Cyclic voltammetry (CV) was performed to characterize the catalytic properties of the microbial populations in biofilm on the electrodes. The potential scan from −0.4 V to + 0.4 V was performed at a scan rate of 1mV/s. The cyclic voltammograms (Figure 3.9)

show the presence of redox peaks for the different electrodes. A higher redox peak observed for POCO3 bio-anode (Figure 3.9) compared to the other electrodes indicate that biofilm formed on POCO3 electrode is very effective in oxidizing the substrate and transfer of electrons. In case of the POCO3 and G347 materials, the multiple redox peaks suggest that more than one microorganism participated in electricity production. To some extent, the CV data correlated with the result from the microbial analysis (section 3.5).
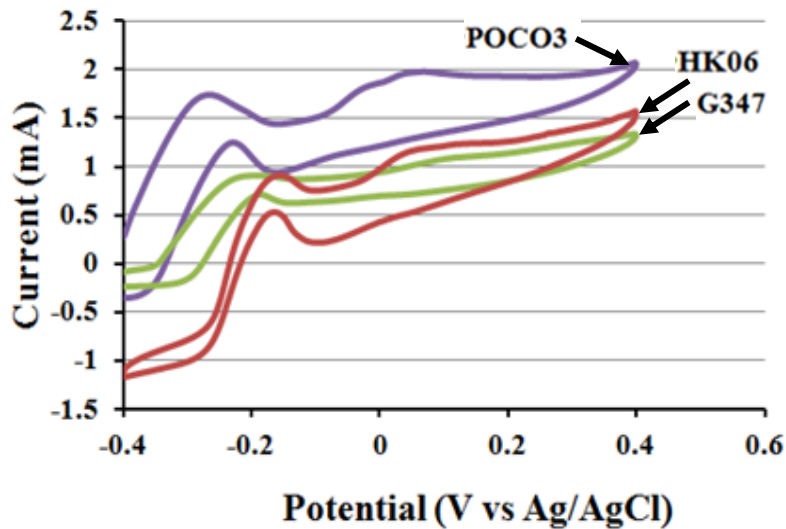
Figure 3.9 Cyclic voltammogram of bacterial biofilm on SCMFC graphite plate electrodes.

3.3.7 Principal component analysis

Principle components (PCs) are linear combinations of the measured variables. The PCA bi-plots indicate that the electrodes are different from each another and it also shows an association between the material properties and the MFCs performance variables and the electrodes (Figure 3.10). The PCA showed two PCs. The first PC explained 64.15 % of the variance and the second PC explained 35.85% of the variance in the data set (Figure 3.10). The PCA also highlights similarities and differences between the three

electrodes. The length of each vector indicates the dominance of the various factors. In this case, none of the factors were dominant. Principal components 1 and 2 combined explained 100% of the variance in the data set. According to Varmuza and Filzmose (2009), if the objects points are positioned in a plane, PC1 and PC2 are able to represent the data structure. These authors also state that the sum of the variances preserved by PC1 and PC2 is close to 100%.

Energy efficiency, COD removal, coulombic efficiency and maximum power density are positively correlated with PC1 while the internal resistance and specific gravity are negatively correlated with PC1. The flexural strength and shore hardness were correlated with PC2. Vectors in the same direction reinforce their effect, those at 90° are independent and when placed in the opposite direction, they work against each other. In this study, the coulombic efficiency is negatively affected by the internal resistance and notice the energy efficiency is correlated with COD removal.
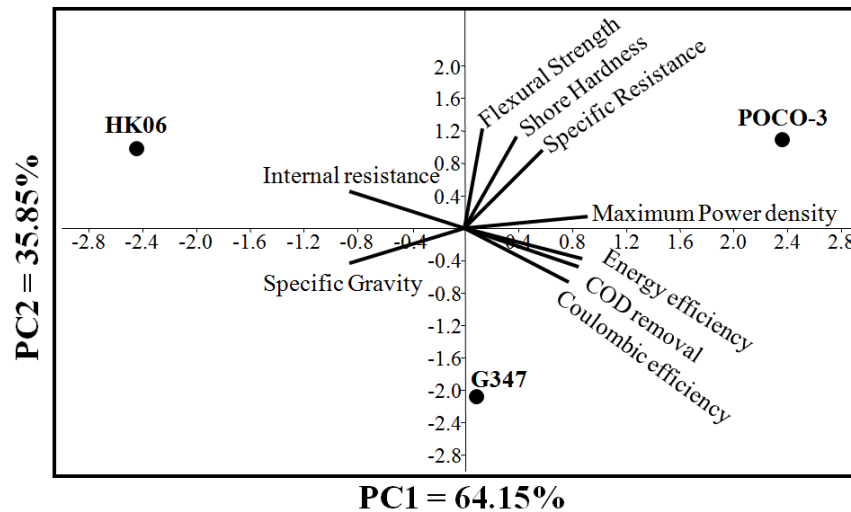
Figure 3.10 Principal component analysis of graphite plate electrodes properties and efficiencies.

3.4 Conclusion

The performance of different graphite plate anode materials in single and double chamber MFCs was detected in this study. The selection of electrode material is essential in the design of MFCs. This research contributes to the advancement of MFCs since it provides tools for selecting suitable anode graphite materials to construct laboratory scale MFCs. Of the three graphite electrodes, the best grade was selected based on power generation, biofilm formation and cost. This study has clearly indicated the variation in the electricity generation and biofilm formation using different grades of graphite plate electrode. The findings have significant impact in understanding the performance of electrode material and depicted relevant parameters required for comparison. The conclusions from this study are as follows:

1. Electricity generation and microbial biofilm communities on anodes are affected by the physio-chemical properties of graphite electrodes.

2. Selection of a graphite plate electrode should not be based on the power output but also the cost of the material.

3. The greatest power density was observed for the POCO3 material. The trend for increasing electricity generation was as follows: POCO3 > G347 > HK06.

4. Microbial analysis showed that the dominant populations are dependent on the graphite characteristics.

5. Selecting electrodes for optimum electricity generation is important in the development of laboratory scale and full-scale MFCs.

Further suggested experimental work should consider the following:

1. Perform similar studies in continuous flow MFCs.

2. Further comparison of the graphite plate electrodes using wastewater or substrates from full-scale waste production facilities.

3. Considering other components including different types of cathodes for cost and performance comparison.

4. Assess the scalability of graphite plate electrodes for pilot and full-scale applications.

3.5 References

Aelterman, P., Rabaey, K., Clauwaert, P., and Verstraete, W. (2006) Microbial fuel cells for wastewater treatment. *Water Sci. Technol.* **54**(8): 9–15.

Ahn, Y., and Logan, B.E. (2010) Effectiveness of domestic wastewater treatment using microbial fuel cells at ambient and mesophilic temperatures. *Bioresour. Technol.* **101**(2): 469–475.

Almiron, M.A., Roset, M.S., and Sanjuan, N. (2013) The aggregation of *Brucella abortus* occurs under microaerobic conditions and promotes desiccation tolerance and biofilm formation. *Open Microbiol. J.* **7**: 87–91.

APHA, AWWA, and WPCF. (2005) Standard methods for the examination of water and wastewater, 21st edn. Washington, D.C: American Public Health Association.

Bond, D.R. and Lovley, D.R. (2003) Electricity production by *Geobacter sulfurreducens* attached to electrodes. *Appl. Environ. Microbiol.* **69**(3): 1548–1555.

Cha, J., Kim, C., Choi, S., Lee, G., Chen, G., and Lee, T. (2009) Evaluation of microbial fuel cell coupled with aeration chamber and bio-cathode for organic matter and nitrogen removal from synthetic domestic wastewater. *Water Sci. Technol.* **60**(6): 1409–1418.

Chaganti, S.R., Lalman, J.A., and Heath, D.D. (2012) 16S rRNA gene based analysis of the microbial diversity and hydrogen production in three mixed anaerobic cultures. *Int. J. Hydrogen Energy* **37**(11): 9002–9017.

Cheng, S., Liu, H., and Logan, B.E. (2006) Increased performance of single-chamber microbial fuel cells using an improved cathode structure. *Electrochem. Commun.* **8**(3): 489–494.

Chew, J., Zilm, P.S., Fuss, J.M., and Gully, N.J. (2012) A proteomic investigation of *Fusobacterium nucleatum* alkaline-induced biofilms. *BMC Microbiol.* **12**(1): 189.

Du, Z., Li, H., and Gu, T. (2007) A state of the art review on microbial fuel cells: A promising technology for wastewater treatment and bioenergy. *Biotechnol. Adv.* **25**(5): 464–482.

Franks, A. and Nevin, K. (2010) Microbial fuel cells, a current review. *Energies* **3**(5): 899–919.

Kargi, F., and Eker, S. (2009) High power generation with simultaneous COD removal using a circulating column microbial fuel cell. *J. Chem. Technol. Biotechnol.* **84**(7): 961-965.

Liu, H., Cheng, S., and Logan, B.E. (2005) Production of electricity from acetate or butyrate using a single-chamber microbial fuel cell. *Environ. Sci. Technol.* **39**(2): 658–662.

Liu, H., and Logan, B.E. (2004) Electricity generation using an air-cathode single chamber microbial fuel cell in the presence and absence of a proton exchange membrane. *Environ. Sci. Technol.* **38**(14): 4040-4046.

Logan, B.E. (2008) Microbial fuel cells. New York, NY: John Wiley and Sons.

Logan, B.E. (2012) Essential data and techniques for conducting microbial fuel cell and other types of bioelectrochemical system experiments. *ChemSusChem.* **5**(6): 988–994.

Logan, B.E., and Regan, J.M. (2006) Electricity-producing bacterial communities in microbial fuel cells. *Trends Microbiol.* **14**(12): 512-518.

Lovley, D.R., Ueki, T., Zhang, T., Malvankar, N.S., Shrestha, P.M., Flanagan, K.A., Aklujkar, M., Butler, J.E., Giloteaux, L., Rotaru, A.E., Holmes, D.E., Franks, A.E., Orellana, R., Risso C., and Nevin, K.P. (2011) Geobacter: the microbe electric's physiology, ecology, and practical applications. *Adv. Microb. Physiol.* **59**: 1–100.

Rabaey, K., and Rozendal, R.A. (2010) Microbial electrosynthesis—revisiting the electrical route for microbial production. *Nat. Rev. Microbiol.* **8**(10): 706-716.

Rabaey, K., and Verstraete, W. (2005) Microbial fuel cells: novel biotechnology for energy generation. *Trends Biotechnol.* **23**(6): 291–298.

Rahimnejad, M., Ghoreyshi, A.A., Najafpour, G., and Jafary, T. (2011) Power generation from organic substrate in batch and continuous flow microbial fuel cell operations. *Appl. Energy* **88**(11): 3999–4004.

Ringeisen, B.R., Henderson, E., Wu, P.K., Pietron, J., Ray, R., Little, B., et al. (2006) High power density from a miniature microbial fuel cell using *Shewanella oneidensis* DSP10. *Environ. Sci. Technol.* **40**(8): 2629–2634.

Sun, Y., Wei, J., Liang, P., and Huang, X. (2011) Electricity generation and microbial community changes in microbial fuel cells packed with different anodic materials. *Bioresour. Technol.* **102**(23): 10886–10891.

Varmuza, K., and Filzmoser, P. (2009) Introduction to multivariate statistical analysis in chemometrics. Boca Raton, FL: CRC press.

Virdis, B., Rabaey, K., Yuan, Z., and Keller, J. (2008) Microbial fuel cells for simultaneous carbon and nitrogen removal. *Water Res.* **42**(12): 3013–3024.

Wei, J., Liang, P., and Huang, X. (2011) Recent progress in electrodes for microbial fuel cells. *Bioresour. Technol.* **102**(20): 9335–9344.

Wiegant, W.M., and Lettinga, G. (1985). Thermophilic anaerobic digestion of sugars in upflow anaerobic sludge blanket reactors. *Biotechnol. Bioeng.* **27**(11): 1603–1607.

CHAPTER 4

EVALUATING ANODE MATERIALS FOR MICROBIAL FUEL CELLS

4.1 Introduction

The popularity of microbial fuel cells (MFCs) has risen exponentially over the past 5 to 10 years because the technology has the potential of harvesting energy from chemicals in wastewaters directly in the form of electricity (Lefebvre et al. 2011). However, MFCs for the large scale treatment of wastewaters still face problems of scale up from laboratory experiments and slow rates of substrate degradation (Franks and Nevin, 2010). The reasons that limited translation of laboratory-scale processes to full-scale are 1) the cost of the electrodes, and 2) the diminished power at larger scales (Logan et al., 2015). However, Logan et al. (2015) argues that the main difficulty is not an intrinsic loss of power at larger scales, but maintaining reactor geometry relative to electrode configurations and densities as larger reactors are built to handle greater water flows.

A typical MFC consists of an anodic chamber and a cathodic chamber separated by a proton exchange membrane (PEM) as in the case of two chamber MFC. A single chamber MFC eliminates the need for the cathodic chamber by exposing the cathode directly to air (Du et al., 2007). Du et al. (2007) has summarized the components and the materials used to construct MFCs (Table 4.1). All the components listed in Table 4.1 are required for the proper operation of MFCs except the cathode chamber which can be avoided and replaced with an air-cathode. The air-cathode can be constructed from carbon cloth, carbon black powder, platinium catalyst and polytetrafluoroethylene (PTFE) solution (Shewa et al., 2014).

Electricity generation in an MFC is accomplished by (i) microbial catabolism, (ii) electron transfer from microbes to the anode, (iii) reduction of electron acceptors at the cathode, and (iv) proton transfer from the anode to cathode (Watanabe, 2008). MFC power generation and performance is governed by several parameters which include the following: 1) physical factors including fuel cell configuration, anolyte volume, electrode materials, membrane. 2) biological factors such as nature of microbes used along with their growth and synergistic interaction with the electrode, mechanism of electron transfer from the microbes and the role of electron shuttlers and 3) operational factors such as nature of electron donor, organic load, retention time, redox condition (pH) and microenvironment (Mohan et al., 2013).

Table 4.1 Basic components of microbial fuel cells (Du et al., 2007).

Items	Materials	Remarks
Anode	Graphite, graphite felt, carbon paper, carbon-cloth, Pt, Pt black, reticulated vitreous carbon (RVC)	Necessary
Cathode	Graphite, graphite felt, carbon paper, carbon-cloth, Pt, Pt black, RVC	Necessary
Anodic chamber	Glass, polycarbonate, Plexiglas	Necessary
Cathodic chamber	Glass, polycarbonate, Plexiglas	Optional
Proton exchange system	Proton exchange membrane: Nafion, Ultrex, polyethylene/poly(styrene-co-divinylbenzene); salt bridge, porcelain septum, or solely electrolyte	Necessary
Electrode catalyst	Pt, Pt black, MnO_2, Fe^{3+}, polyaniline, electron mediator immobilized on anode	Optional

Comparing research data from many different studies is difficult according to Noll (2006). Data summarized by Noll (2006) on MFC performance from numerous publications concluded that the difficulty in comparing results reported is due to the absence of key experimental parameters. The other main challenge in comparing MFC performances is the use of a wide variety of MFC configurations and construction materials (Pant et al, 2012). For example, comparing data for MFC treating different wastewaters is difficult because data for different organic feed stock types tested under identical conditions is lacking (Larrosa-Guerrero et al., 2010).

Watanabe (2008) indicated that the reactor configuration largely influences the bioelectrochemical processes and the total MFC performance. Watanabe (2008) further argues that a distinct feature of an MFC is that its performance is largely dependent on hardware rather than on microbial activity. The anode electrode is one of the hardware components of MFCs (Table 4.1). In nearly all bioelectrochemical system (BES) studies, researchers have been using graphite (or carbon) as the anode materials because it is (Hamelers et al., 2010): (i) well compatible with electrochemically active biofilms, (ii) widely available in high specific area structures, and (iii) relatively inexpensive.

Using better performing electrode materials can improve the performance of an MFC because different anode materials result in different activation polarization losses (Du et al., 2007). In Chapter 3 of this thesis, different types of graphite plate electrodes were compared (Shewa et al., 2014). The objective of this work was to evaluate the performance of three different graphite plates, brush and graphite felt electrodes. The air-cathodes used in this study for all MFCs were identical and constructed from carbon cloth.

The particular air-cathode design was selected because this type of electrode could be used in full-scale systems (Logan 2008).

4.2 Materials and methods

4.2.1 MFCs configuration

The single chamber microbial fuel cells (SCMFCs) and equipment used in this study are shown in Figure 4.1. The SCMFCs were constructed from acrylic (Figure 4.2) and the details of the anodes and electrodes are described in subsequent sections.
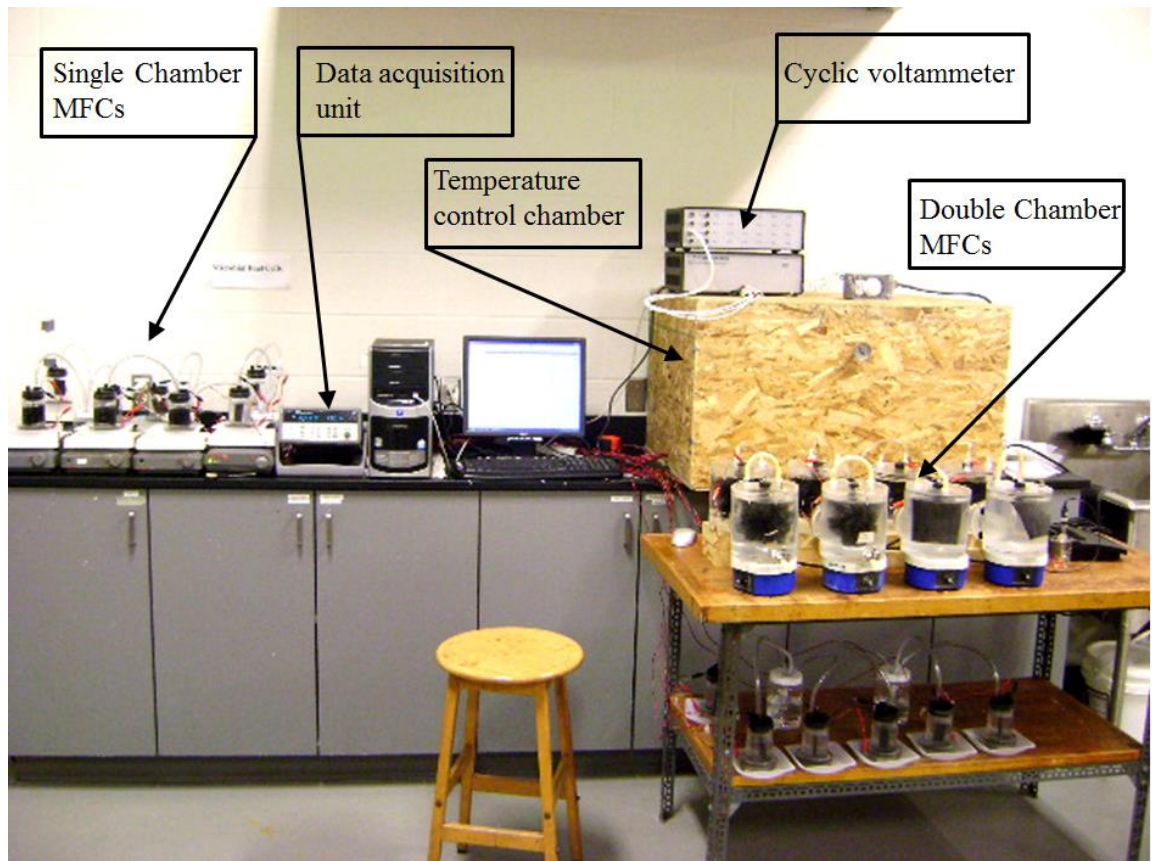
Figure 4.1 Experimental set up.

Figure 4.2 Digital picture of the SCMFC.

4.2.1.1 Cathode

The air-cathodes (Figure 4.3) for the SCMFCs were constructed according to the method and procedure described in Chapter 3 using carbon cloth, carbon black powder, platinium catalyst and polytetrafluoroethylene (PTFE) solution. The steps followed to construct the air-cathodes are described in Appendix D.
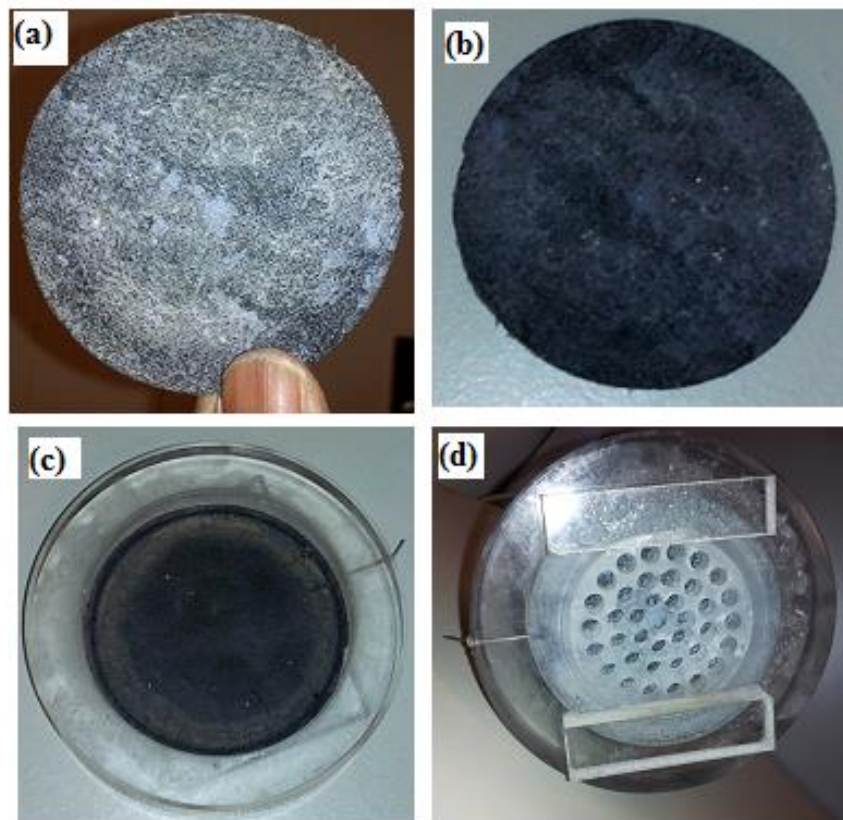
Figure 4.3 Digital picture of air-cathode: a) Air-cathode exposed to the air (four diffusion layers), b) Air-cathode exposed to the medium, c) Air-cathode fixed to the acrylic bottom, and d) Digital picture showing the perforated acrylic air-cathode support.

4.2.2.1 Anode

The brush electrode (Figure 4.4a) was purchased from the Mill-Rose Co. (Mentor OH, USA). The graphite felt (GF-S6 Graphite, 6 mm thick) was purchased from Electrosynthesis Company, Inc. (Lancaster, NY, USA) (Figure 4.4b). The solid graphite electrodes (POCO3, HK06 and G347) used for the comparison are shown and described in Chapter 3. To aid the comparison of the electrodes, the dimensions of the five anode electrodes were maintained at a volume of 5 cm^3.

Figure 4.4 Digital picture showing: a) Graphite fiber brush anode and b) Graphite felt anode used in SCMFCs.

4.2.2 MFCs operation

All the SCMFCs were seeded with a mixed anaerobic culture obtained from a municipal wastewater treatment facility (Chatham, ON). The liquid medium added to the SCMFCs contained the ingredients described in Chapter 3. The SCMFCs were operated at the same operating conditions employed in Chapter 3 (Table 4.2). All experiments were conducted in triplicate.

Table 4.2 Operating conditions of SCMFCs.

S.No.	Parameter description	Value
1	Temperature	21±1°C
2	Anodic working liquid volume	130 mL
3	External resistance	1000 ohms
4	Substrate concentration (glucose)	500 mg L^{-1}
5	Initial pH	7

4.2.3 Measurements and data analysis

The voltage (V) was monitored every 5 minutes using an Agilent data acquisition system (34970A Keithley, USA). The polarization data for maximum power density

determination was obtained by changing the resistors over different time intervals as described by Shewa et al. (2014). When the resistors were changed over a single cycle, sufficient time was allowed to achieve steady-state conditions (Logan, 2012). The coulombic and energy efficiencies were calculated using the procedure reported by Shewa et al. (2014). Tukey's test was performed to compare and statistically evaluate the means. A principal component analysis (PCA) was used for data analysis and interpretation (Appendix E2). The PCA was performed using PAST version 2.17b, a Paleontological statistics software package for education and data analysis (Hammer et al., 2001).

4.3 Results and discussion

4.3.1 Electricity generation efficiency

The main advantage of an MFC is that it can generate combustion-less, pollution-free bioelectricity directly from the organic matter (Rittmann, 2008). Power density curves and polarization curves obtained by varying the external circuit resistances from 1.5 to 1,000,000 ohms (single-cycle method) showed that the carbon brush electrodes produced more power compared to the other four electrodes. The LSV polarization data (at a scan rate of 0.1 mV/s) in this study is in agreement with single- and multiple-cycle polarization curves as reported in studies conducted by Velasquez-Orta et al. (2009).

To estimate the power per unit surface to putative power output per unit reactor volume, one can consider that 100-500 m^2 of anode surface can be installed per m^3 anodic reactor volume (Rabaey et al., 2005). Hence, according to Rabaey et al. (2005), the state of the art power supply ranges from approximately 1 to 1800 W per m^3 anode

reactor volume installed. To be consistent, in this study electricity generated from each MFC was compared and reported per unit reactor volume and per m^2 of air-cathode surface area.

Maximum power densities of 510±55 and 100±15 mW m^{-2}, were observed in experiments conducted with graphite fiber brush and felt anodes, respectively (Figure 4.5). The power densitiy obtained from SCMFCs configured with graphite fiber brush anode was approximately 5-fold larger than the values observed with graphite felt anodes and also larger than the power densities for SCMFCs operating with graphite plate electrodes (Table 4.3). This indicates that the higher surface area brush electrodes were likely more favorable for biofilm formation compared to the other electrodes.
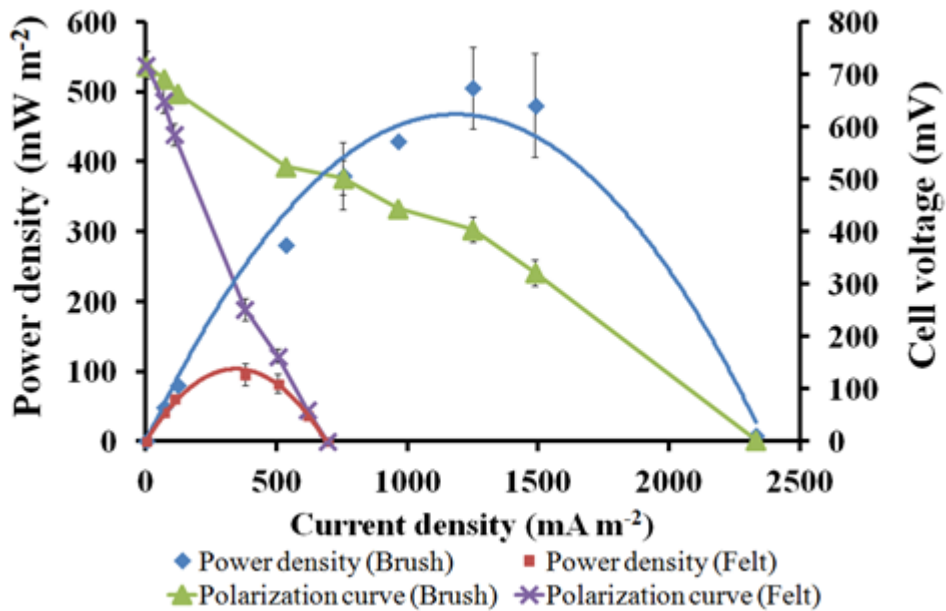
Figure 4.5 Polarization and power density curves as a function of current density for SCMFCs configured with brush and felt anodes.

Table 4.3 Power (P) and current (I) densities of SCMFCs provided with different types of anodes.

Type of electrode*	Normalized to working volume		Normalized to Cathode surface area		Internal resistance
	I (mA m^{-3})	P (mW m^{-3})	I (mA m^{-2})	P (mW m^{-2})	R_{in} (ohms)
POCO3	8145	2680	1080	355	310
HK06	770	280	100	40	3670
G347	3930	1480	520	195	735
Graphite fiber Brush	12040	4040	1500	510	230
Graphite felt	2990	900	330	100	770

*Note: POCO3, HK06 and G347 are graphite plate electrodes (Shewa et al., 2014)

4.3.2 Selection of best performing electrode

In addition to electricity generation, MFCs are able to remove COD from wastewaters. The COD removal efficiency of the SCMFCs configured with the five different anodes used in this study were evaluated and the results are presented in Figure 4.6. A comparison of the mean COD removal efficiencies show that POCO3 has the highest COD removal efficiency and the trend for increasing COD removal efficiency is as follows: POCO3 > G347 > Brush > Felt > HK06. The COD removal efficiency trend is not in agreement with the electricity generation data reported in section 3.3. In addition, the Tukey's test indicates that the COD removal efficiencies of POCO3, G347, brush and felt are statistically the same except that felt and HKO6 are statistically different. Therefore, selecting the best performing becomes difficult based on both the electricity generation values and COD removal efficiencies. Similar studies conducted by Larrosa-Guerrero et al. (2010) reported the same observation on COD removal efficiency. Larrosa-Guerrero et al. (2010) compared six anode materials for a MFC system and

observed the COD removal efficiency of biofilms formed on the different anode materials under closed circuit was statistically the same.
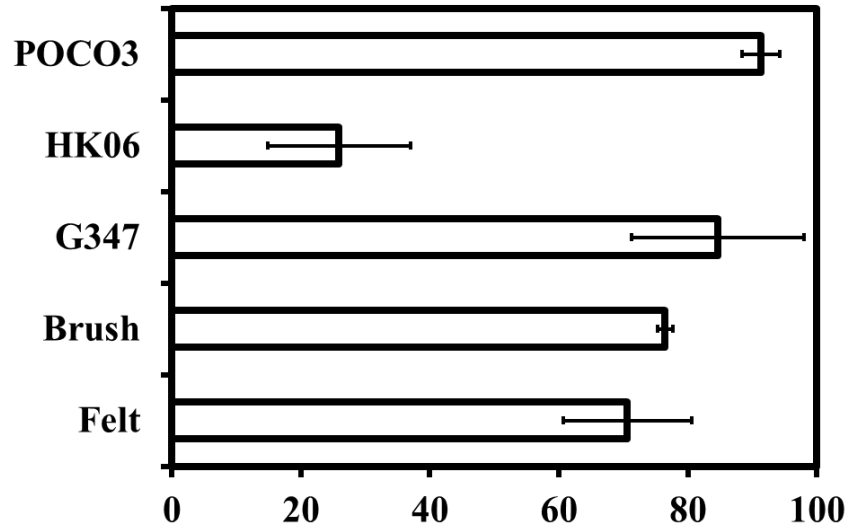
Figure 4.6 COD removal efficiencies of SCMFCs provided with different electrodes.

Selecting the five anode materials for the SCMFC was performed using the power density and the other MFC performance evaluation parameters which include coulombic efficiency and energy efficiency. The results obtained from the performance evaluation of the SCMFCs are presented in Table 4.4.

Table 4.4 Efficiency of SCMFCs configured with different electrodes.

Type of Electrode	Columbic efficiency (%)	Energy efficiency (%)	COD removal (%)
POCO3	10.95±3.10	2.10±0.60	91.30±2.90
HK06	2.55±0.20	0.10±0.00	25.95±11.00
G347	11.80±1.45	1.70±0.20	84.65±13.30
Brush	25.75±3.25	8.03±1.00	76.45±1.15
Felt	14.00±2.00	2.05±0.30	70.60±10.00

It is apparent from Tables 4.3 and 4.4 that among the five anodes used in this study, the graphite fiber brush electrode is the best performing anode material based on electrical power generation. A possible explanation for this might be that carbon brush fiber has a larger surface area available for microbial growth and electron transfer compared to the other electrodes (Drapcho et al., 2008). A study conducted by Logan et al. (2007) has also shown that brush anodes with high surface areas and a porous structure can produce high power densities, and therefore have qualities that make them ideal for scaling up MFC systems.

Further analysis conducted with PCA (Figure 4.7) indicated that there is significant difference in the overall performance of the electrodes. The PCA generated four principle components. The first principal component (PC1) explained 78.01 % of the variance; PC2 explained 17.74%, PC3 accounted for 4.14% and the PC4 accounted for 0.11%. Therefore, the first and second principal components explained 96% of the total variance between the samples. The PCA bi-plots (Figure 4.7) indicate that the energy efficiency, coulombic efficiency and power density are positively correlated or provide the same information.
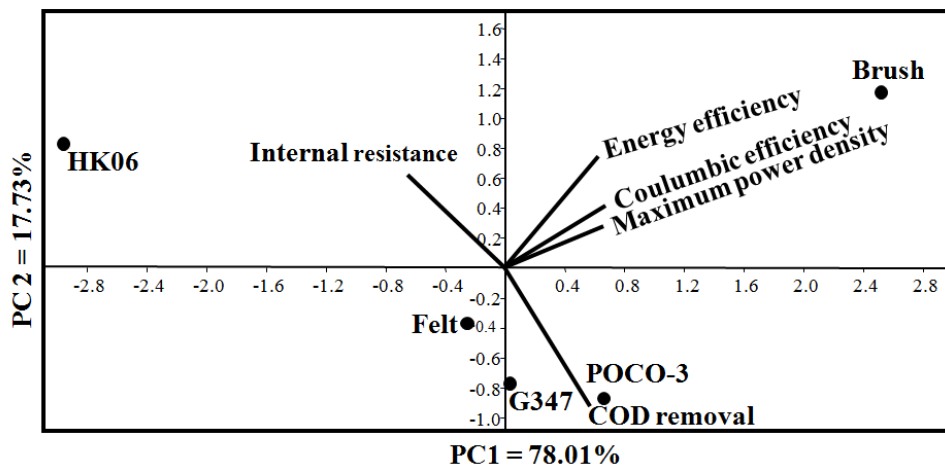
Figure 4.7 Principal component analysis of anode electrodes performance and efficiencies.

4.4 Conclusions

Different anode materials used in MFCs were evaluated under identical operating conditions. Based on the results of this study, the graphite carbon brush electrode was the preferred option. The highest energy generation was observed for the SCMFCs provided with graphite fiber brush anode. The trend for increasing electricity generation was as follows: Brush > POCO3 > G347 > Felt > HK06. The SCMFCs provided with the best performing anode (graphite fiber brush) generated maximum current and power densities of 12040 ± 3030 mA m^{-3} and 4040 ± 610 mW m^{-3}, respectively. The corresponding maximum current and power densities normalized to the cathode area were 1500 ± 215 mA m^{-2} and 510 ± 55 mW m^{-2}, respectively.

4.5 References

Drapcho, C.M., Nhuan, N.P., and Walker, T.H. (2008) Biofuels engineering process technology. New York, NY: McGraw-Hill, pp. 303–328.

Du, Z., Li, H., and Gu, T. (2007) A state of the art review on microbial fuel cells: A promising technology for wastewater treatment and bioenergy. *Biotechnol. Adv.* **25**(5): 464–482.

Franks, A. and Nevin, K. (2010) Microbial fuel cells, a current review. *Energies* **3**(5): 899–919.

Hamelers, B., Sleutels, T.H., Jeremiasse, A., Post, J.W., Strik, D.P., and Rozendal, R.A. (2010) Technological factors affecting BES performance and bottlenecks towards scale up. In *Bioelectrochemical systems: from extracellular electron transfer to biotechnological application*. Reaby K., Angenet L., Schroder U., and Keller J. eds. London: IWA Publishing, pp. 205–223.

Hammer, Ø., Harper, D.A.T., and Ryan, P.D. (2001) Paleontological statistics software package for education and data analysis. *Palaeontol. Electron.* **4**(1): 9–18.

Larrosa-Guerrero, A., Scott, K., Katuri, K.P., Godinez, C., Head, I.M., and Curtis, T. (2010) Open circuit versus closed circuit enrichment of anodic biofilms in MFC: Effect on performance and anodic communities. *Appl. Microbiol. Biotechnol.* **87**(5): 1699–1713.

Lefebvre, O., Uzabiaga, A., Chang, I.S., Kim, B.H., and Ng, H.Y. (2011) Microbial fuel cells for energy self-sufficient domestic wastewater treatment-a review and discussion from energetic consideration. *Appl. Microbiol. Biotechnol.* **89**(2): 259–270.

Liu, H., Cheng, S., and Logan, B.E. (2005) Power generation in fed-batch microbial fuel cells as a function of ionic strength, temperature, and reactor configuration. *Environ. Sci. Technol.* **39**(14): 5488–5493.

Logan, B.E. (2008) Microbial fuel cells. New York, NY: John Wiley and Sons.

Logan, B.E. (2012) Essential data and techniques for conducting microbial fuel cell and other types of bioelectrochemical system experiments. *ChemSusChem* **5**(6): 988–994.

Logan, B., Cheng, S., Watson, V., and Estadt, G. (2007) Graphite fiber brush anodes for increased power production in air-cathode microbial fuel cells. *Environ. Sci. Technol.* **41**(9): 3341–3346.

Logan, B.E., Wallack, M.J., Kim, K.-Y., He, W., Feng, Y., and Saikaly, P.E. (2015) Assessment of microbial fuel cell configurations and power densities. *Environ. Sci. Technol. Lett.* **2**(8): 206–214.

Mohan, S.V., Srikanth, S., Velvizhi, G., and Babu, M.L. (2013) Microbial fuel cells for sustainable bioenergy generation: Principles and perspective applications. In *Biofuel Technologies*: *Recent Developments*. Gupta, V.K., and Tuohy, M.G. eds. Berlin-Heidelberg: Springer, pp. 335–368.

Noll, K. (2006) Microbial fuel cells. In *Fuel cell technology: Reaching towards commercialization*. Sammes, N. ed. London: Springer, pp. 277–296.

Pant, D., Singh, A., Van Bogaert, G., Irving Olsen, S., Singh Nigam, P., Diels, L., and Vanbroekhoven, K. (2012) Bioelectrochemical systems (BES) for sustainable energy production and product recovery from organic wastes and industrial wastewaters. *RSC Adv.* **2**(4): 1248-1263.

Rabaey, K., Lissens, G., and Verstraete, W. (2005) Microbial fuel cells: performances and perspectives. In *Biofuels for fuel cells: Renewable energy from biomass fermentation*. Lens, P., Westermann, P., Haberbauer, M., and Moreno, A. eds. IWA Publishing, London, pp. 377–399.

Ren, Z.J. (2013) The Principle and Applications of Bioelectrochemical Systems. In *Biofuel Technologies*: *Recent Developments*. Gupta, V.K., and Tuohy, M.G. eds. Berlin-Heidelberg: Springer, pp. 501–527.

Rittmann, B.E. (2008) Opportunities for renewable bioenergy using microorganisms. *Biotechnol. Bioeng.* **100**(2): 203–212.

Shewa, W.A., Chaganti, S.R., and Lalman, J.A. (2014) Electricity generation and biofilm formation in microbial fuel cells using plate anodes constructed from various grades of graphite. *J. Green Eng*. **4**(1): 13–32.

Velasquez-Orta, S.B., Curtis, T.P., and Logan, B.E. (2009) Energy from algae using microbial fuel cells. *Biotechnol. Bioeng.* **103**(6): 1068–1076.

Watanabe, K. (2008) Recent developments in microbial fuel cell technologies for sustainable bioenergy. *J. Biosci. Bioeng.* **106**(6): 528–536.

CHAPTER 5

PRODUCING ELECTRICITY USING A MICROBIAL FUEL CELL FED FEEDSTOCK CHEMICALS PRODUCED FROM THE PHOTOCATALYSIS OF A LIGNIN MODEL CHEMICAL

5.1 Introduction

Lignin (from the Latin word *lignum*, wood) is a highly branched polymer of phenylpropanoid compounds in plant cell walls. After cellulose, lignin is the second most abundant organic compound in plants, representing approximately 30% of the organic carbon in the biosphere (Boerjan et al., 2003). According to Tonucci et al. (2012), using lignin as a feedstock is becoming more attractive for the following reasons: 1) Production is not dependent on the supply and cost of fossil fuel supplies; 2) An Increase lignin use will lead to increase pulp production; and 3) The feedstock is readily available in large quantities.

Approximately 30 million tonnes of lignin is produced anually from wood pulping (Hatakeyama and Hatakeyama , 2010). This complex cross-linked polymeric structure of phenolic monomers is impermeable and resistant to enzymatic cleavage (Yoo et al, 2013). The recalcirant chemical structure and stability of lignin makes biological degradation difficult. Therefore, the treatment of wastewaters from paper and pulp industries and other facilities that generate lignin-rich effluents is a potential challenge.

Metal oxides such as TiO_2, ZnO, ZrO_2, CeO_2 and metal sulfides such as CdS and ZnS have been used to photodegrade various pollutants (Gogate and Pandit, 2004). Titanium dioxide (TiO_2) is preferentially used because of its ability to completely

degrade a wide array of organic compounds to CO_2 plus H_2O (Bhatkhande et al., 2002; Gogate and Pandit, 2004; Dalrymple et al., 2007). In addition to simple carbon chemicals, TiO_2 has been used to completely degrade lignin in the presence of ultraviolet light (Tanaka et al., 1999; Machado et al. 2000).   Other reasons for selecting TiO_2 are related to stability under various conditions, easy of availability and a relatively low cost (Vogelpohl and Kim, 2004; Ahmed et al., 2011). Titanium dioxide exists primarily as anatase, rutile and brookite. Anatase was selected because it is catalytically more active in comparison to the rutile and brookite phases (Bouzouba et al., 2005; Hengerer et al., 2000).

The heterogenous photocatalysis reaction shown as Equation 5.1 can be divided into several steps according to Chong et al. (2010). In the first step, organic contaminant(s) are transferred from the liquid phase and onto the TiO_2 surface. The next step involves adsorption of organic contaminant(s) onto the photon activated TiO_2 surface (i.e. surface activation by photon energy occurs simultaneously in this step). After adsorption, the adsorbed contaminant(s) undergo photocatalysis on the TiO_2 surface. Next, the intermediate(s) from the TiO_2 surface desorb and finally, the intermediate(s) are transferred from the interface region and into the bulk liquid.

$$Organic\ Chemcials \xrightarrow{TiO_2/h\nu} Intermediate(s) \rightarrow\rightarrow\rightarrow CO_2 + H_2O \qquad (5.1)$$

Controlling the photocatalytic process to produce biodegradable intermediates from complex carbon chemicals has been reported using model lignin compounds such as syringol and guaiacol (Lalman and Ray, 2011).   Ray and Lalman (2011) reported controlling TiO_2 photocatalytic conditions to produce short chain carbon compounds can be utilized to produce energy by anaerobic digestion or microbial fuel cells (MFCs).

Microbial fuel cells (MFCs) are a recently developed microbial electrochemical technology (Logan and Rabaey, 2012) that convert reduced carbon containing chemicals to electricity. According to Rabaey and Verstraete (2005), the advantages of using MFCs include the following: 1) A high conversion efficiency is achieved by the conversion of substrate energy to electricity, 2) Efficient operation at ambient and at low temperatures distinguishes the technology from current bio-energy processes, 3) Gas treatment is not required because carbon dioxide is major off-gas, 4) Energy input is not required for aeration provided the cathode is passively aerated, and 5) The potential for application in areas lacking electricity infrastructure is enormous.

Using pure cultures in MFCs is impractical, primarily because of contamination from microorganisms in feedstocks.   An alternative approach is to use mixed cultures from municipal treatment facilitates, soil, and composting sources, because according to many reports, these sources contain significant levels of electrogenic bacteria (Watanabe, 2008; Jiang et al., 2010). Mixed culture systems have been shown to achieve higher power densities in comparison to pure cultures in many circumstances (Drapcho et al., 2008; He et al., 2005; Nevin et al., 2008). A recent study conducted by Fu et al. (2013) comparing pure culture and mixed culture inoculated MFCs reported that the pure culture exoelectrogens produced a current significantly lower than (less than 10%) mixed culture inoculated MFCs.

Employing MFCs to treat wastewaters has been reported by numerous researchers (Aelterman et al., 2006; Ahn and Logan, 2010; Cha et al., 2009; Kargi and Eker, 2007; Kalathil et al., 2012; Vidris et al., 2008). However, to date, no study has examined treating waste containing lignin using MFCs or a combined treatment process plus a

MFC.   The objectives of this study were to produce intermediate biodegradable chemicals from a model lignin compound using photolysis and to produce electricity from the intermediate chemicals using an MFC.

5.2. Materials and methods

The process schematic used in the study is shown in Figure 5.1. Photocatalysis of the lignin model compound was performed using TiO_2. Details of the photocatalysis process and electricity production process using an MFC are described in sections 2.4 and 2.5.
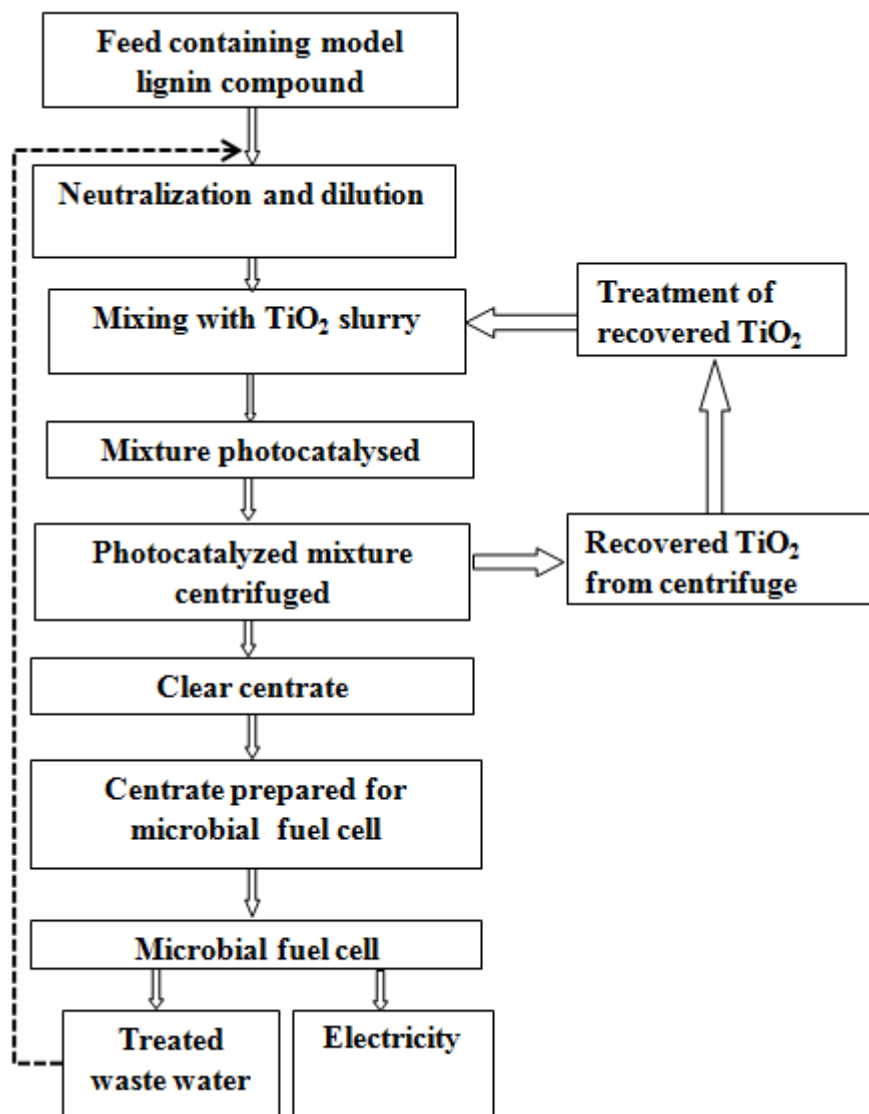
Figure 5.1 Experimental process flow chart.

5.2.1 MFC microbial culture source

The single chamber MFCs (SCMFCs) were inoculated with cultures from active and well-functioning two chamber MFCs. The two chamber MFCs were inoculated with mixed anaerobic cultures which were obtained from a municipal wastewater treatment facility (Chatham, ON).

5.2.2 Biological oxygen demand (BOD) test inocula

The seed for the BOD test was raw domestic wastewater obtained from the Lou Romano wastewater treatment plant (Windsor, ON).

5.2.3 Medium and chemicals

Two solutions, designated as A and B, were used to feed the MFCs. Solution A contained the following ingredients: 500 mg L^{-1} glucose, 310 mg L^{-1} NH_4Cl, 130 mg L^{-1} KCl, 4225 mg L^{-1} $NaH_2PO_4.H_2O$, 7400 mg L^{-1} $Na_2HPO_4.12H_2O$, 10 mg L^{-1} yeast extract and 1 mL L^{-1} of a mineral solution. Solution B contained effluent from the photo-chemical reactor (393 ± 2 mg COD L^{-1}) plus all the other constituents mentioned for solution A except glucose.

The nutrient solution was prepared in accordance with the procedure described by Wiegant and Lettinga (1985) and contained the following (Spectrum Chemicals, CA): (mg per L of distilled water): $NaHCO_3$, 6000; NH_4HCO_3, 70; KCl, 25; K_2HPO_4, 14; $(NH_4)_2SO_4$, 10; yeast extract, 10; $MgCl_2.4H_2O$, 9; $FeCl_2.4H_2O$, 2; resazurin, 1; EDTA, 1; $MnCl_2$ $4H_2O$, 0.5; $CoCl_2.6H_2O$, 0.15; Na_2SeO_3, 0.1; $(NH_4)_6MoO_7.4H_2O$, 0.09; $ZnCl_2$, 0.05; H_3BO_3, 0.05; $NiCl_2.6H_2O$, 0.05; and $CuCl_2.2H_2O$, 0.03. All the nutrient chemicals were 99% pure and procured from Sigma Aldrich (St. Louis, MO).

5.2.4 Photocatalysis

Photocatalysis was conducted using sodium lignosulfonate (LS) (99% purity) (Sigma-Aldrich, (St. Louis, MO). A stock suspension of TiO_2 nanoparticles (in aqueous) was prepared and stored at 21°C in sealed 20 ml vials. The stock solutions of TiO_2 were

sonicated in an ultrasonic bath (VWR, Mississauga, ON) for approximately 10-15 min to ensure homogeneous mixing prior to preparing the reaction solution.

Three different TiO_2 anatase nanoparticles sizes (5 nm, 10 nm and 32 nm) (Alfa Aesar, Ward Hill, MA) were used in this investigation and the size selected was based on optimum COD removal. Characteristics for the three different TiO_2 nanoparticles are shown in Table 5.1.

Table 5.1 TiO_2 catalyst surface area (Choquette-Labbé et al. (2014)).

Particle Size (nm)	Surface Area ($m^2\,g^{-1}$)
5[1]	275±15[2]
10[1]	131±12[2]
32[1]	47±2[2]

[1] Particle size as per manufacturer specifications (Alfa Aesar, Ward Hill, MA)
[2] Surface area ($m^2\,g^{-1}$) of the TiO_2 nanoparticles were determined using a Brunauer–Emmett–Teller (BET) gas adsorption technique in a Quantachrome NOVA 1200e surface area analyzer (Quantachrome Instruments, Boynton Beach, FL). The instrument temperature was set at 77 K and nitrogen (BOC, Windsor, ON) was the adsorbate.

Photocatalytic reactions were performed in a modified Rayonet RPR−100 UV photocatalytic chamber (Figure 5.2) (The Southern New England Ultraviolet Company, CT). Configuring this apparatus was previously described by Choquette-Labbé et al. (2014).
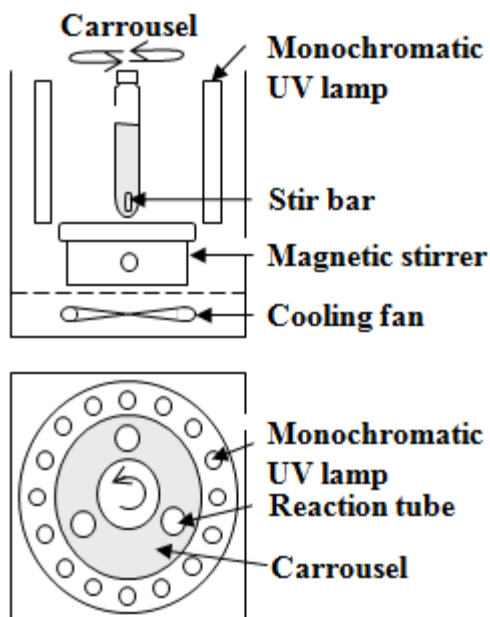
Figure 5.2 Schematic of the photo-reactor.

The photo-reactor was configured with 16 RPR-3000 photochemical UV lamps (Southern New England Ultraviolet Co., Branford, CT). The lamps are able to emit 300 nm UV light. The irradiance (9 mW cm^{-2}) was measured using a UVX Radiometer (UV Process Supply, Chicago, IL). The UV lamps were turned on 1 hr before initiating the experiment to obtain a stable light intensity. The reaction tubes were placed on the carrousel and rotated at a fixed rpm.

The reaction vessels (25 mm ID x 250 mm) were constructed from Pyrex® and fused quartz tubing (UV transmitting clear fused quartz (GE 214, Technical Glass Products Inc., Painesville Twp., OH)). The Pyrex® upper portion of the vessel was connected to the fused quartz bottom using a graded seal (Technical Glass Products, Inc., Painesville Twp., OH). The reaction tubes were wrapped in aluminium foil before placing them in the reaction chamber to prevent initiation of the reaction from extraneous light sources.

The total liquid volume was maintained at 50 mL and consisted of TiO_2 slurry plus LS. The solutions were prepared using Milli-Q® water and the mixtures were purged for 2 minutes with oxygen (BOC Gases Division ltd, Windsor, ON). After purging, the tubes were sealed immediately with Teflon® septa and an aluminium crimp cap.

Over the duration of the reaction, the reaction vessels were positioned into slots placed on a 10-rpm carrousel in the reaction chamber. All experiments were conducted in triplicate.

The effluent from the photo-chemical reactor was centrifuged (Marathon 3200R centrifuge, fisher-scientific, Blaine, MN) at 3000 rpm for 20 minutes to separate the TiO_2 particles from the aqueous solution. The clear centrate was removed and stored prior to feeding to the MFCs.

The chemical oxygen demand (COD) and biological oxygen demand (BOD) of liquid samples were determined in accordance with *Standard Methods* (APHA et al., 2005). The levels of CO_2, H_2 and CH_4 in the gas samples from the photocatalytic reactors and MFCs were determined using a Varian-3600 (Palo Alto, CA) gas chromatograph (GC) configured with a thermal conductivity detector (TCD). A 2 m long $\times$ 2 mm I.D. Carbon Shin column (Alltech, Deerfield, IL) was used to conduct the gas analysis. The GC injector, detector and oven temperatures were set at 100 ºC, 200 ºC, and 200 ºC, respectively. The carrier gas used was N_2 at a flow rate of 15 mL min^{-1}. The detection limits for CO_2, H_2 and CH_4 were 25 μL per 160 mL bottle, 10 μL per 160 mL bottle, and 25 μL per 160 mL bottle, respectively.

5.2.5 Microbial fuel cell

5.2.5.1 Microbial fuel cell set up

The microbial fuel cell (working volume 130 mL) and the air-cathode were constructed as previously described by Shewa et al. (2014). The anodes used were carbon brush electrodes (Mill-Rose Co., Mentor, OH). The carbon brush electrode (9 cm long and 9 cm in outer diameter) consisted of a Panex 35 carbon fiber fill (400,000 tips per inch) fixed to a Titanium stem wire which was 12.5 cm long and 0.135 cm in diameter. A schematic of the SCMFC is shown in Figure 5.3.
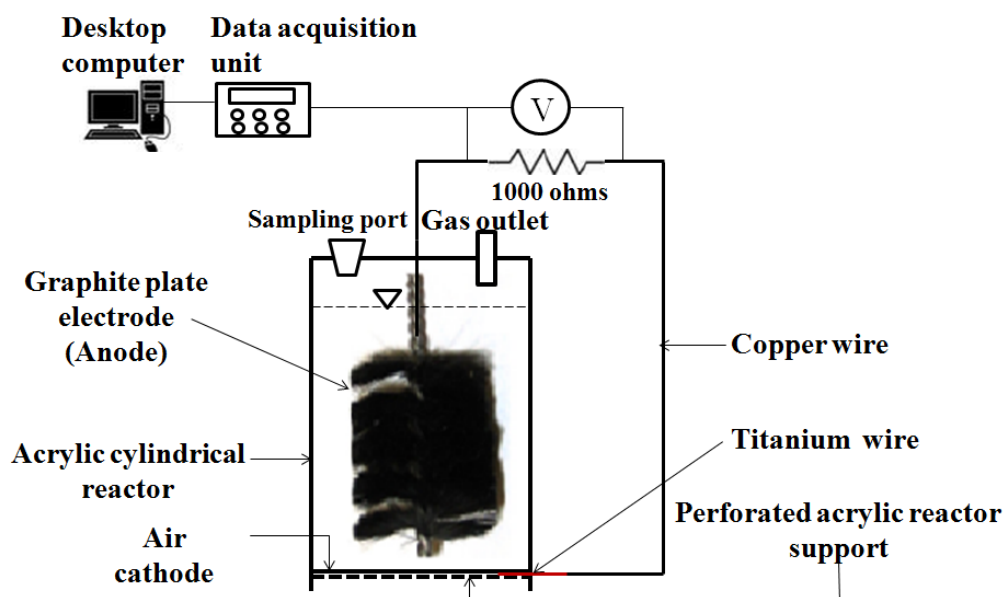
Figure 5.3 Schematic of the single-chamber microbial fuel cell.

The SCMFCs were operated in batch mode. The SCMFCs were fed repeatedly with fresh solution A or solution B until the voltage decreased to less than 20±5 mV. The time to decrease to below 20±5 mV was designated as one feeding cycle.

5.2.5.2 Data acquisition and analytical methods

Cell voltages (V) of each MFC were sampled every 5 min using an Agilent 34970A data acquisition unit connected to a PC. A full channel scan was performed for all MFCs and the data was stored for analysis. The potential of the anode and cathode electrodes were measured versus an Ag/AgCl reference electrode (Part no. CHI111; CH instruments Inc., Austin, TX) with the anode or the cathode as the working electrode. This was conducted by varying the circuit load (external resistance). The different external resistances used were 1,000,000, 10,000, 5,600, 1,000, 680, 470, 330, 220, 100, 47, 8.2 and 1.5 Ω, with each resistance connected to the circuit for 15 min. The potential (V) was used to calculate the current (I).

Cyclic voltammetry (CV) was performed using a computer-controlled potentiostat (CHI684; CH Instruments, Austin, TX) in a three electrode cell consisting of an anode as the working electrode with a counter platinum electrode and a Ag/AgCl reference electrode. The polarization and power density curves for SCMFCs were obtained using linear sweep voltammetry (LSV).

The coulombic efficiencies (C_E) for SCMFCs fed with solution A and solution B were calculated using Equations 5.2 and 5.3, respectively (Logan, 2008).

$$C_E = \frac{M_s \int_0^{t_b} I dt}{F b_{es} v_{An} \Delta c} \qquad (5.2)$$

M_s is the molecular weight of the substrate, t_b is time for one feeding cycle, F is Faraday's constant, b_{es} is number of moles of electrons per mole of substrate, v_{An} is the volume of liquid in the anode compartment and Δc is the substrate concentration change over a feeding cycle.

$$C_E = \frac{M \int_0^{t_b} I dt}{Fb\,v_{An}\,\Delta COD} \tag{5.3}$$

where *M* is the molecular weight of oxygen (32), *b* is the number of electrons exchanged per mole of oxygen (4) and *ΔCOD* is the change in the chemical oxygen demand (COD) over a feeding cycle.

5.3. Results and discussion

5.3.1 Photocatalytic degradation

5.3.1.1 Irradiation time

Preliminary studies using LS photocatalytic degradation byproducts were performed to assess the optimum irradiation time required for the photocatalytic degradation experiments. The irradiation time profile for the degradation of LS (500 mg L^{-1}) at different TiO_2 concentrations indicated an increase in CO_2 production and COD removal efficiency with an increase in the irradiation time. Longer irradiation time resulted in the conversion of LS and intermediate chemicals to CO_2 and H_2O. Long irradiation time resulted in higher energy consumption and higher retention time. With complete mineralization, the BOD available for electricity production was eliminated.

The intent of this study was to control LS degradation to produce biodegradable intermediates. The optimum illumination time to achieve maximum production of these intermediates was 4 hr. Therefore, unless otherwise stated, all subsequent photocatalytic degradation experiments were carried out with a 4-hr irradiation time.

5.3.1.2 Effect of particle size

In this study, a LS concentration of 500 mg L^{-1} (683 mg COD L^{-1}) was selected to assess the effects of various parameters affecting the photocatalytic process. Of the three TiO_2 particle sizes selected (Table 5.1), the greatest COD removal was observed for the 10 nm TiO_2 particle (Figure 5.4). Studies conducted by Almquist and Biswas (2002) indicated that, at an effective particle size less than 30 nm, the apparent photoactivity increases sharply with particle size and the apparent photoactivity decreases with increasing particle size greater than 30 nm. According to work reported by Choquette-Labbé et al. (2014), for the photocatalytic degradation of phenol and phenol derivatives using 5, 10 and 32 nm TiO_2, the predicted optimum particle size was 11 nm. Studies by Almquist and Biswas (2002) are also consistent with this study when comparing the effect of 5 nm and 10 nm TiO_2 particles on photooxidation reactions.
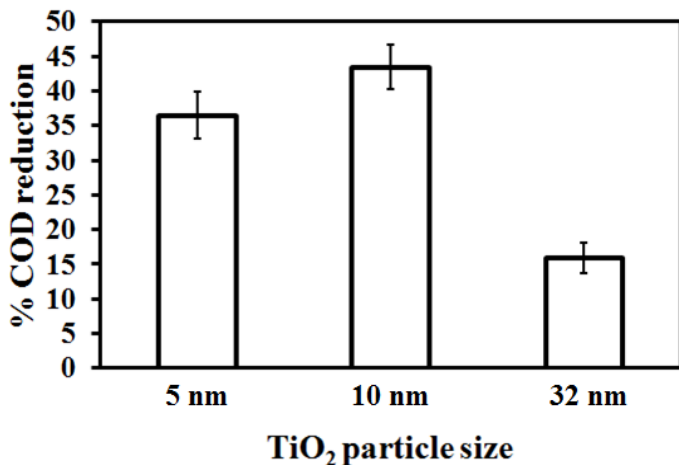
Figure 5.4 Effect of particle size on COD reduction.

5.3.1.3 Effect of catalyst concentration

Several studies have indicated different optimum catalyst loadings for different chemicals at varying concentration. The reasons for this variation in the optimum

catalyst concentration values from different studies could be due to variation in the reactant type and concentration, aeration, irradiation time, reactor size and geometry/design, irradiation wavelength and intensity of the light source and operating conditions of the photoreactor such as temperature, pH, rpm) (Chin et al., 2007; Ray, 2010; Mozia, 2010). The effect of catalyst loading on LS degradation was examined by varying the TiO_2 concentration from 0.5 g L^{-1} to 3.5 g L^{-1}. According to Ahmed et al. (2011a), operating at an optimum catalyst loading is required to ensure efficient photon absorption and to avoid using excess catalyst. The data shown in Figure 5.5 indicates the highest COD removal efficiency was observed at a catalyst concentration of 1 g L^{-1}. The COD removal efficiency increase with increasing catalyst concentration to 1 g L^{-1}; however, at greater levels, the removal efficiency remained constant. Hence, an optimum TiO_2 concentration of 1 g L^{-1} was selected to degrade LS at a 4-hr irradiation time and at 10 rpm. Note the CO_2 yield increased sharply as the TiO_2 concentration increased to 1g L^{-1} is similar to data observed for the COD removal efficiency (Figure 5.5 and Figure 5.6).
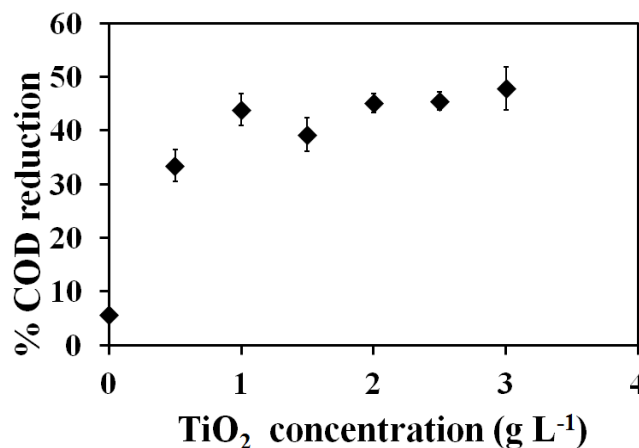
Figure 5.5 COD reduction of LS as a function of TiO_2 catalyst concentration.
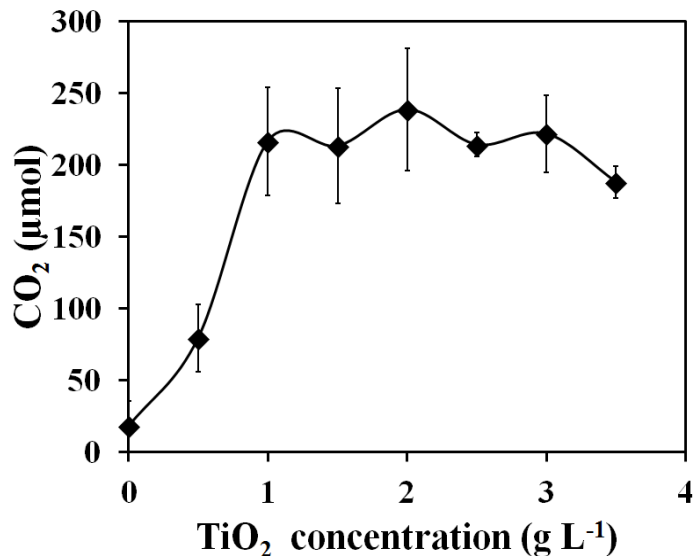
Figure 5.6 CO_2 yield as a function of TiO_2 catalyst concentration.

Beyond a threshold catalyst level, the constant COD removal is likely attributed to many factors. One factor is the formation of catalyst clusters at higher concentrations. According to Verma and Dixit (2012), cluster formation leads to less surface area and hence, less catalytic sites. Ahmed et al. (2011b) reported that increasing the catalyst loading beyond an optimum level results in non-uniform light intensity distribution and hence, lower reaction rates.

5.3.1.4 Effect of oxygen purging and rotation

The dissolved oxygen in the reaction mixture had a significant effect on the degradation process. Dijkstra et al. (2001) reported that oxygen addition directly into a reactor caused an appreciable increase in the photocatalytic degradation rate. During LS photo-degradation with and without purging with air, the % COD removed were 43.9±3.0 and 22.2±2.5, respectively (Figure 5.7). Similar studies by Pekakis et al. (2006) on the

photcatalytic degradation of textile wastewater with and without air sparging reported % COD reduction values of 40% and 23%, respectively.
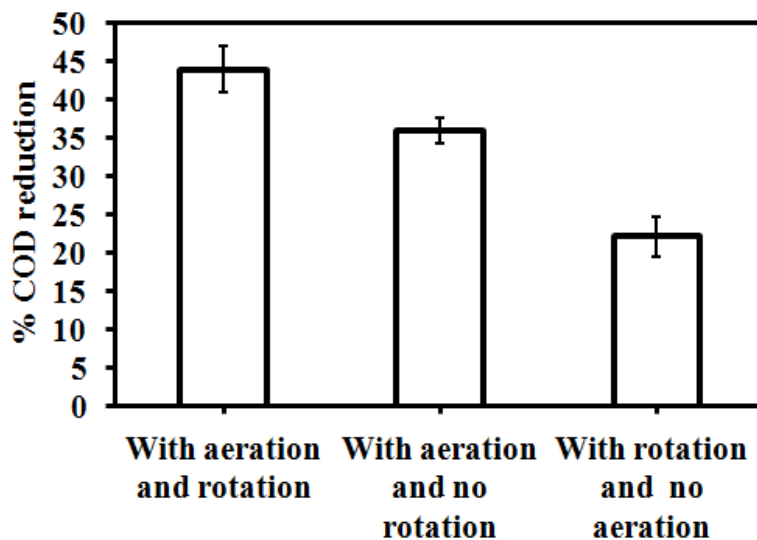
Figure 5.7 Effect of aeration on COD reduction.

The batch reactors in this study were rotated at 10 rpm to attain uniform illumination. Photocatalytic degradation was examined with and without rotation. The results indicate a final COD of 393 ± 2 mg L^{-1} and 448 ± 11 mg L^{-1} with and without rotation, respectively, at an initial pH of 8.0, an initial COD of 683 mg COD L^{-1}, 1.0 g L^{-1} TiO_2 and a 4-hr reaction time. Only a 7.9 % difference in COD removal efficiency (Figure 5.7) was observed as a result of operating the reactors with and without rotation.

5.3.1.5 Impact of photocatalytic degradation on biodegradability

The low BOD observed for LS before photocatalysis indicate it is recalcitrant to the inocula (Table 5.2). After photocatalysis, under conditions of 4-hr irradiation, an initial pH of 8.0, 10 rpm, a TiO_2 particle size and using 1 g L^{-1} 10 nm catalyst particles, the BOD_5 (Table 5.2) observed was attributed to the biodegradable organic compounds formed during the photocatalytic degradation of LS. A detailed chemical analysis of the

organic compounds formed during photocatalysis was not determined in this study. However, studies conducted by Tonucci et al. (2012) have indicated the formation of low molecular compounds such as methanol, formic acid, acetic acid, and small amounts of C-2 and C-3 alcohols after the photocatalytic oxidation of lignin. Lalman and Ray (2011) have also identified short chain fatty acids produced from the photocatalysis of a model lignin compound. Similar studies conducted by Velegraki et al. (2006) converted a bio resistant and toxic compound (acid orange 7) to more readily biodegradable byproducts using TiO_2-mediated photocatalysis.

Table 5.2 BOD, COD and gas production data.

Initial concentration (mg L^{-1})		Concentration after photocatalysis (mg L^{-1})		Gas production (mL g^{-1} COD)	
COD	BOD_5	COD	BOD_5	H_2	CH_4
685	0	395	150	0.45	121.00

Note 1: BOD_5 = 5-day BOD

The BOD_5 of pretreated LS (COD = 393±2 mg L^{-1}) was 150.6±9.0 mg L^{-1}. Using this data, the BOD_5/COD ratio is approximately 0.38.   Dark fermentation of the photocatalysis byproducts was conducted under batch conditions for 4 days at 37±1°C. The gas production yield from dark fermentation was 121 mL CH_4 per g COD_{added}. Note the theoretical amount of CH_4 produced from glucose is 350 mL CH_4 per g COD_{added}. Hu and Stuckey (2006) reported maximum methane production of approximately 83% from dilute wastewaters using a novel submerged anaerobic membrane bioreactor. In this study, with 4 hours of batch fermentation, approximately 50% of the theoretical quantity was attained.

5.3.1.6 Effluent pH

The initial pH of the reaction mixture and the final pH of the effluent from the photocatalytic reactor were compared (Figure 5.8). In all cases, the pH decreased and the decrease in pH was likely attributed to the formation of volatile fatty acids and CO_2 during LS photo-degradation. A maximum change in pH of approximately 2.1 was observed in reactors fed 1 g L^{-1} TiO_2 after 4 hour of irradiation.
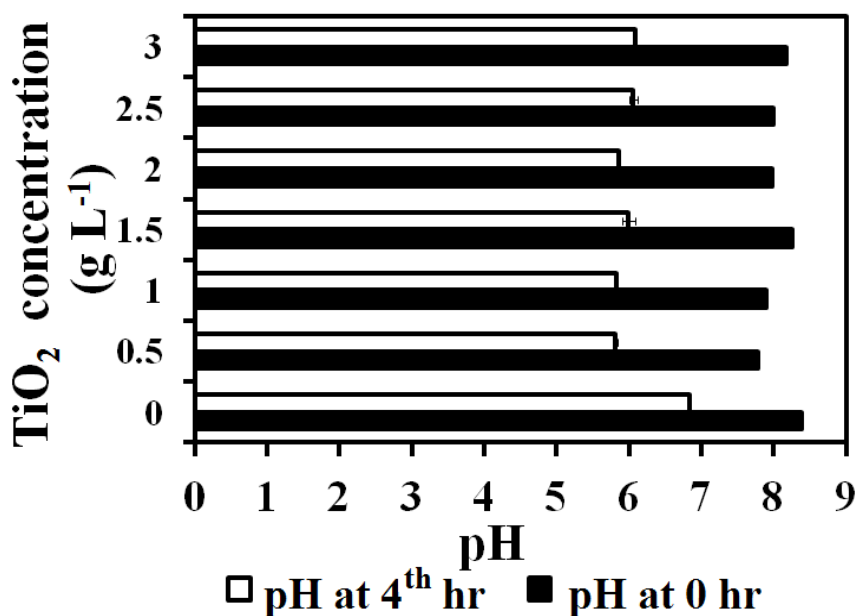
Figure 5.8 Initial and final pH conditions in photo-reactors operating at different TiO_2 loadings.

5.3.2 Microbial fuel cell performance

5.3.2.1 Characterization of the SCMFCs

Characterizing the SCMFCs was performed using solution A, the glucose containing feedstock. The SCMFCs were initially operated at $21\pm1°C$ for 7 cycles (Figure 5.9 a) and then at $37\pm1°C$ for 4 cycles (Figure 5.9 b). Work by Ahan and Logan (2010) indicated that temperature is an important factor affecting treatment efficiency and power

generation and the performance of MFCs was higher under high temperature conditions when compared to lower temperature conditions.
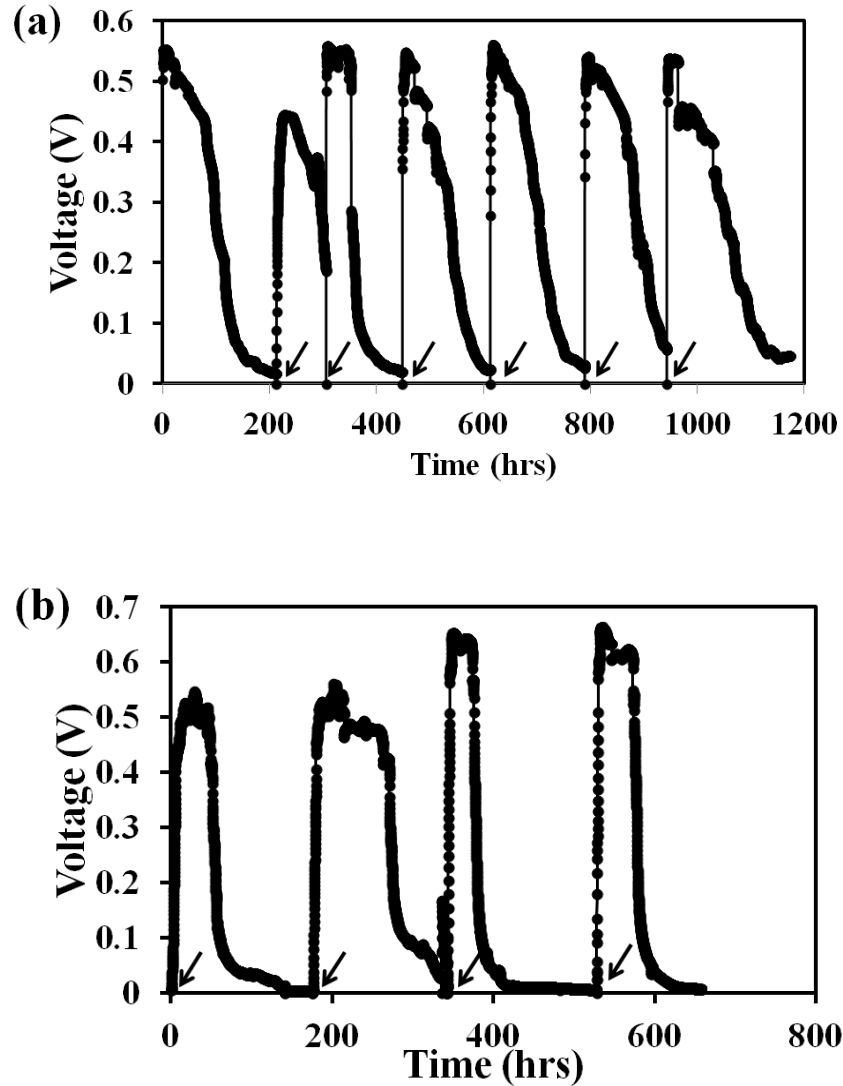
Figure 5.9 Voltage generation from glucose (500 mg L^{-1}) in SCMFC at (a) 21°C and (b) 37°C. Arrows indicate addition of fresh solution.

The SCMFCs produced repeatable and stable voltages in all the feeding cycles at 21±1°C and 37±1°C. The maximum voltage obtained at 21°C was 535±40 mV. In comparison, the maximum voltage for the SCMFCs operating at 37°C reached 660±10 mV. This voltage increase could be due to increase in the population and acclimatization

of electrogenic microbes to the mesophilic temperature condition (Jiang et al., 2010). A voltage increase of approximately 23% was observed when comparing data for $21\pm1\,^{\circ}C$ and $37\pm1\,^{\circ}C$.

The maximum current and power densities were determined using linear sweep voltammetry (LSV) (Figure 5.10). The LSV study was conducted by varying the potential of the working electrode at a scan rate of 1 mV s^{-1}. The data show that at $21\pm1\,^{\circ}C$, maximum current and power densities were 1615 mA m^{-2} and 690 mW m^{-3}, respectively. At $37\pm1\,^{\circ}C$, the maximum current and power densities increased to 2265 mA m^{-2} and 850 mW m^{-3}, respectively (Table 5.3). The temperature increase from $21\pm1\,^{\circ}C$ to $37\pm1\,^{\circ}C$ resulted in a 40% and 23% increase in the current and power densities, respectively. In similar studies by Jiang et al. (2010), MFCs operating at 15°C and at 30°C verified that higher temperatures increased the bacterial activity, which in return enhanced the power output and reduced the internal resistance.
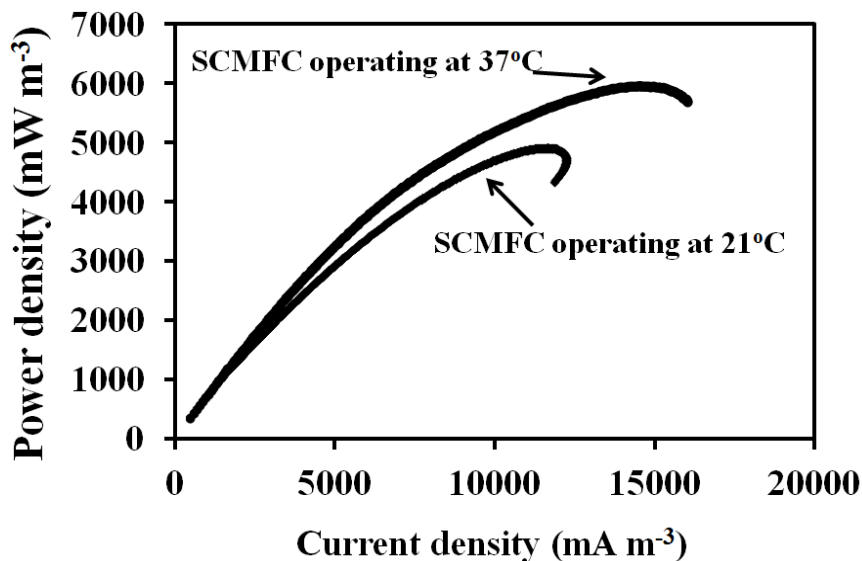
Figure 5.10 Polarization and power density curves at ambient and mesophilic temperatures in glucose (Solution A) fed SCMFCs.

Table 5.3 Maximum current and power density of SCMFCs operated at ambient and mesophilic temperatures for glucose (Solution A) fed SCMFCs.

Temp-erature (°C)	Current density		Power density		Internal resistance
	(mA m^{-3})	(mA m^{-2})	(mW m^{-3})	(mW m^{-2})	(ohms)
21±1	11320±865	1615±125	4845±370	690±55	270±20
37±1	15890±1940	2265±280	5970±10	850±1	175±40

Electrode potentials measurements at 21±1°C and 37±1°C were performed by varying the circuit load as described in section 2.5.2 (Figure 5.11). This data indicate that the oxidation-reduction potential of the SCMFCs increased when the operating temperature was increased from 21±1°C to 37±1°C.
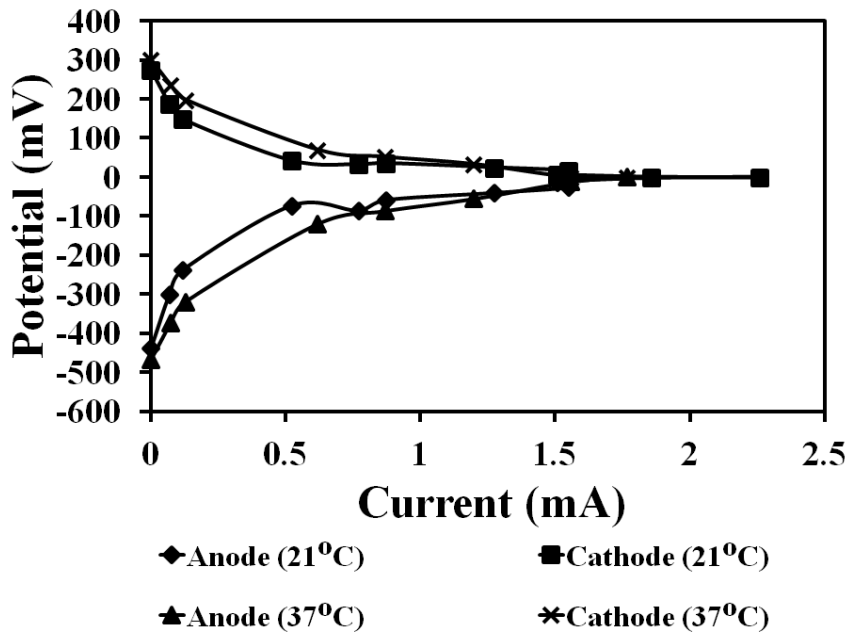
Figure 5.11 Oxidation-reduction potential of electrodes in glucose (Solution A) fed SCMFCs.

5.3.2.2 Electricity generation of SCMFCs fed a pretreated lignin model compound

The maximum voltage produced from the pretreated LS in one feeding cycle was 270±10 mV. A typical voltage generation pattern for one feeding cycle is shown in Figure 5.12. Notice the voltage increased to a maximum within 3 hours and gradually decreased to 20 mV after approximately 80 hr as the substrate was depleted. The rapid voltage increase is likely attributed to the presence of electrochemical active biofilms attached to the anode, rather than the microbes in the medium. Similar observations were reported by Fu et al. (2013) who performed experiments using MFCs inoculated with mixed cultures.
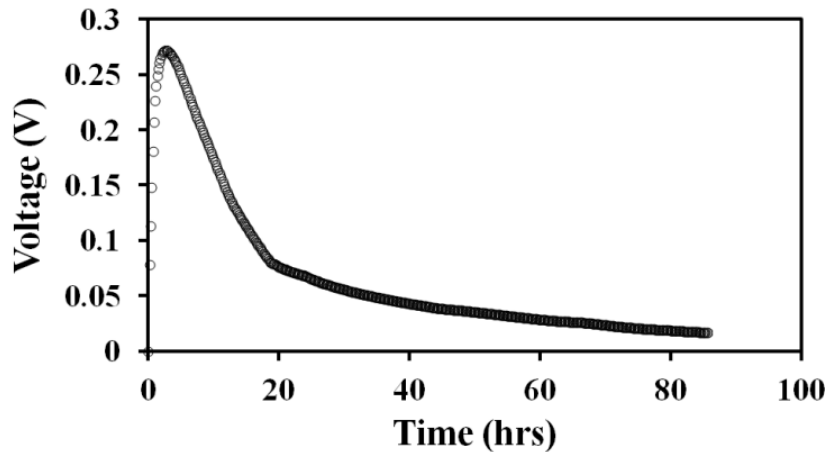
Figure 5.12 Voltage generation from pretreated lignosulfonate (Solution B) in SCMFCs at 21°C for one feeding cycle after attaining a stable voltage. Values are averages of triplicates.

The SCMFCs fed solution B generated maximum current and power densities of 3925±280 mA m^{-3} and 1165±210 mW m^{-3}, respectively (Figure 5.13). The corresponding maximum current and power densities normalized to cathode area are 560±40 mA m^{-2} and 165±30 mW m^{-2}, respectively (Figure 5.14).
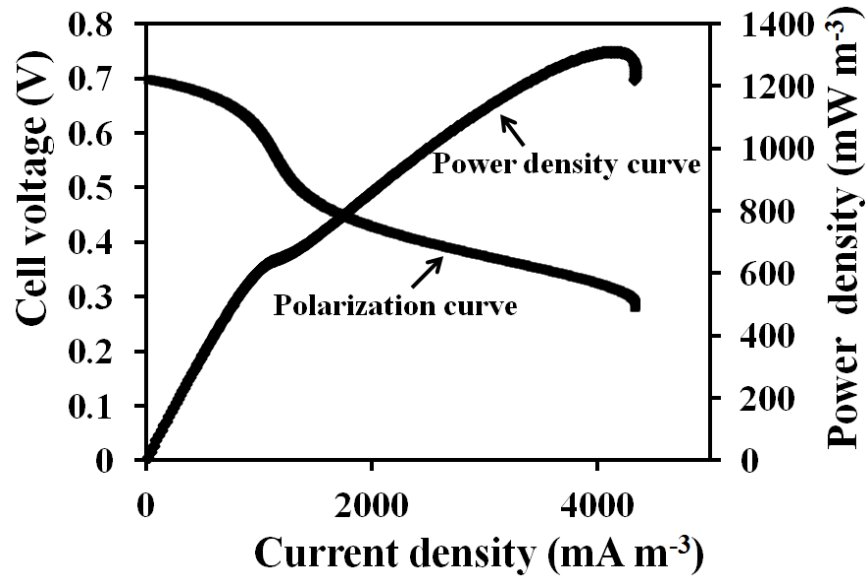
Figure 5.13 Typical power density and polarization curves (normalized to working volume) in pretreated lignin (Solution B) fed SCMFCs.
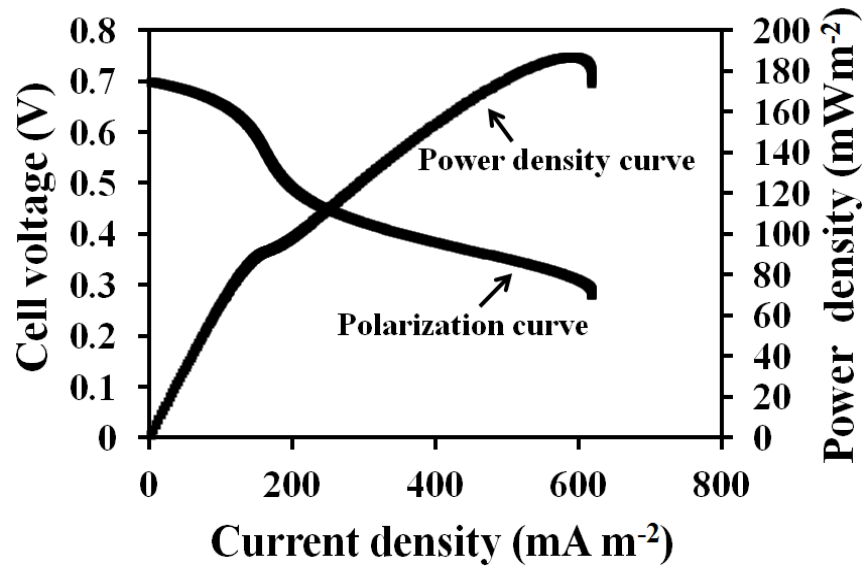
Figure 5.14 Typical power density and polarization curves (normalized to cathode surface area) for a pretreated lignin model compound (Solution B) fed SCMFCs operating at 21°C.

5.3.2.3 Microbial biofilm voltammetry

In this study, cyclic voltammetry (CV) was employed to acquire qualitative data related to electrochemical reactions and to locate redox potentials of the electroactive species of the SCMFCs. The potential scan from -0.5 V to $+0.5$ V was performed at a scan rate of 1 mV s^{-1}

According to Zhao et al. (2009), multiple peaks in the cyclic voltammograms of bioelectrochemical system are likely due to multi-step parallel or consecutive (series) mechanisms or to the presence of several different redox species. The multiple redox peaks (Figure 5.15) in the cyclic voltammograms in the SCMFCs fed with glucose (Solution A) indicate the presence of several redox species. Peaks observed for SCMFCs fed with pretreated LS (Solution B) indicate the presence of electrogenic bacteria attached to the brush electrode (Figure 5.15). The data suggest electrogenic microorganisms such as *Geobacter sulfurreducens*, *Shewanella oneidensis* MR-1, *Rhodoferax ferrireducens*, *Aeromonas hydrophila*, *Hansenula anomala* could be involved in the electron transfer process (Wang et al., 2008).
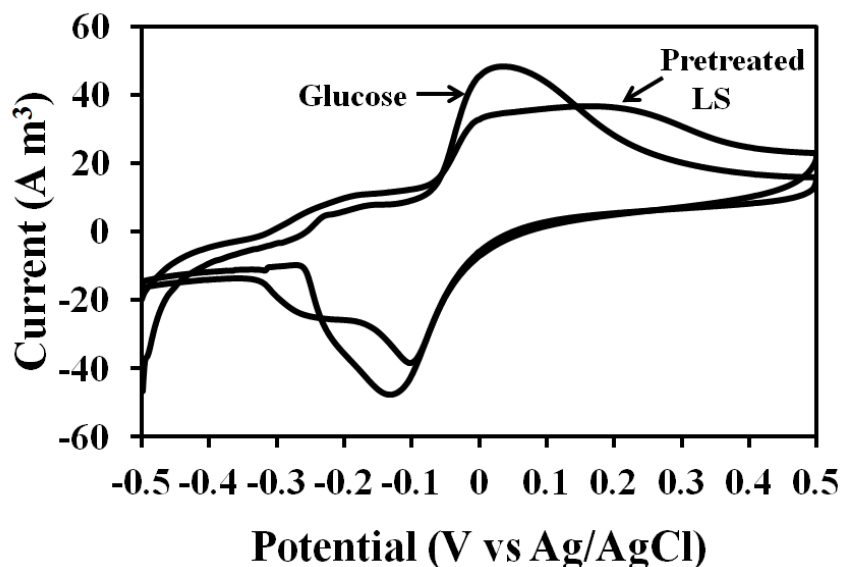
Figure 5.15 Cyclic voltammogram for MFCs operating at 21°C.

5.3.2.4 Treatment efficiency

The photocatalysis reaction converted LS into biologically degradable organic compounds and at the same time reduced the COD from 683 mg L^{-1} to 393 mg L^{-1} (43% COD removal efficiency). The SCMFC further reduced the COD from 393 mg L^{-1} to 94 mg L^{-1} (76% COD removal efficiency). The two processes were able to remove approximately 86% of the COD due to LS. The data indicate that integrating photocatalyis with an MFC could serve as a potential option for COD removal from lignin-rich wastewaters. Studies conducted by Liu et al. (2012) for single chamber MFCs fed a complex steroidal drug industrial effluent reported a COD removal efficiency of 84%.

5.3.2.5 Coulombic efficiency

Comparing C_{ES} reported in the literature is difficult because of differences in substrate type and concentration used and the MFC configurations. Reported C_E values

ranging from 14-20% for glucose and low values of up to 8% have been reported for wastewaters (Lee et al., 2008; Lu et al., 2009). The coulombic efficiency in this study at $21\pm1^{o}C$ was $4.7\pm0.4\%$. Park and Zeikus (2002) reported a low coulombic efficiency of 4% for *Shewanella putrefacians* culture fed lactate and a MFC configured with a Mn(IV)-graphite anode and an air-cathode. Jadhav and Ghangrekar (2009) investigated the performance of an MFC exposed to low operating temperature while treating a synthetic wastewater also found a C_E of 5%. Other similar studies carried out by Zhao et al. 2012 also reported a C_E of $2.8 \pm 0.5\%$ using cattle manure as a substrate.

The lower C_E value in this study is likely due to the consumption of substrate by non-electrogenic bacteria. The possible electron sinks in the SCMFCs could be attributed to biomass formation as well as the formation of soluble organic products, H_2 and CH_4 (Lee et al., 2008). Diffusion of oxygen into the SCMFC chamber may also result in aerobic degradation of the substrates leading to a decrease in C_E (Cheng et al. (2006). In current studies, the authors have observed that at $37\pm1^{o}C$, a coulombic efficiency of 17.2 ± 1.1 % was obtained using pretreated LS (COD = 393 ± 2 mg L^{-1}).

5.4 Conclusion

The pretreatment of LS using TiO_2 photocatalysis under illumination for 4 hrs revealed that the optimum TiO_2 size and loading were 10 nm and 1 g L^{-1}, respectively. The SCMFCs fed photocatalysed LS carbon byproducts and operating at $21^{o}C$ were able to produce maximum current and power densities of 3925 ± 280 mA m^{-3} and 1165 ± 208 mW m^{-3}, respectively. The corresponding maximum current and power densities normalized to cathode area were 560 ± 40 mA m^{-2} and 165 ± 30 mW m^{-2}, respectively.

Photocatalysis together with bioelectrochemical degradation removed 86% of the LS COD.

This investigation demonstrated that combining photocatalysis together with bioelectrochemical degradation can be useful for generating electricity from a model lignin chemical. The process and method suggested by this study could be useful to the pulp and paper and sugar cane milling industries as well as corn processors and other facilities generating waste containing lignin.

5.5 References

Aelterman, P., Rabaey, K., Clauwaert, P., and Verstraete, W. (2006) Microbial fuel cells for wastewater treatment. *Water Sci. Technol.* **54**(8): 9–15.

Ahmed, S., Rasul, M.G., Brown, R., and Hashib, M.A. (2011a) Influence of parameters on the heterogeneous photocatalytic degradation of pesticides and phenolic contaminants in wastewater: A short review. *J. Environ. Manage.* **92**(3): 311–330.

Ahmed, S., Rasul, M.G., Martens, W.N., Brown, R., and Hashib, M.A. (2011b) Advances in heterogeneous photocatalytic degradation of phenols and dyes in wastewater: A review. *Water Air Soil Pollut.* **215**(1-4): 3–29.

Ahn, Y., and Logan, B.E. (2010) Effectiveness of domestic wastewater treatment using microbial fuel cells at ambient and mesophilic temperatures. *Bioresour. Technol.* **101**(2): 469–475.

Almquist, C.B., and Biswas, P. (2002) Role of synthesis method and particle size of nanostructured TiO_2 on its photoactivity. *J. Catal.* **212**(2): 145–156.

APHA, AWWA, and WPCF. (2005) Standard methods for the examination of water and wastewater, 21st edn. Washington, D.C: American Public Health Association.

Bhatkhande, D.S., Pangarkar, V.G., and Beenackers, A.A. (2002) Photocatalytic degradation for environmental applications - a review. *J. Chem. Technol. Biotechnol.* **77**(1): 102–116.

Boerjan, W., Ralph, J., and Baucher, M. (2003) Lignin biosynthesis. *Annu. Rev. Plant Biol.* **54**(1): 519–546.

Bouzoubaa, A., Markovits, A., Calatayud, M., and Minot, C. (2005) Comparison of the reduction of metal oxide surfaces: TiO_2-anatase, TiO_2-rutile and SnO_2-rutile. *Surf. Sci.* **583**(1): 107–117.

Cha, J., Kim, C., Choi, S., Lee, G., Chen, G., and Lee, T. (2009) Evaluation of microbial fuel cell coupled with aeration chamber and bio-cathode for organic matter and nitrogen removal from synthetic domestic wastewater. *Water Sci. Technol.* **60**(6): 1409–1418.

Cheng, S., Liu, H., and Logan, B.E. (2006) Increased performance of single-chamber microbial fuel cells using an improved cathode structure. *Electrochem. Commun.* **8**(3): 489–494.

Chin, S.S., Lim, T.M., Chiang, K., and Fane, A.G. (2007) Factors affecting the performance of a low-pressure submerged membrane photocatalytic reactor. *Chem. Eng. J.* **130**(1): 53–63.

Chong, M.N., Jin, B., Chow, C.W.K., and Saint, C. (2010) Recent developments in photocatalytic water treatment technology: A review. *Water Res.* **44**(10): 2997–3027.

Choquette-Labbé, M., Shewa, W.A., Lalman, J.A., and Shanmugam, S.R. (2014) Photocatalytic degradation of phenol and phenol derivatives using a nano-TiO_2 catalyst: integrating quantitative and qualitative factors using response surface methodology. *Water* **6**(6), 1785–1806.

Dalrymple, O.K., Yeh, D.H., and Trotz, M.A. (2007) Removing pharmaceuticals and endocrine-disrupting compounds from wastewater by photocatalysis. *J. Chem. Technol. Biotechnol.* **82**(2): 121–134.

Dijkstra, M.F.J., Buwalda, H., De Jong, A.W.F., Michorius, A., Winkelman, J.G.M., and Beenackers, A.A.C.M. (2001) Experimental comparison of three reactor designs for photocatalytic water purification. *Chem. Eng. Sci.* **56**(2): 547–555.

Drapcho, C.M., Nhuan, N.P., and Walker, T.H. (2008) Biofuels engineering process technology. New York, NY: McGraw-Hill, pp. 303–328.

Fu, Q., Kobayashi, H., Kawaguchi, H., Vilcaez, J., Wakayama, T., Maeda, H., and Sato, K. (2013) Electrochemical and phylogenetic analyses of current-generating microorganisms in a thermophilic microbial fuel cell. *J. Biosci. Bioeng.* **115**(3): 268–271.

Gogate, P.R., and Pandit, A.B. (2004) A review of imperative technologies for wastewater treatment I: Oxidation technologies at ambient conditions. *Adv. Environ. Res.* **8**(3): 501–551.

Hatakeyama, H., and Hatakeyama, T. (2010) Lignin structure, properties, and applications. *Adv. Polym. Sci.* **232**(1): 1–63.

He, Z., Minteer, S.D., and Angenent, L.T. (2005) Electricity generation from artificial wastewater using an upflow microbial fuel cell. *Environ. Sci. Technol.* **39**(14): 5262–5267.

Hengerer, R., Bolliger, B., Erbudak, M., and Grätzel, M. (2000) Structure and stability of the anatase TiO_2 (101) and (001) surfaces. *Surf. Sci.* **460**(1): 162–169.

Hu, A.Y., and Stuckey, D.C. (2006) Treatment of dilute wastewaters using a novel submerged anaerobic membrane bioreactor. *J. Environ. Eng.* **132**(2): 190–198.

Jadhav, G.S., and Ghangrekar, M.M. (2009) Performance of microbial fuel cell subjected to variation in pH, temperature, external load and substrate concentration. *Bioresour. Technol.* **100**(2): 717–723.

Jiang, D., Li, B., Jia, W., and Lei, Y. (2010) Effect of inoculum types on bacterial adhesion and power production in microbial fuel cells. *Appl. Biochem. Biotechnol.* **160**(1): 182–196.

Kalathil, S., Lee, J., and Cho, M.H. (2012) Efficient decolorization of real dye wastewater and bioelectricity generation using a novel single chamber biocathode-microbial fuel cell. *Bioresour. Technol.* **119**: 22–27.

Kargi, F., and Eker, S. (2009) High power generation with simultaneous COD removal using a circulating column microbial fuel cell. *J. Chem. Technol. Biotechnol.* **84**(7): 961–965.

Lalman, J.A., and Ray, S. (2011) Patent application publication number: *US 2011/0084231 A1.* Washington, DC: U.S. Patent and Trademark Office.

Lee, H.S., Parameswaran, P., Kato-Marcus, A., Torres, C.I., and Rittmann, B.E. (2008) Evaluation of energy-conversion efficiencies in microbial fuel cells (MFCs) utilizing fermentable and non-fermentable substrates. *Water Res.* **42**(6): 1501–1510.

Liu, R., Gao, C., Zhao, Y.G., Wang, A., Lu, S., Wang, M. Maqbool, F., and Huang, Q. (2012). Biological treatment of steroidal drug industrial effluent and electricity generation in the microbial fuel cells. *Bioresour. Technol.*, **123**: 86-91.

Logan, B.E. (2008) Microbial fuel cells. New York, NY: John Wiley and Sons.

Logan, B.E., and Rabaey, K. (2012) Conversion of wastes into bioelectricity and chemicals by using microbial electrochemical technologies. *Science* **337**(6095): 686–690.

Lu, N., Zhou, S., Zhuang, L., Zhang, J., and Ni, J. (2009) Electricity generation from starch processing wastewater using microbial fuel cell technology. *Biochem. Eng. J.* **43**(3): 246–251.

Machado, A.E.H., Furuyama, A.M., Falone, S.Z., Ruggiero, R., Perez, D.D.S., and Castellan, A. (2000) Photocatalytic degradation of lignin and lignin models, using titanium dioxide: The role of the hydroxyl radical. *Chemosphere* **40**(1): 115–124.

Mozia, S. (2010) Photocatalytic membrane reactors (PMRs) in water and wastewater treatment. A review. *Sep. Purif. Technol.* **73**(2): 71-91.

Nevin, K.P., Richter, H., Covalla, S.F., Johnson, J.P., Woodard, T.L., Orloff, A.L., et al. (2008) Power output and columbic efficiencies from biofilms of *Geobacter sulfurreducens* comparable to mixed community microbial fuel cells. *Environ. Microbiol.* **10**(10): 2505–2514.

Park, D., and Zeikus, J. (2002) Impact of electrode composition on electricity generation in a single-compartment fuel cell using *Shewanella putrefaciens*. *Appl. Microbiol. Biotechnol.* **59**(1): 58–61.

Pekakis, P.A., Xekoukoulotakis, N.P., and Mantzavinos, D. (2006) Treatment of textile dyehouse wastewater by TiO_2 photocatalysis. *Water Res.* **40**(6): 1276–1286.

Rabaey, K., and Verstraete, W. (2005) Microbial fuel cells: novel biotechnology for energy generation. *Trends Biotechnol.* **23**(6): 291–298.

Ray, S. (2010) Developing an efficient nanocatalyst system for enhanced photocatalytic degradation of toxic aqueous contaminants. PhD Thesis. University of Windsor, Windsor, Ontario, Canada.

Shewa, W.A., Chaganti, S.R., and Lalman, J.A. (2014) Electricity generation and biofilm formation in microbial fuel cells using plate anodes constructed from various grades of graphite. *J. Green Eng*. **4**(1): 13–32.

Tanaka, K., Calanag, R.C.R., and Hisanaga, T. (1999) Photocatalyzed degradation of lignin on TiO$_2$. *J. Mol. Catal. A Chem.* **138**(2): 287–294.

Tonucci, L., Coccia, F., Bressan, M., and D'Alessandro, N. (2012) Mild photocatalysed and catalysed green oxidation of lignin: A useful pathway to low-molecular-weight derivatives. *Waste and Biomass Valorization* **3**(2): 165–174.

Velegraki, T., Poulios, I., Charalabaki, M., Kalogerakis, N., Samaras, P., and Mantzavinos, D. (2006) Photocatalytic and sonolytic oxidation of acid orange 7 in aqueous solution. *Appl. Catal. B Environ.* **62**(1): 159–168.

Verma, A., and Dixit, D. (2012) Photocatalytic degradability of insecticide Chlorpyrifos over UV irradiated titanium dioxide in aqueous phase. *Int. J. Environ. Sci.* **3**(2): 743–755.

Virdis, B., Rabaey, K., Yuan, Z., and Keller, J. (2008) Microbial fuel cells for simultaneous carbon and nitrogen removal. *Water Res.* **42**(12): 3013–3024.

Vogelpohl, A., and Kim, S.M. (2004) Advanced oxidation processes (AOPs) in wastewater treatment. *J. Ind. Eng. Chem. (Seoul, Repub. Korea),* **10**(1): 33–40.

Wang, X., Feng, Y., Ren, N., Wang, H., Lee, H., Li, N., and Zhao, Q. (2009) Accelerated start-up of two-chambered microbial fuel cells: Effect of anodic positive poised potential. *Electrochim. Acta* **54**(3): 1109–1114.

Watanabe, K. (2008) Recent developments in microbial fuel cell technologies for sustainable bioenergy. *J. Biosci. Bioeng.* **106**(6): 528–536.

Wiegant, W.M., and Lettinga, G. (1985). Thermophilic anaerobic digestion of sugars in upflow anaerobic sludge blanket reactors. *Biotechnol. Bioeng.* **27**(11): 1603–1607.

Yoo, C.G., Wang, C., Yu, C., and Kim, T.H. (2013) Enhancement of enzymatic hydrolysis and klason lignin removal of corn stover using photocatalyst-assisted ammonia pretreatment. *Appl. Biochem. Biotechnol.* **169**(5): 1648–1658.

Zhao, F., Slade, R.C.T., and Varcoe, J.R. (2009) Techniques for the study and development of microbial fuel cells: an electrochemical perspective. *Chem. Soc. Rev.* **38**(7): 1926–1939.

Zhao, G., Ma, F., Wei, L., Chua, H., Chang, C.C., and Zhang, X.J. (2012) Electricity generation from cattle dung using microbial fuel cell technology during anaerobic acidogenesis and the development of microbial populations. *Waste Manage.* **32**(9): 1651–1658.
.

CHAPTER 6

OPTIMIZING THE PHOTOCATALYTIC DEGRADATION OF A MODEL LIGNIN CHEMICAL USING THE BOX-BEHNKEN DESIGN AND CONVERTING THE DEGRADATION BYPRODUCTS INTO ELECTRICITY

6.1 Introduction

Converting complex organic chemicals in biomass and lower molecular weight monomeric components such as sugars and oils into sustainable chemicals and fuels is a rapidly evolving research area (Bruijnincx and Roman-Leshkov, 2014). Biomass is an alternative to fossil resources because it is the only source of carbon neutral compounds which can be utilized to produce fuels and chemicals (Climent et al., 2014). According to Alonso et al. (2010), starches, triglycerides and lignocellulosics are major classes of feedstocks derived from biomass which can be utilized for producing fuels and chemicals. Lignocellulosics, another class of feedstock, are abundant and a relatively inexpensive non-edible source that can be used instead of expensive starches (Climent et al., 2014). Utilizing lignocellulosic biomass is essential because converting starch-based feedstocks into biofuels and chemicals is the main cause of decreasing food supplies and elevated prices.

Lignin and cellulose are abundant; however, they are not easily converted into useful products using microbial technologies (Schwartz, 2007). Producing electricity directly from cellulose or lignin using bioelectrochemical systems is also a challenge. The lack of a single microbe to hydrolyze cellulose and degrade solid substrates has been resolved by Ren et al. (2007). Ren et al. (2007) reported electricity production from cellulose by

employing a binary culture of *C. cellulolyticum* and *G. sulfurreducens*. In similar studies, Hassan et al. (2014) also demonstrated electricity generation from rice straw (without pretreatment) in microbial fuel cells (MFCs) inoculated with a mixed culture containing cellulose-degrading bacteria. Although, non-woody substrates such as rice straw have been utilised in MFCs, no study has demonstrated electricity production from lignin, a complex biopolymer containing three monolignol monomers (p-coumaryl alcohol, coniferyl alcohol, and sinapyl alcohol) or lignin byproducts (Freudenberg and Nash, 1968).

Many researchers have assessed combining an advanced oxidation process (as pre-treatment or post-treatment) and biological systems to treat a diverse array of industrial effluents containing recalcitrant chemicals (Oller et al., 2011). Pokhrel and Viraraghavan (2004) suggested that combining physicochemical and biological treatment processes is a long-term solution for treating pulp and paper mill effluents containing lignin plus lignin byproducts. Duran et al (1994) reported using fungi to treat an industrial influent containing lignin compounds. They indicated the potential of using photochemical and biological methods to treat Kraft treatment effluent. Studies conducted by Pekakis et al. (2006) on textile effluents have shown photocatalytic oxidation was as an effective pre-treatment step prior to biological treatment. Similar studies conducted by Velegraki et al. (2006) also revealed that chemical oxidation was utilized as a pre-treatment step to convert bioresistant compounds into biodegradable byproducts.

Many researchers have reported the partial degradation of complex carbon structures in short chain chemicals by advanced oxidation processes (AOPs) (Wu and Zhou, 2001; De Morais and Zamora, 2005; Chamarro et al., 2011; Yurdakal and Augugliaro, 2012;

Shewa and Lalman, 2014). Converting a chemical such as lignosulfonate (LS), a model lignin compound, into simple short chain biodegradable carbon chemicals is feasible by controlling the photocatalytic reaction steps before ultimately producing CO_2. According to Shewa and Lalman (2014), single-chamber microbial fuel cells (SCMFCs) were used to produce electricity from a photocatalytic pretreated LS liquor.

The photocatalytic degradation of organic compounds is affected by parameters such as type of photocatalyst and composition, light intensity, initial substrate concentration, amount of catalyst, pH of the reaction medium, mixing, ionic components in aqueous solution, solvent type, oxidizing agents/electron acceptors, mode of catalyst application and catalyst calcination temperature (Ahmed et al., 2011b). Optimizing these factors is important to ensure the feasibility of employing a photocatalytic process as a pretreatment option. In work reported by Shewa and Lalman (2014), a one-factor-at-a-time approach was used to optimize the photocatalytic process. Although this conventional optimization approach is widely acceptable, the reported outcomes could be insignificant and have less predictive power if the condition for one operating parameter changes (Chong et al, 2010). Hence, many researchers prefer to use multi-variable design of experiments and statistical modelling tools to optimize processes such as photocatalytic degradation.

Several response surface methodologies (RSM) designs available for statistical modelling include Box-Behnken (BBD), central composite design (CCD), and the Doehlert matrix. A comparison between the BBD and other response surface designs (CCD, Doehlert matrix, and three-level full-factorial design) has demonstrated that the BBD and Doehlert matrix are slightly more efficient than the CCD but much more

efficient than the three-level full factorial designs (Ferreira et al., 2007). Myers et al. (2009) have also indicated that the BBD is an efficient option and an important alternative to the CCD method. Therefore, in this study, the BBD is used to model and optimize the photocatalytic degradation of LS.

The objectives of this study were to optimize the production of biodegradable chemicals derived from the photocatalytic treatment of a model lignin compound and to assess electricity production in MFCs fed the biodegradable chemicals.

6.2 Materials and Methods

6.2.1 Photocatalysis

6.2.1.1 Photoreactor system

Photocatalysis was conducted using sodium lignosulfonate (LS) (99% purity, Sigma-Aldrich; St. Louis, MO). TiO$_2$ anatase nanoparticles were procured from Alfa Aesar (Ward Hill, MA, USA). Characteristics of the TiO$_2$ nanoparticles were described in work reported by Choquette-Labbé et al. (2014).

A stock suspension of TiO$_2$ (10,000 mg L^{-1}) nanoparticles (in aqueous) was prepared and stored at 21°C in sealed 20 ml vials. TiO$_2$ stock solutions were sonicated in an ultrasonic bath (VWR, Mississauga, ON) for approximately 10 - 15 min to ensure homogeneous mixing prior to reaction solution preparation.

Photocatalytic reactions were performed in a modified Rayonet RPR–100 UV photocatalytic chamber (The Southern New England Ultraviolet Company, CT). Configuration of the apparatus and the procedures to execute the photocatalytic degradation experiment were reported by Shewa and Lalman (2014).

6.2.1.2 Experimental design and optimization study

TiO$_2$ particles (10 nm) and an irradiation time of 4 hr was used based on work reported by Shewa and Lalman (2014). The factors (independent variables) used in this study were the substrate concentration (X_1), TiO$_2$ concentration (X_2) and mixing (revolutions per minute (RPM)) (X_3). The optimum value of TiO$_2$ concentration = 1000 mg L^{-1} obtained in Chapter 5 using one-at-a-time experimental design method was used as center point for X_2. A LS concentration of 500 mg L^{-1} and RPM of 10 which were used to assess the effects of various parameters affecting the photocatalytic process in Chapter 5 were used as centre points of factors X_1 and X_3, respectively. The experimental design is shown in Table 6.1. The natural (uncoded) independent variables (X_1, X_2 and X_3) are coded according to Equation 6.1 (Yetilmezsoy et al., 2009). The total number of runs was selected based on the BBD (15 experiments with 3 center point runs).

$$x_i = \frac{(X_i - X_0)}{\Delta X_i} \tag{6.1}$$

where x_i is dimensionless coded value of the ith independent variable, X_i is the uncoded value of the ith independent variable, X_0 is the uncoded ith independent variable at the center point, and ΔX_i is the step change value.

Table 6.1 Experimental design parameters.

Factor	Model Term	Low (-1)	Middle (0)	High (1)	Step Change Values (ΔXi)
LS concentration (mg L^{-1})	X_1	250	500	750	250
TiO$_2$ concentration (mg L^{-1})	X_2	500	1000	1500	500
RPM	X_3	5	10	15	5

Note: 1 mg L^{-1} of LS = 1.4 mg COD L^{-1}.

The response surface model was developed using a statistical regression equation (Equation 6.2) (Yetilmezsoy et al., 2009).

$$Y = \beta_o + \sum_{i=1}^{k} \beta_i x_i + \sum_{i=1}^{k} \beta_{ii} x_i^2 + \sum_{i=1}^{k} . \sum_{j=1}^{k} \beta_{ij} x_i x_j + \varepsilon \qquad (6.2)$$

where Y is the process response or output (dependent variable), k is the number of the patterns, i and j are the index numbers for the pattern, β_0 is the free or offset term called the intercept term, $x_1, x_2,..., x_k$ are the coded independent variables, β_i is the first-order (linear) main effect, β_{ii} is the quadratic (squared) effect, β_{ij} is the interaction effect, and ε is the "error" in the system that include effects such as measurement error on the response, other sources of variation that are inherent in the process or system (background noise, or common cause variation in the language of statistical process control), and the effect of other variables (Myers and Montgomery, 2002).

MINITAB 16 (Minitab Inc., State College, PA), a statistical software program, was used to determine the second-order polynomial model and obtain the response surface. An analysis of variance (ANOVA) was performed to evaluate the model. The numerical optimization function in the Minitab software, based on the D-optimality index, was used to locate the maximum response within the factor space under evaluation (Chaganti et al., 2012a). Validation of the model was conducted using the Anderson–Darling statistic (ADS) (Stephens, 1974).

6.2.2 Microbial fuel cell configuration and operation

Single chamber MFCs (SCMFCs) were inoculated with cultures from two chamber MFCs which were previously used for other studies. The two chamber MFCs were inoculated with a mixed anaerobic culture which was obtained from a municipal

wastewater treatment facility (Chatham, ON). Configuration of the MFCs was reported by Shewa and Lalman (2014).

The medium added to the SCMFCs contained the following: glucose or PrLS, 310 mg L^{-1} NH_4Cl, 130 mg L^{-1} KCl, 4,225 mg L^{-1} $NaH_2PO_4.H_2O$, 7,400 mg L^{-1} $Na_2HPO_4.12H_2O$, 10 mg L^{-1} yeast extract and 1 mL L^{-1} of a mineral solution. The mineral solution was prepared in accordance with the procedure described by Wiegant and Lettinga (1985) and contained the following (Spectrum Chemicals, CA): (mg per L of distilled water): $MgCl_2$ $4H_2O$, 9; $FeCl_2.4H_2O$, 2; resazurin, 1; EDTA, 1; $MnCl_2.4H_2O$, 0.5; $CoCl_2.6H_2O$, 0.15; Na_2SeO_3, 0.1; $(NH_4)_6MoO_7.4H_2O$, 0.09; $ZnCl_2$, 0.05; H_3BO_3, 0.05; $NiCl_2.6H_2O$, 0.05; and $CuCl_2.2H_2O$, 0.03. All the SCMFCs were operated at $37\pm1^{\circ}C$ in a temperature-controlled chamber. Fresh SCMFC solution was added when the voltage decreased to below 20 mV.

6.2.3 Analytical procedures and calculations

Voltage, electrochemical analysis (cyclic voltammetry (CV)) and linear swipe voltammetry (LCV)) measurements were performed using procedures described by Shewa and Lalman (2014) and Shewa et al. (2014). Chemicals in the PrLS were identified using liquid chromatography-mass spectrometry (LC-MS). The LC-MS analysis was performed at McMaster University (Hamilton, Ontario) using a Quattro Ultima, a quadrupole-hexapole-quadrupole (QHQ) mass spectrometer, which was interfaced to a liquid chromatograph (LC). The LC (Waters 2695, Milford, MA) was configured to a photo-diode array (PDA) detector together with a ternary pump system, a column compartment with temperature control and an auto sampler. The PDA detection wavelength was set at 254 nm. Samples were eluted with acetic acid (3000 ppm):

methanol (65:35 v/v) at a flow rate of 0.2 ml min^{-1}. The samples were analyzed with a Zorbax Eclpse Plus C18, 100 X 3.0 mm X 3.5 micron column which was maintained at 50 ºC.

COD and BOD were determined in accordance with *Standard Methods for the Examination of Water and Wastewater* (APHA et al., 2005). Samples from SCMFCs for COD analysis were prepared by filtering through a 0.2 µm filter.

The coulombic efficiencies (C_E) for SCMFCs were determined using Equation 6.3 (Logan, 2008).

$$C_E = \frac{M\int_0^{t_b} I dt}{Fb v_{An} \Delta COD} \tag{6.3}$$

where M is the molecular weight of oxygen (32), t_b is time for one feeding cycle, I is the current, F is Faraday's constant, b is the number of electrons exchanged per mole of oxygen (4), v_{An} is the volume of liquid in the anode compartment and ΔCOD is the change in the chemical oxygen demand (COD) over a feeding cycle.

6.2.4 Microbial analysis

Biofilm samples were removed from the SCMFCs brush anode electrodes for microbial analysis. DNA was isolated from the microbial samples, according to Chaganti et al. (2012b). The DNA was quantified and the PCR amplified using universal bacterial and Archaeal PCR primers for the 16S rRNA gene targeting the V5-V6 region. The PCR was performed in two steps. In step 1, the targeted V5-V6 region was amplified and in step 2, barcodes were included to prepare the library for the next generation sequencing. The protocol for step 1 PCR was as follows: 95°C for 150 s followed by 27 cycles of

95°C for 30 s, 50°C for 30s and 72°C for 1 min and a final elongation at 72°C for 10 min. The protocol of step 2 PCR was as follows: 95°C for 150 s followed by 8 cycles of 95°C for 30 s, 60°C for 30s and 72°C for 1 min and a final elongation at 72°C for 5 min. Both the forward and reverse primers used in step 1 of the PCR method included a 12 bp tail at the 5' end which was bound by the corresponding primer ("UniA" and "UniB") used in step 2 of the PCR. Step 2 of the PCR includes the next generation sequencing adapters (UniA" and "UniB). The forward primer used in step 2 of the PCR included multiplex identifiers (10 to 12 bp) allowed assigning sequences to the original sample and 4 bp key. After step 2 of the PCR, the amplicons were visualized on a 1.5 % agarose gel and the targeted band was excised from the gel and purified using a Qiagen MinElute gel extraction kit (Qiagen Inc., Toronto, Ontario, Canada). Each purified DNA amplicon was pooled at equal concentrations for sequencing. Prior to sequencing, all the PCR amplicon types were assessed for fragment size distribution and DNA concentration using an Agilent 2100 Bioanalyzer with a high sensitive DNA chip (Agilent Technologies, Mississauga, Canada). The samples were adjusted to a final concentration of 26 pM and attached to the surface of Ion Sphere particles (ISPs) using an Ion PI™ Template OT2 200 Kit (Life Technologies, Canada) according to the manufacturer's instructions. Manual enrichment of the resulting ISPs resulted in $> 90\%$ templated-ISPs. The templated-ISPs which were sequenced on "314" micro-chips using the Ion Torrent Personal Genome Machine (PGM; Life Technologies, USA) 125 cycles (500 flows) resulted in an expected average read length of > 220 bp for the Ion Express Template 200 chemistry. After sequencing, the individual sequence reads were filtered within the PGM software to remove any low quality and polyclonal sequences. Sequences matching the

PGM 3′ adaptor were also automatically trimmed. All PGM quality filtered data were exported as FastQ files. The resulting sequencing data sets were uploaded to the Metagenome Rapid Annotation using Subsystem Technology (MG-RAST) server (http://metagenomics.nmpdr.org/), checked for low-quality reads prior to de-replication, annotation and assignment of phylogenetic identification as described by Meyer et al. (2008).

6.3 Results and discussion

6.3.1 Photocatalytic degradation

6.3.1.1 Effects of selected factors on response variable (BOD₅ to COD ratio)

The two dimensional contour plots and three dimensional surface plots, generated using Minitab, was used to assess effects of the LS concentration, TiO_2 concentration and RPM on the BOD_5/COD ratio. The contour plot provides a two-dimensional view where all points along the same line indicate a constant response. Similarly, the surface plot shows a three-dimensional view which provides an enhanced understanding of the response surface. The concentric contours (Figures 6.1 a-c) and the three-dimensional surface plots (Figures 6.2 a-c) indicate the presence of a maximum response point. The peak response was located at the mid-point of factor levels ($X_1 = 500$ mg L^{-1}, $X_2 = 1000$ mg L^{-1} and $X_3 = 10$). As the factor values move away from the mid-value of the factors, the response decreases.

Increasing the catalyst concentration is a route leading to increasing the number of photocatalytic active surface sites and hence, an increase in the number of •OH radicals. However, beyond a threshold catalyst level, the turbidity retarded the reaction progress

by preventing UV light from penetrating to initiate the degradation process (Rauf et al., 2011). In this study, a similar outcome was observed as the TiO_2 concentration increased to 1000 mg L^{-1}, the BOD_5/COD increased and then decreased as TiO_2 concentration was increased to 1500 mg L^{-1} (Figures 6.1 a-b). Rabindranathan et al. (2003) reported an increase and subsequent decease in the reponse variable with increasing TiO_2 levels for the photocatalytic degradation of phosphamidon.
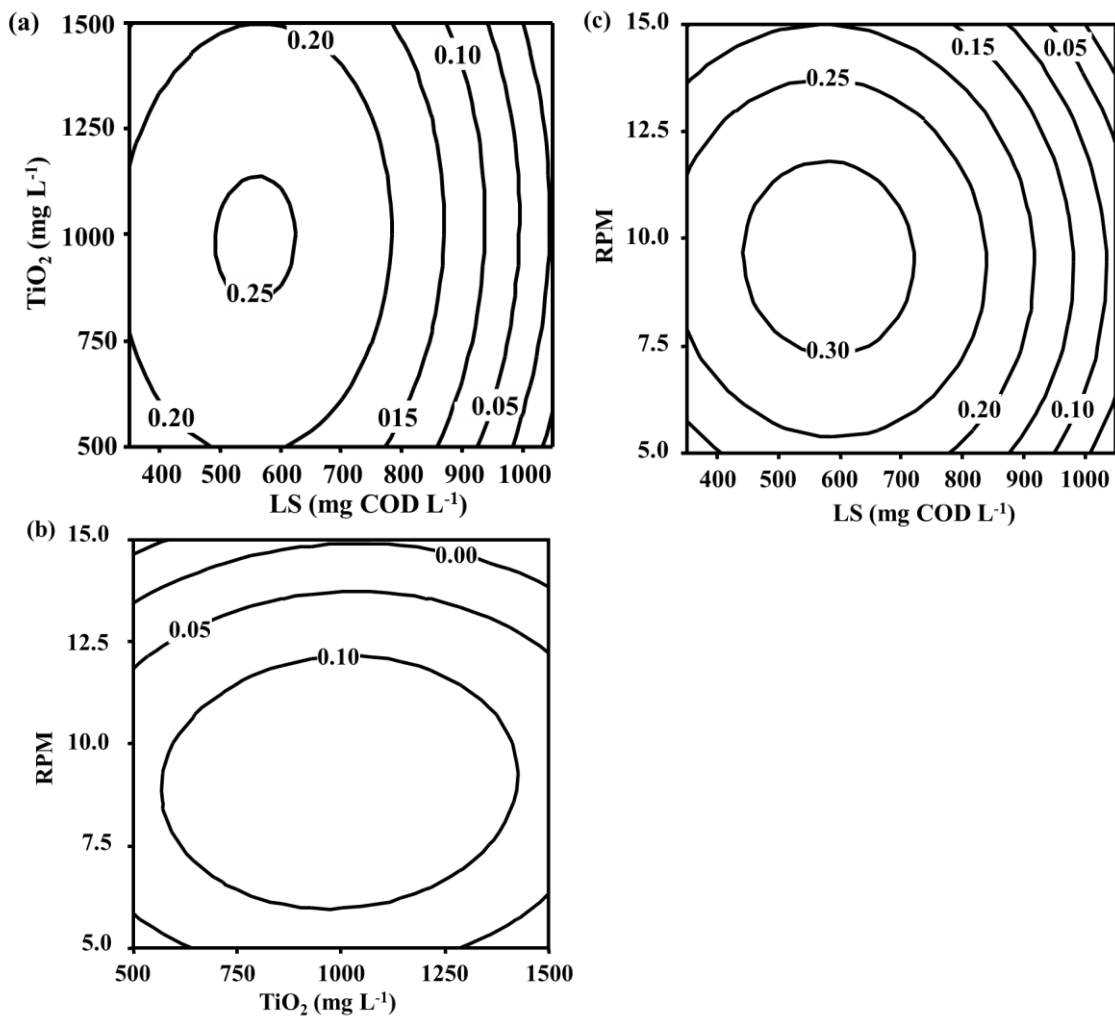
Figure 6.1 Contour plots of the BOD_5 to COD ratio of LS after photocatalysis as a function of a) TiO_2 and LS concentrations, b) RPM and TiO_2 concentration and c) RPM and LS concentration. Hold values (RPM = 15, LS = 1050 mg COD L^{-1} and TiO_2= 1500 mg L^{-1})
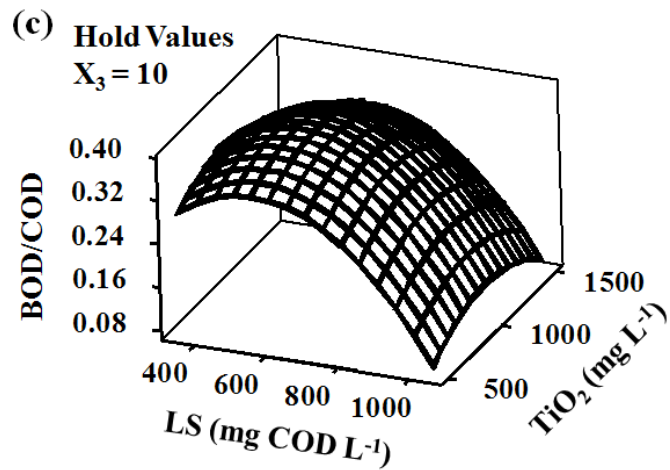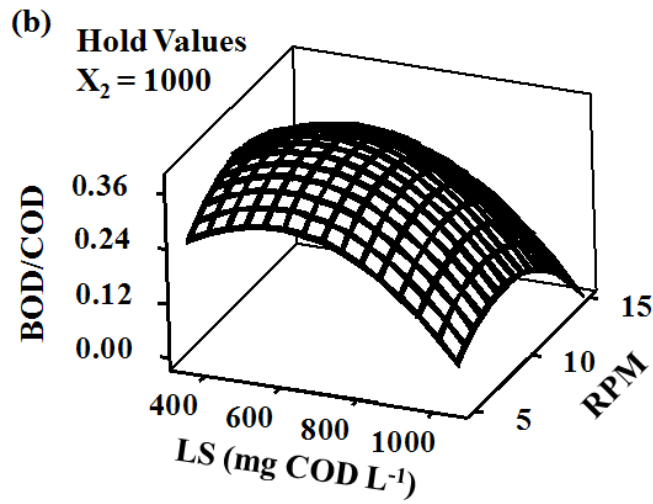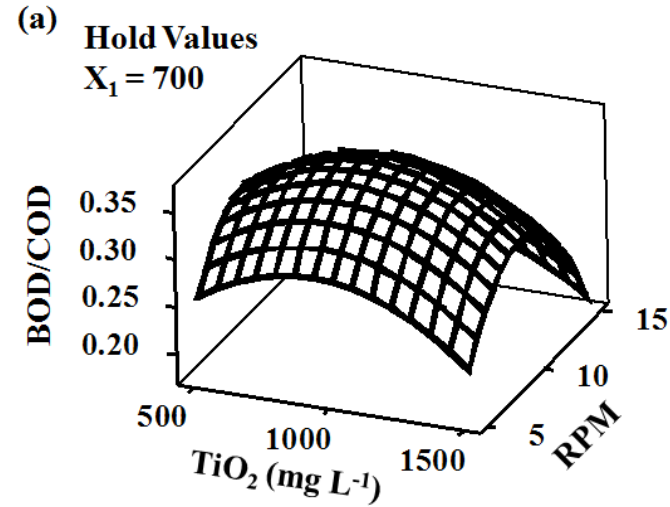
Figure 6.2 Response surface plot fitted from the experimental results of the Box-Behnken design (BBD).

With increasing LS concentrations up to approximately 500 mg COD L^{-1}, the BOD$_5$/COD ratio increased; however, a decrease was observed at levels greater than 500 mg COD L^{-1} (Figures 6.1a and 6.1c). The reduced degradation beyond an initial substrate threshold level could be attributed to the saturation of catalytic sites and the inadequate production of reactive species such as $^\bullet OH$ and $^\bullet O_2^-$ (Ahmed et al., 2011a). Interference of reaction intermediates formed by the degradation of LS could also lead to a decrease in the degradation efficiency which resulted in a low BOD$_5$/COD ratio (Tzikalos et al., 2013). Similar studies by Bahnemann et al. (2007) on the influence of the initial substrate concentration on the photocatalytic degradation rate noted that the propham degradation rate increased to a threshold level with increasing substrate concentrations and with increasing the substrate concentration, the degradation rate decreased.

The effect of each factor on the response variable was also investigated using the main effects plot. The main effects plot (Figure 6.3) shows the response mean value for each factor. The magnitude of the vertical displacement is an indication of the strength of the main effect on a factor. The large vertical displacement for X_1 (LS concentration) suggest that the LS concentration has the largest effect on the BOD$_5$/COD ratio when compared to the TiO$_2$ concentration (X_2) and RPM (X_3).
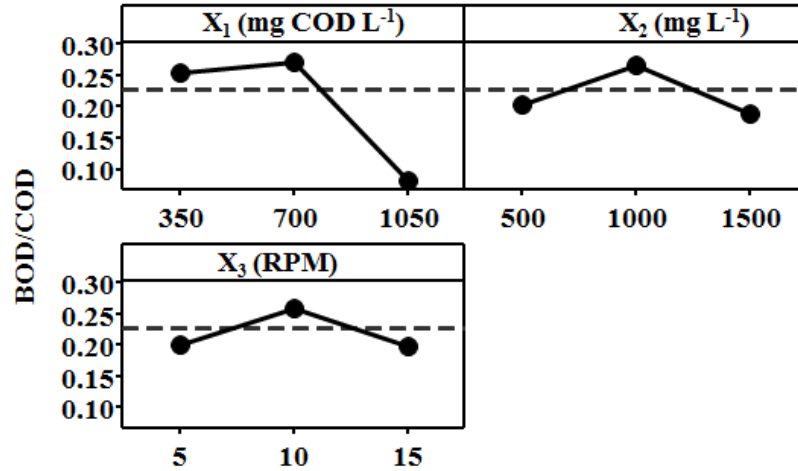
Figure 6.3 Main effect plots for the experimental factors.

Interactions plots are used to assess interaction between the different factors. An interaction is present when the response at a factor level is dependent on the level(s) of other factors. Parallel lines indicate no interaction and non-parallel lines indicate a high degree of interaction. Interaction between the factors under consideration is shown in Figure 6.4 and Table 6.2. Although interaction is shown between the three variables, none of the interactions were significant ($p > 0.005$).
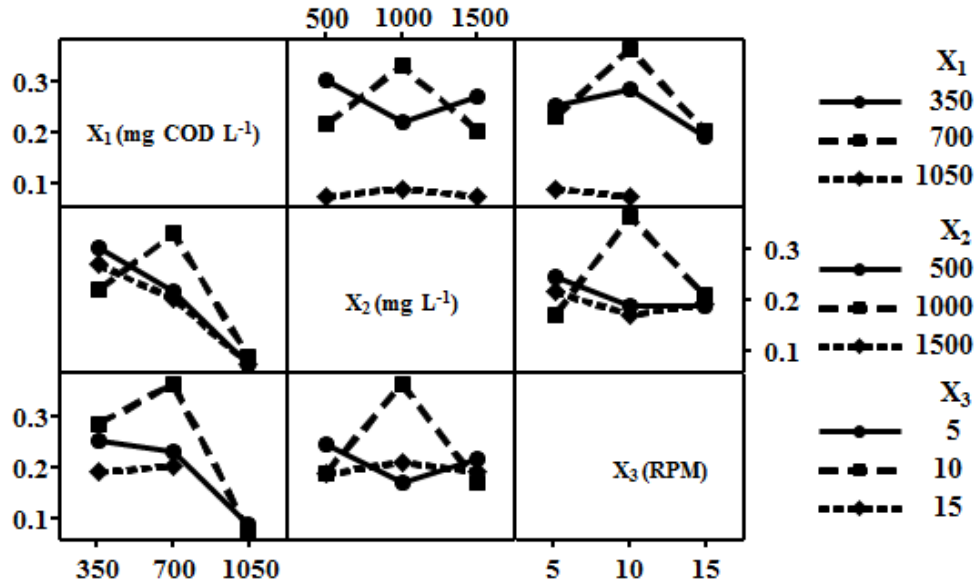
Figure 6.4 Interaction plots showing effects of experimental factors on BOD_5 to COD ratio.

Table 6.2 ANOVA results for the experimental response at different factor levels (at 95% confidence level)

Source	DF	Seq SS	Adj SS	Adj MS	F	P	
Regression	9	0.135295	0.135295	0.015033	58.57	0.000	S
Linear		0.045325	0.054920	0.018307	71.32	0.000	S
X_1	1	0.044004	0.054199	0.054199	211.15	0.000	S
X_2	1	0.000448	0.000448	0.000448	1.75	0.243	NS
X_3	1	0.000873	0.006088	0.006088	23.72	0.005	S
Square		0.089233	0.085311	0.028437	110.79	0.000	S
X_1*X_1	1	0.044631	0.052050	0.052050	202.78	0.000	S
X_2*X_2	1	0.009160	0.009684	0.009684	37.73	0.002	S
X_3*X_3	1	0.035442	0.034465	0.034465	134.27	0.000	S
Interaction		0.000737	0.000737	0.000246	0.96	0.481	NS
X_1*X_2	1	0.000280	0.000280	0.000280	1.09	0.344	NS
X_1*X_3	1	0.000151	0.000151	0.000151	0.59	0.478	NS
X_2*X_3	1	0.000306	0.000306	0.000306	1.19	0.325	NS
Residual Error		0.001283	0.001283	0.000257			
Lack-of-Fit	3	0.001283	0.001283	0.000428			
Pure Error	2	0.000000	0.000000	0.000000			
Total	14	0.136579					

Notes: $R^2 = 99.06\%$, R^2 (predicted = 82.91%, R^2 (adjusted) = 97.37%; S = significant; NS = Not significant; DF = Degrees of freedom; Seq SS = Sequential sum of squares; Adj SS = Adjusted sum of squares; Adj MS = Adjusted mean square; * = multiplication sign.

6.3.1.2 Model assessment

The Anderson-Darling statistic (ADS) for the developed model (Section 6.3.3.1) confirmed a normal-fit for the probability distribution of the residuals (Figure 6.5). The observed ADS (0.265) for the model response was less than the critical ADS value of 0.752 for a sample size of 39 at a 5% significance level. The associated p-value (0.641) of the ADS which was greater than 0.05 confirmed a normal distribution of the residuals.
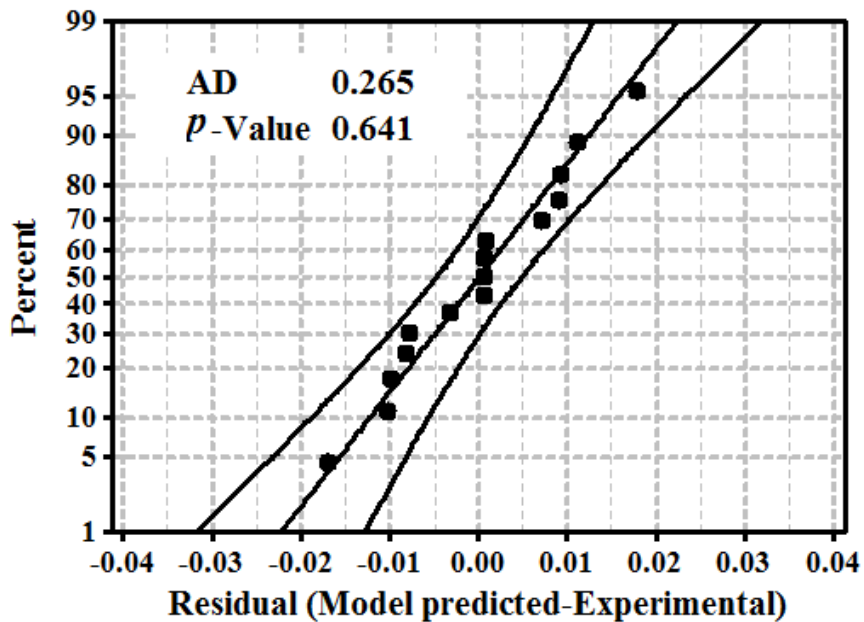
Figure 6.5 Anderson-Darling normality plot of the residuals.

6.3.1.2 Optimizing the photocatalytic degradation process

According to Ahmed et al. (2011b), optimization of the degradation parameters is crucial from the perspective of efficient design and application of photocatalytic oxidation process to ensure sustainable operation. Assessing the adequacy of a second-order model was conducted in accordance with Myers et al. (2009). A second-order model equation for the response variable (BOD_5/COD ratio) was developed as a function of the independent factors (Equation 6.4).

$$Y = 0.365154 - 0.098223X_1 - 0.007487X_2 - 0.030171X_3 - 0.131667X_1{}^2 -$$

$$0.052880X_2{}^2 - 0.101924X_3{}^2 + 0.008366X_1 * X_2 - 0.008345X_1 * X_3 + 0.008747X_2 *$$

$$X_3 \hspace{6cm} (6.4)$$

where Y is the predicted BOD$_5$ to COD ratio and X_1, X_2 and X_3 are the factor values in coded units.

The ANOVA (Table 6.2) indicates terms not significant ($p > 0.005$). The non-significant terms were removed with a resulting modified quadratic equation (Equation 6.5).

$$Y = 0.365154 - 0.098223X_1 - 0.030171X_3 - 0.131667X_1{}^2 - 0.052880X_2{}^2$$

$$- 0.101924X_3{}^2 \hspace{5cm} (6.5)$$

The regression model (Equation 6.4) explained 99.06% of the variation in the response variable. The model is predictive, since the calculated F-value (58.57) is greater than the critical F-value (3.4). This shows that the model equation is reliable within the range of factors under consideration. The experimental factors along their experimental and predicted responses based on Equation 6.5 are shown in Table 6.3.

Table 6.3 Box-Behnken design matrix for experimental factors along their experimental and predicted responses.

| Run # | Factors | | | Response (BOD$_5$/COD) | | | | Residual |
| | LS conc. (mg COD L^{-1}) | TiO$_2$ conc. (mg L^{-1}) | RPM | Experimental | | Predicted | | |
				Average	STD	Average	STD	
1	350	1000	5	0.252	0.027	0.252	0.029	0.001
2	1050	1000	5	0.090	0.013	0.072	0.028	0.018
3	700	500	5	0.246	0.023	0.257	0.002	-0.010
4	700	1500	5	0.216	0.011	0.224	0.009	-0.008
5	350	500	10	0.304	0.087	0.295	0.071	0.009
6	1050	500	10	0.074	0.009	0.082	0.006	-0.008
7	350	1500	10	0.270	0.015	0.263	0.019	0.007
8	1050	1500	10	0.073	0.004	0.083	0.024	-0.010
9	700	1000	10	0.366	0.083	0.365	0.078	0.001
10	350	1000	15	0.191	0.014	0.208	0.024	-0.017
11	700	1000	15	0.230	0.028	0.233	0.015	-0.003
12	700	500	15	0.188	0.017	0.179	0.019	0.009
13	700	1500	15	0.193	0.016	0.181	0.018	0.011

Notes: STD = Standard deviation; The average and standard deviation are based on triplicate samples.

In this study, a maximum BOD$_5$/COD ratio (0.3859) was obtained under optimum conditions of an initial LS concentration of 569 mg COD L^{-1}, a TiO$_2$ concentration of 944 mg L^{-1} and at 9 RPM (Figure 6.6). A stock PrLS feed was prepared based on the optimum conditions for subsequent experiments with SCMFCs. LC-MS analysis was employed to identify compounds produced from LS photocatalysis. The structure of PrLS compounds identified using the m/z ratio and molecular weight are shown in Table 6.4. A typical LC-MS spectrum is presented in Appendix B (Figure B1). Characterization of the compounds (Table 6.4) revealed the presence of biodegradable compounds which include acetic acid (m/z = 59) and muconic acid (m/z = 141). The findings of this study

are consistent with those of Nakamura et al. (2004) who reported similar compounds produced from the ozonolysis of sodium lignosulfonate.

		X_1	X_2	X_3
Optimal	High	1050.0	1500.0	15.0
D=0.92961	Cur	[569.19]	[944.44]	[9.34]
	Low	350.0	500.0	5.0
Composite Desirability 0.92961				
Maximum BOD/COD =0.3859 D=0.92961				
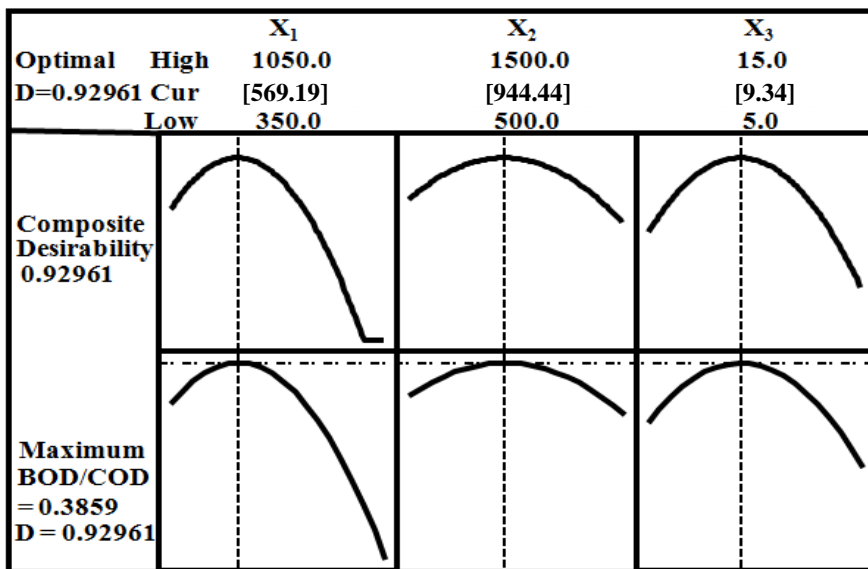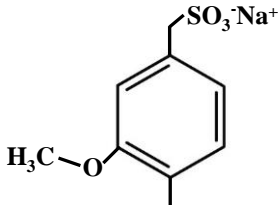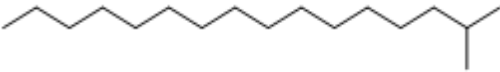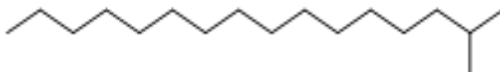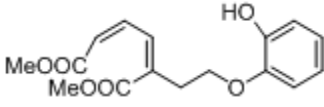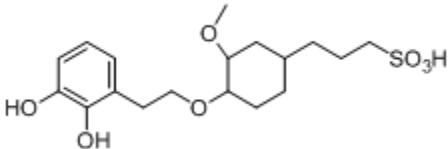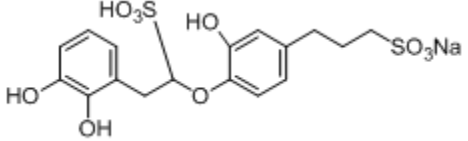
Figure 6.6 Optimality plot locating optimum factor levels for maximized response.

Table 6.4 Compounds identified in PrLS.

m/z	Molecular weight	Structure
59	60	
141	142	$C_2H_6O_4$
179	180	

m/z	Molecular weight	Structure
223	224	A benzene ring with $SO_3^-Na^+$ group and H_3C-O group attached.
239	240	Branched alkane chain, $C_{17}H_{36}$
240	240	Branched alkane chain, $C_{17}H_{36}$
305	306	Structure with MeOOC groups and phenol (HO) ring connected via ether linkage.
387	388	Structure with methoxy, HO, OH, and SO_3H groups on cyclohexane and benzene rings.
469	470	Structure with HO_3S, HO, OH, and SO_3Na groups.

6.3.2 Microbial fuel cell performance

6.3.2.1 Voltage generation and adaptation to pretreated LS

The maximum theoretical voltage output that can be produced from glucose fed to an air-cathode MFC, estimated from the biological redox tower of electron donors and acceptors, is 1.25 V (He and Angenent, 2006). The glucose fed SCMFCs used in this

study generated 620±30 mV. The 50.4% voltage efficiency of the SCMFCs is comparable with the voltage efficiency of SCMFCs fed organic substrates (Liu et al., 2005; Cheng et al., 2006). The lower values of maximum voltages are attributed to internal potential losses in MFCs (Hamelers et al., 2010).

In this study, the SCMFCs were initially operated using a glucose feed. After achieving a stable and repeatable voltage of 620±30 mV with the glucose feed, the SCMFCs were acclimated to PrLS by employing a feeding procedure divided into three stages (Figure 6.7). In the first and second feeding stages, the feed contained 1/3 of PrLS and 2/3 of glucose and 2/3 of PrLS and 1/3 of glucose, respectively. In the third (final) phase, the feed was composed of only PrLS. The COD of the feeds in all phases were maintained constant. The maximum voltages achieved in each phase are shown in Table 6.5. The maximum voltage obtained when the fed was changed to only PrLs was reduced to 410±50 mV (a decreased of 34.5% when compared to feeding glucose). The lower voltage when the feed was changed to PrLS is likely attributed to the complexity of PrLS compared to glucose (El-Chakhtoura et al., 2014). However, note the maximum voltage achieved from PrLS is comparable to those reported in other studies which used a feed containing complex organic chemicals (Wang et al., 2008; Yang et al., 2013).
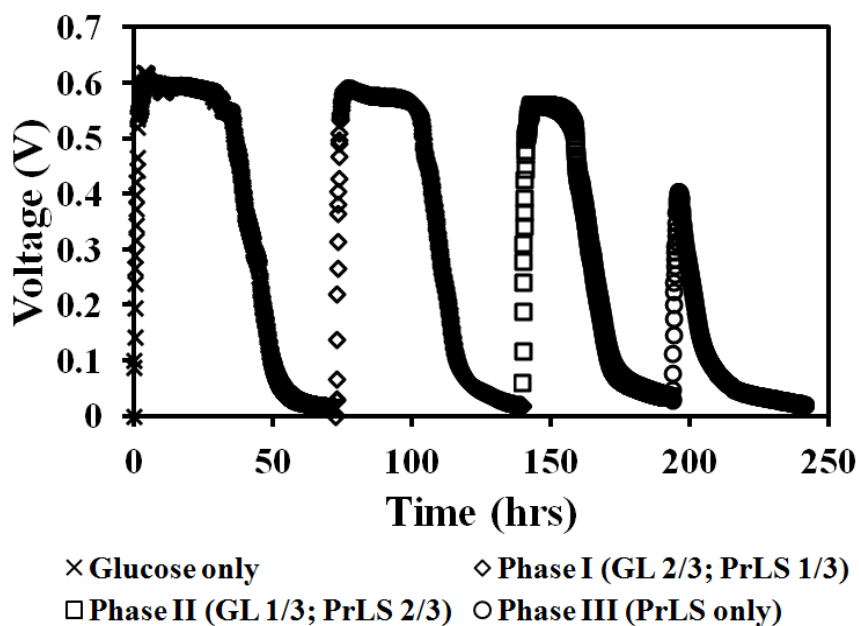
Figure 6.7 Voltage production from GL (glucose) and PrLS (pretreated lignosulfonate) at mesophilic temperature for one feeding cycle after acheiving a stable and repeatable voltage.

Table 6.5 Maximum voltages obtained with GL and PrLS.

	Maximum Voltage (V)	
Substrate	**Average**	**STD**
Glucose (GL) only	0.620	0.030
GL(2/3); PrLS(1/3)	0.590	0.010
GL(1/3); PrLS(2/3)	0.565	0.035
PrLS only	0.405	0.050

Note: GL= Glucose; PrLS = Pretreated liginosulfonate; STD = Standard deviation

6.3.2.2 Comparative electricity generation

Different operating conditions, surface area and type of electrodes as well as type of microorganisms are factors to consider when comparing the performance of MFCs (Pant et al., 2010). In spite of the difficulties associated with comparing the performance of MFCs, Pant et al. (2010) compiled a comprehensive inventory of power output as a

134

function of substrate type and concentration, inoculum source and type of MFC. Comparing data from this study with other studies is difficult because electricity production from PrLS using SCMFCs has not been reported by other researchers. The comparison was instead primarily based on the performance of SCMFCs fed glucose to SCMFs fed PrLS (Table 6.6).

Table 6.6 Electrochemical properties and efficiencies of SCMFCs fed with GL and PrLS.

Substrate	Current density		Power density		V_{max} (mV)	OCV_{max} (mV)	R (Ω)	CE (%)	η_{COD} (%)
	mA m^{-3}	mA m^{-2}	mW m^{-3}	mW m^{-2}					
Glucose	10490	1390	3315	440	620	850	230	17	82
PrLS	6560	870	1880	250	405	805	340	18	78

Note: V_{max} = Maximum voltage; OCV_{max} = Maximum open circuit voltage; R = Internal resistance; CE = Coulombic efficiency; η_{COD} = COD removal efficiency

The power generation from SCMFCs fed PrLS was monitored under similar conditions as SCMFCs fed glucose. The COD of the feed containing either glucose or PrLS was maintained at 390 mg COD L^{-1}. The PrLS fed SCMFCs generated maximum current and power densities of 6,555±360 mA m^{-3} and 1,880±105 mW m^{-3}, respectively. The corresponding maximum current and power densities normalized to the cathode area were 870±50 mA m^{-2} and 250±15 mW m^{-2}, respectively.

SCMFCs fed PrLS generated less electricity when compared to those fed glucose (Figures 6.8 and 6.9). The lower power generation from a feed containing PrLS is likely due to the presence of complex organic compounds which were not be easily oxidized by electrogenic bacteria. The internal resistance (R_{in}) of the SCMFCs fed with glucose (230 ohms) was greater than that of PrLS fed SCMFCs (340 ohms). According to Rabaey and Verstraete (2005), the internal resistance is dependent on the electrolyte resistance

between the electrodes as well as the membrane resistance. The difference in the internal resistance may be attributed to the difference in the type of substrate fed to the SCMFCs. Wang et al. (2012) deduced that when compared to MFCs utilizing glucose or acetate, the internal resistance of MFCs powered by waste-activated sludge was slightly greater.
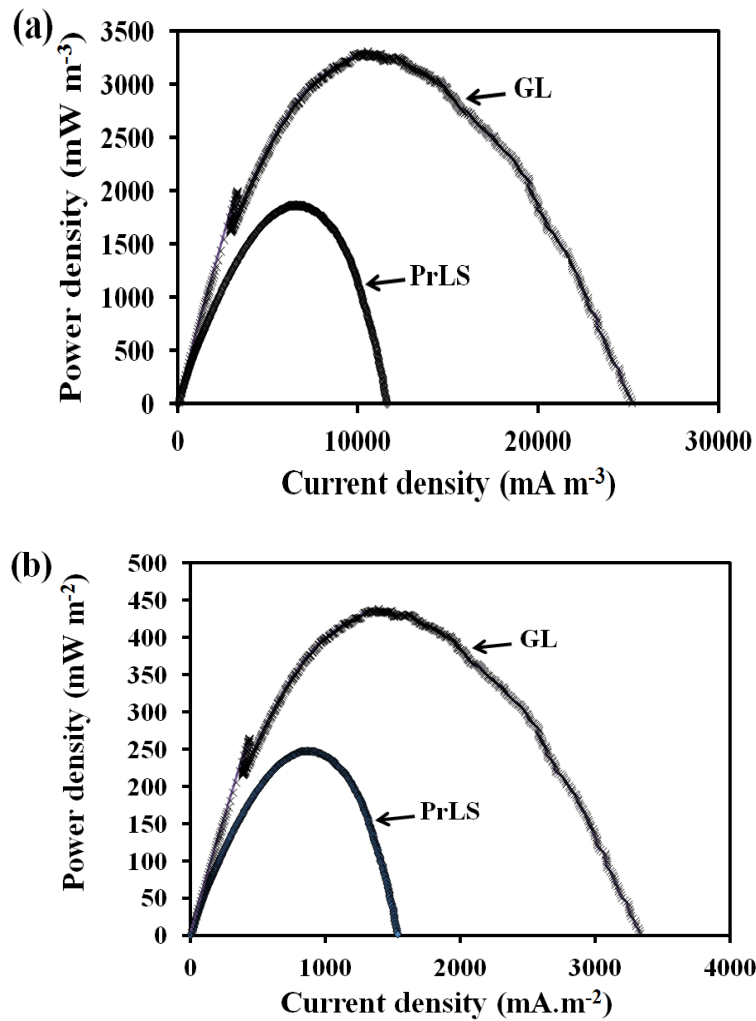
Figure 6.8 Power density curves normalized to (a) working volume and (b) cathode surface area. Note: GL= Glucose; PrLS = Pretreated liginosulfonate.
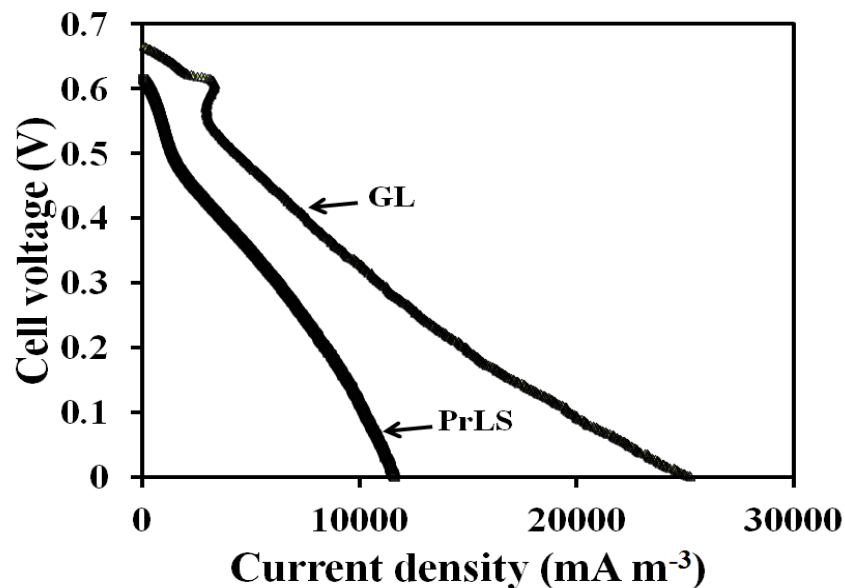
Figure 6.9 Polarization curves of SCMFCs fed GL (glucose) and PrLS (pretreated lignosulfonate).

6.3.2.3 COD removal and coloumbic efficiency

The COD removal efficiency for glucose (390 mg/L as COD) fed SCMFCs of 82.1 % (Table 6.6) was the same as reported by Lee et al. (2008) who reported a COD reduction of 82% for MFCs fed glucose (384 mg/L as COD). The COD removal efficiency of the PrLS fed SCMFCs was 77.6±2.3% which is slightly lower than the SCMFCs fed glucose (82.1%). The lower COD removal in PrLs fed SCMFCs compared to those fed glucose is likely caused by the presence of complex non-biodegradable organic compounds. Similar studies conducted by Liu et al. (2012) reported COD removal efficiencies ranging from 70% to 82% for SCMFCs fed different concentrations of steroidal drug production wastewater. Treatment of the remaining undegraded PrLS chemicals in the effluent was not examined; however, an added photocatlytic process could be utilized to remove the remaining 22.4% COD.

The coulombic efficiency is the fraction of the electrons from degraded organic matter that flows in the electrical circuit (Hamelers et al., 2010). According to Hamelers et al. (2010), reported coulombic efficiencies for MFCs range from 5% to 38%, and depended on the reactor design, type of wastewaters, temperature etc. Despite the lower power generated by the PrLS fed SCMFCs compared to glucose fed SCMFCs, the coloumbic efficiency (Table 6.6) was approximately the same for the glucose (17.1±1.2%) and the PrLS (17.7±1.2%) fed SCMFCs.

6.3.2.4 Microbial community analysis

The bacterial population as well as bacterial activity are important components for producing electricity (Liu et al., 2012). The work conducted in this study not only demonstrated the utilisation of PrLS for power generation but it also illustrated the diversity of the microbial community needed for degrading complex organic structures.

In this study, the similar microbial sequences for biofilm samples were clustered into operational taxonomic units based on a 97% identity aligned with the Greengenes core set (DeSantis et al., 2006) and taxonomy was assigned using the RDP (ribosomal database project) classifier (Cole et al., 2009). Greengenes is a web application tool which provides access to 16S rRNA sequence alignment for browsing, blasting, probing and downloading (http://greengenes.lbl.gov/cgi-bin/nph-index.cgi). RDP (https://rdp.cme.msu.edu) is a compilation of analytical tools which provides quality-controlled, aligned and annotated bacterial and Archaeal 16S rRNA sequences, and fungal 28S rRNA sequences. The detailed diversity and abundance of microbial communities are presented in Appendix F (Tables F1 and F2).

Comparing the glucose and PrLS fed SCMFCs bacterial communities was conducted at phylum-level (Figure 6.10). The major phyla in the glucose fed SCMFCs were *Bacteroidetes* (36.0%) and *Proteobacteria* (32.6%). In the PrLS fed SCMCs, the most abundant phyla were *Bacteroidetes* (30%) and *Firmicutes* (10.1%). The bacterial diversity detected is in agreement with bacterial diversity reported by Beecroft et al. (2012) who conducted studies to assess the performance and to semi-quantitatively determine the bacterial community dynamics of biofilm on the anode in MFCs fed sucrose. The phylogenetic analysis performed by Beecroft et al. (2012) revealed a diverse bacterial community consisting mainly of the phyla *Firmicutes* and *Bacteroidetes* and different classes of the phylum *Proteobacteria*. Similar studies conducted by Yusoff et al. (2013) revealed that *Proteobacteria* (38.4%), *Bacteroidetes* (30.5%) and *Firmicutes* (15.9%) were the three major phyla attached to the anode.
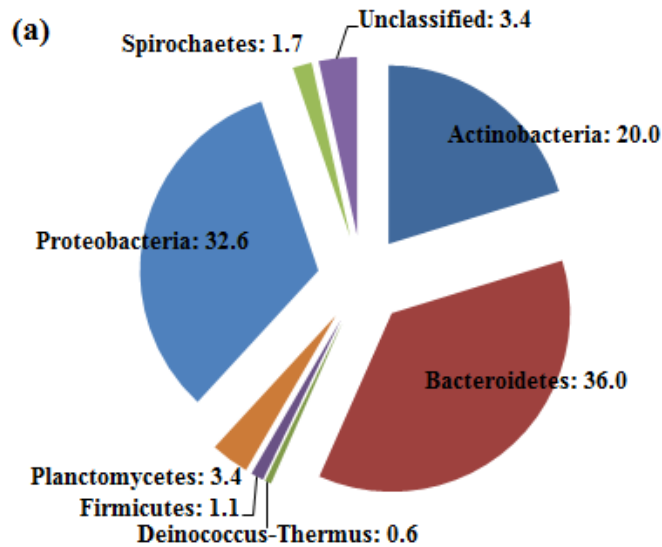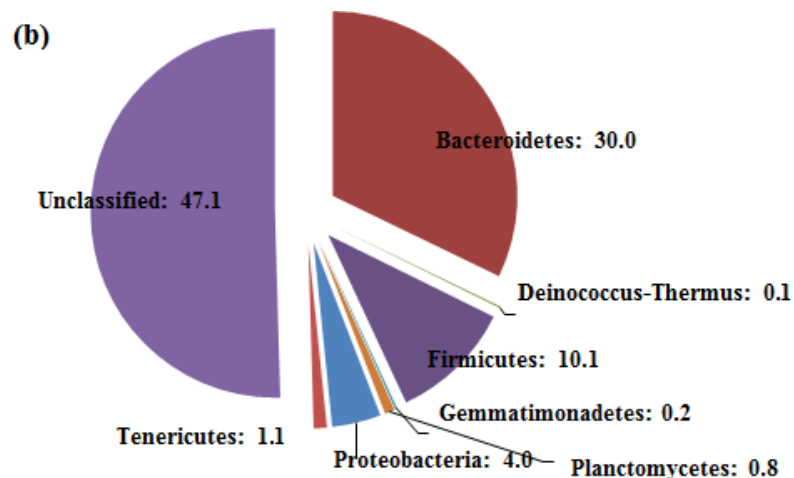
Figure 6.10 Phylum-level relative abundance of dominant bacterial a) Glucose fed SCMFCs and b) PrLS fed SCMFCs. Note: The numerical values on the chart represent the percent microorganisms.

Approximately one-half of the bacteria (47.1%) are unclassified in PrLS fed SCMFCs as compared to 3.4% in glucose fed SCMFCs (Figure 6.10). The large percent of unclassified bacteria in PrLS fed SCMFCs is attributed to bacterial communities utilizing the photocatalytic degradation products as a carbon source.

6.4 Conclusions

This study demonstrated the effectiveness of a two-stage process where photocatalysis is followed by MFCs to treat lignin compounds and generate electricity. The findings have significant impact in understanding the performance of SCMFCs fed with PrLS in comparison to those fed glucose.

The optimization and the modeling of the photocatalytic degradation process of the model lignin compound (LS) performed using a Box-Behnken design indicate that the factor values for a maximum BOD_5/COD ratio are the initial LS concentration of 569 mg COD L^{-1}, a TiO_2 concentration of 944 mg L^{-1} and a mixing rate at 9 RPM. The model

employed in this study is suitable for the photocatlytic degradation study because the experimental values are in agreement with the predicted values and the assessment of the mathematical model revealed that the quadratic model is adequate under the conditions examined.

The PrLS (390 mg COD L^{-1}) fed SCMFCs, operating at $37\pm1^{o}C$, generated maximum current and power densities of $6{,}555\pm360$ mA m^{-3} and $1{,}880\pm105$ mW m^{-3}, respectively. The corresponding maximum current and power densities normalized to the cathode area were 870 ± 50 mA m^{-2} and 250 ± 15 mW m^{-2}, respectively. The SCMFCs removed 77.6 ± 2.3 % of the COD of PrLS and achieved a coloumbic efficiency of $17.7\pm1.2\%$.

6.5 References

Ahmed, S., Rasul, M.G., Brown, R., and Hashib, M.A. (2011a) Influence of parameters on the heterogeneous photocatalytic degradation of pesticides and phenolic contaminants in wastewater: A short review. *J. Environ. Manage.* **92**(3): 311–330.

Ahmed, S., Rasul, M.G., Martens, W.N., Brown, R., and Hashib, M.A. (2011b) Advances in heterogeneous photocatalytic degradation of phenols and dyes in wastewater: A review. *Water Air Soil Pollut.* **215**(1-4): 3–29.

Alonso, D.M., Bond, J.Q., and Dumesic, J.A. (2010) Catalytic conversion of biomass to biofuels. *Green Chem.* **12**: 1493.

APHA, AWWA, and WPCF. (2005) Standard methods for the examination of water and wastewater, 21st edn. Washington, D.C: American Public Health Association.

Bahnemann, W., Muneer, M., and Haque, M.M. (2007) Titanium dioxide-mediated photocatalysed degradation of few selected organic pollutants in aqueous suspensions. *Catal. Today* **124**(3): 133–148.

Beecroft, N.J., Zhao, F., Varcoe, J.R., Slade, R.C.T., Thumser, A.E., and Avignone-Rossa, C. (2012) Dynamic changes in the microbial community composition in microbial fuel cells fed with sucrose. *Appl. Microbiol. Biotechnol.* **93**(1): 423–437.

Bruijnincx, P.C., and Román-Leshkov, Y. (2014) Sustainable catalytic conversions of renewable substrates. *Catal. Sci. Technol.* **4**(8): 2180–2181.

Chaganti, S.R., Kim, D.H., Lalman, J.A., and Shewa, W.A. (2012a) Statistical optimization of factors affecting biohydrogen production from xylose fermentation using inhibited mixed anaerobic cultures. *Int. J. Hydrogen Energy* **37**(16): 11710–11718.

Chaganti, S.R., Lalman, J.A., and Heath, D.D. (2012b) 16S rRNA gene based analysis of the microbial diversity and hydrogen production in three mixed anaerobic cultures. *Int. J. Hydrogen Energy* **37**(11): 9002–9017.

Chamarro, E., Marco, A., and Esplugas, S. (2001) Use of Fenton reagent to improve organic chemical biodegradability. *Water Res.* **35**(4): 1047–1051.

Cheng, S., Liu, H., and Logan, B.E. (2006) Power densities using different cathode catalysts (Pt and CoTMPP) and polymer binders (Nafion and PTFE) in single chamber microbial fuel cells. *Environ. Sci. Technol.* **40**(1): 364–369.

Chong, M.N., Jin, B., Chow, C.W.K., and Saint, C. (2010) Recent developments in photocatalytic water treatment technology: A review. *Water Res.* **44**(10): 2997–3027.

Choquette-Labbé, M., Shewa, W.A., Lalman, J.A., and Shanmugam, S.R. (2014) Photocatalytic degradation of phenol and phenol derivatives using a nano-TiO_2 catalyst: integrating quantitative and qualitative factors using response surface methodology. *Water*, **6**(6): 1785–1806.

Climent, M.J., Corma, A., and Iborra, S. (2014) Conversion of biomass platform molecules into fuel additives and liquid hydrocarbon fuels. *Green Chem.* **16**(2): 516–547.

Cole, J.R., Wang, Q., Cardenas, E., Fish, J., Chai, B., Farris, R.J., Kulam-Syed-Mohideen, A.S., McGarrell, D.M., Marsh, T., Garrity, G.M., and Tiedje J.M. (2009) The ribosomal database project: improved alignments and new tools for rRNA analysis. *Nucleic Acids Res.* **37**: D141–D145.

DeSantis T.Z, Hugenholtz P., Larsen N., Rojas M., Brodie E.L, Keller K., Huber, T., Dalevi, D., Hu, P., and Andersen G.L. (2006) Greengenes, a chimera-checked 16S rRNA gene database and workbench compatible with ARB. *Appl. Environ. Microbiol*. **72**(7):5069-72.

Duran, N., Esposito, E., Innocentini-Mei, L., and Canhos, V. (1994) A new alternative process for kraft E1 effluent treatment. *Biodegradation* **5**:13–19.

El-Chakhtoura, J., El-Fadel, M., Rao, H.A., Li, D., Ghanimeh, S., and Saikaly, P.E. (2014) Electricity generation and microbial community structure of air-cathode microbial fuel cells powered with the organic fraction of municipal solid waste and inoculated with different seeds. *Biomass and Bioenergy* **67**: 24–31.

Ferreira, S.C., Bruns, R.E., Ferreira, H.S., Matos, G.D., David, J.M., Brandao, G.C., da Silva, E.G.P., Portugal, L.A., dos Reis, P.S., Souza, A.S., and Dos Santos, W.N.L. (2007) Box-Behnken design: An alternative for the optimization of analytical methods. *Anal. Chim. Acta* **597**(2): 179-186.

Freudenberg, K., and Nash, A.C. (1968). Constitution and biosynthesis of lignin. Berlin: Springer-Verlag.

Hamelers, B., Sleutels, T.H., Jeremiasse, A., Post, J.W., Strik, D.P., and Rozendal, R.A. (2010) Technological factors affecting BES performance and bottlenecks towards scale up. In *Bioelectrochemical systems: from extracellular electron transfer to biotechnological application*. Reaby K., Angenet L., Schroder U., and Keller J. eds. London: IWA Publishing, pp. 205–223.

Hassan, S.H. a., Gad El-Rab, S.M.F., Rahimnejad, M., Ghasemi, M., Joo, J.-H., Sik-Ok, Y., et al. (2014) Electricity generation from rice straw using a microbial fuel cell. *Int. J. Hydrogen Energy* **39**(17): 9490–9496.

He, Z., and Angenent, L.T. (2006) Application of bacterial biocathodes in microbial fuel cells. *Electroanalysis* **18**(19–20): 2009–2015.

Lee, H.S., Parameswaran, P., Kato-Marcus, A., Torres, C.I., and Rittmann, B.E. (2008) Evaluation of energy-conversion efficiencies in microbial fuel cells (MFCs) utilizing fermentable and non-fermentable substrates. *Water Res*. **42**(6): 1501–1510.

Liu, H., Cheng, S., and Logan, B.E. (2005) Production of electricity from acetate or butyrate using a single-chamber microbial fuel cell. *Environ. Sci. Technol.* **39**(2): 658–662.

Liu, R., Gao, C., Zhao, Y.G., Wang, A., Lu, S., Wang, M. Maqbool, F., and Huang, Q. (2012). Biological treatment of steroidal drug industrial effluent and electricity generation in the microbial fuel cells. *Bioresour. Technol.*, **123**: 86-91.

Logan, B.E. (2008) Microbial fuel cells. New York, NY: John Wiley and Sons.

De Morais, J.L., and Zamora, P.P. (2005) Use of advanced oxidation processes to improve the biodegradability of mature landfill leachates. *J. Hazard. Mater.* **123**(1-3): 181–186.

Meyer, F., Paarmann, D., D'Souza, M., Olson, R., Glass, E.M., Kubal, M., Paczian, T., Rodriguez, A., Stevens, R., Wilke, A., Wilkening, J., and Edwards, R.A. (2008) The metagenomics RAST server - a public resource for the automatic phylogenetic and functional analysis of metagenomes. *BMC Bioinformatics* **9:**386.

Myers, R. H., and Montgomery, D. C. (2002) Response surface methodology: process and product optimization using designed experiments, 2nd edn. Hoboken, NJ: John Wiley and Sons.

Myers, R. H., Montgomery, D. C., and Anderson-Cook, C. M. (2009) Response surface methodology: process and product optimization using designed experiments, 3rd edn. Hoboken, NJ: John Wiley and Sons.

Nakamura, Y., Daidai, M., and Kobayashi, F. (2004) Ozonolysis mechanism of lignin model compounds and microbial treatment of organic acids produced. *Water Sci. Technol.* **50**(3): 167–172.

Oller, I., Malato, S., and Sánchez-Pérez, J. A. (2011) Combination of advanced oxidation processes and biological treatments for wastewater decontamination-A review. *Sci. Total Environ.* **409**(20): 4141–4166.

Pant, D., Van Bogaert, G., Diels, L., and Vanbroekhoven, K. (2010) A review of the substrates used in microbial fuel cells (MFCs) for sustainable energy production. *Bioresour. Technol.* **101**(6): 1533–1543.

Pekakis, P.A., Xekoukoulotakis, N.P., and Mantzavinos, D. (2006) Treatment of textile dyehouse wastewater by TiO_2 photocatalysis. *Water Res.* **40**(6): 1276–1286.

Pokhrel, D., and Viraraghavan, T. (2004) Treatment of pulp and paper mill wastewater - a review. *Sci. Total Environ.* **333**(1): 37–58.

Rabaey, K., and Verstraete, W. (2005) Microbial fuel cells: novel biotechnology for energy generation. *Trends Biotechnol.* **23**(6): 291–8.

Rabindranathan, S., Devipriya, S., and Yesodharan, S. (2003) Photocatalytic degradation of phosphamidon on semiconductor oxides. *J. Hazard. Mater.* **102**(2): 217–229.

Rauf, M.A., Meetani, M.A., and Hisaindee, S. (2011) An overview on the photocatalytic degradation of azo dyes in the presence of TiO_2 doped with selective transition metals. *Desalination* **276**(1): 13–27.

Ren, Z., Ward, T.E., and Regan, J.M. (2007) Electricity production from cellulose in a microbial fuel cell using a defined binary culture. *Environ. Sci. Technol.* **41**(13): 4781–4786.

Schwartz, K. (2007) Microbial fuel cells: Design elements and application of a novel renewable energy source. *MMG 445 Basic Biotechnol. eJournal* **3**: 20–27.

Shewa, W.A., and Lalman, J.A (2014). Producing electricity using a microbial fuel cell fed with feedstock chemicals produced from the photocatalysis of a lignin model chemical. In: Proceedings of the 87th Annual Water and Environment Federation Technical Exhibition and Conference, 27 September–01 October 2014, New Orleans, LA, USA, pp. 2484–2503.

Shewa, W.A., Chaganti, S.R., and Lalman, J.A. (2014) Electricity generation and biofilm formation in microbial fuel cells using plate anodes constructed from various grades of graphite. *J. Green Eng*. **4**(1): 13–32.

Stephens, M.A. (1974) EDF statistics for goodness of fit and some comparisons. *J. Am. Stat. Assoc.* **69**(347): 730–737.

Tzikalos, N., Belessi, V., and Lambropoulou, D. (2013) Photocatalytic degradation of Reactive Red 195 using anatase/brookite TiO_2 mesoporous nanoparticles: Optimization using response surface methodology (RSM) and kinetics studies. *Environ. Sci. Pollut. Res.* **20**(4): 2305–2320.

Velegraki, T., Poulios, I., Charalabaki, M., Kalogerakis, N., Samaras, P., and Mantzavinos, D. (2006) Photocatalytic and sonolytic oxidation of acid orange 7 in aqueous solution. *Appl. Catal. B Environ.* **62**(1): 159–168.

Wang, X., Feng, Y.J., and Lee, H. (2008) Electricity production from beer brewery wastewater using single chamber microbial fuel cell. *Water Sci. Technol.* **57**(7): 1117–1121.

Wang, Z., Mei, X., Ma, J., and Wu, Z. (2012) Recent advances in microbial fuel cells integrated with sludge treatment. *Chem. Eng. Technol.* **35**(10): 1733–1743.

Wiegant, W.M., and Lettinga, G. (1985). Thermophilic anaerobic digestion of sugars in upflow anaerobic sludge blanket reactors. *Biotechnol. Bioeng.* **27**(11): 1603–1607.

Wu, Z., and Zhou, M. (2001) Partial degradation of phenol by advanced electrochemical oxidation process. *Environ. Sci. Technol.* **35**(13): 2698–2703.

Yang, F., Ren, L., Pu, Y., and Logan, B.E. (2013) Electricity generation from fermented primary sludge using single-chamber air-cathode microbial fuel cells. *Bioresour. Technol.* **128**: 784–787.

Yetilmezsoy, K., Demirel, S., and Vanderbei, R.J. (2009) Response surface modeling of Pb (II) removal from aqueous solution by *Pistacia vera* L.: Box–Behnken experimental design. *J. Hazard. Mater.* **171**(1): 551–562.

Yurdakal, S., and Augugliaro, V. (2012) Partial oxidation of aromatic alcohols via TiO_2 photocatalysis: the influence of substituent groups on the activity and selectivity. *RSC Adv.* **2**(22): 8375.

Yusoff, M.Z.M, Hu, A., Feng, C., Maeda, T., Shirai, Y., Hassan, M.A., and Yu, C.P. (2013) Influence of pretreated activated sludge for electricity generation in microbial fuel cell application. *Bioresour. Technol.* **145**: 90–96.

CHAPTER 7

COMPARING ENERGY GENERATION FROM A FEEDSTOCK GENERATED FROM THE PHOTOCATALYTIC DEGRADATION OF BLACK LIQUOR USING A TWO-STAGE ANAEROBIC DIGESTION PROCESS AND A MICROBIAL FUEL CELL

7.1 Introduction

Energy recovery from waste generated in industrial processes is an important energy management strategy for industries to recognize as energy demand continues to grow (Francis and Chungpaibulpatana, 2014). In biorefineries, lignocellulosic wastes are an important feedstock which is used for energy recovery. Energy recovery processes used in biorefineries can be classified as chemical, thermal and biological. Combustion, pyrolysis, chemical pretreatment followed by biological treatment, anaerobic digestion and gasification followed by biological or catalytic processing are example technologies that can be utilized to produce energy and chemicals.

In biorefineries such as pulp and paper and sugar cane mills, lignocelluosic waste is converted into energy by gasification. Black liquor is a waste generated during the cooking of wood chips. The primary chemical component of black liquor is lignin, a complex heterogeneous aromatic biopolymer (Font et al., 2003). According to Lara et al. (2003), black liquor is also characterized by high alkalinity and a high dissolved solids content.

With increasing high energy and chemical costs and stringent environment regulations, solid waste disposal cost and mill effluent treatment costs, the need for improved energy recovery and chemicals from black liquor has become a critical economic factor in the operation of pulp mills (Tran and Vakkilainen, 2007). In addition to energy recovery form black liquor, the treatment of effluents from pulp and paper industries is an increasing concern.

Aerobic and anaerobic bioprocesses have been used to treat diluted black liquor effluents (Kortekaas et al., 1998); however, low biodegradability as well as toxicity are major impediments and pretreatment prior to biological treatment is necessary to detoxify and facilitate degradation (Leach et al., 1976; Sierra-Alvarez and Lettinga, 1990; Font et al., 2003). According to Font et al. (2003), the low biodegradability of black liquor is due to the presence of lignin and lignin derivatives. Lignin is not easily biodegradable (Angelidaki and Sanders, 2004) because it is insoluble, chemically complex and lack hydrolysable linkages (Reid, 1995). According to Reid (1995), fungi such as basidiomycetes are organisms able to biodegrade lignin; however, the degradation process is relatively slow.

Substrates containing lignin or bacterial cells appear to be the most amendable to pre-treatment for enhancing anaerobic digestion (Carlsson et al., 2012). Shewa and Lalman (2014) have demonstrated the application of an advanced oxidation process to increase the biodegradability and reduce the toxicity of a model lignin compound, sodium lignosulfonate (LS). This was achieved through partial/controlled photocatalytic degradation using TiO_2. Employing pretreatment is useful because toxic and non-biodegradable chemicals can be converted into biodegradable substrates.

Thermal processing technologies such as combustion or gasification are utilized to recovery energy from black liquor. Methane production using anaerobic treatment and electricity production using microbial fuel cells (MFCs) have not been examined as energy recovery options because of the toxicity imposed by chemicals in black liquor on microorganisms.

Anaerobic digestion (AD) is used commercially to treat a variety of organic feedstocks from industries and municipalities. The AD process can be configured with a 1 or 2-stages. A 1-stage AD process combines hydrolysis, acidogenesis, acetogenesis and methanogensis in a single reactor. In comparison, in a 2-stage AD design, hydrolysis, acidogenesis, acetogenesis processes are mediated in the 1st reactor with methanogensis in the 2nd stage. The 2-stage AD process has been used to produce hydrogen plus methane in the 1st and 2nd reactor, respectively (Poggi-Varaldo et al., 2014). The application and advantages of the 2-stage AD process for bio-energy production using a wide range of effluents have been reported by several researchers (Fongsatitkul et al. 2012; Kyazze et al., 2007, Liu et al., 2006; Ueno et al., 2007). Recently, Schievano et al. (2014) compared the 1-stage and 2-stage AD processes. According to Schievano et al. (2014), the overall energy recovery efficiency (8%−43%) was significantly higher for the 2-stage AD process under a variety of experimental conditions.

MFCs are an emerging energy producing technology which are utilized to convert organic chemicals into electricity. MFCs are bioelectrochemical systems that use electrochemically active bacteria (Chang et al., 2006) to generate electricity from organic compounds. Biodegradable organic substrates include simple molecules, such as carbohydrates and proteins, as well as complex mixtures of organic matter present in

sewage, animal and food-processing effluents (Logan, 2009). Logan (2009) has also pointed out that the flexibility of microorganisms to use a range of substrates is a leading reason for utilizing MFCs for producing electricity from biomass. Rabaey et al. (2005) have argued that the overall conversion efficiencies which can be attained are potentially higher for MFCs compared to other processes that produce biofuels such as hydrogen gas, methane (biogas) and bio-ethanol.

The objectives of this study were to convert diluted black liquor into short chain carbon byproducts using TiO_2 photocatalysis and to assess and compare fuel and electricity production from the pretreated black liquor for energy production using a 2-stage AD process and single chamber microbial fuel cells (SCMFCs), respectively.

7.2 Material and methods

Details of the photocatalysis process, AD, and MFCs (Figure 7.1) are described in the following sections.
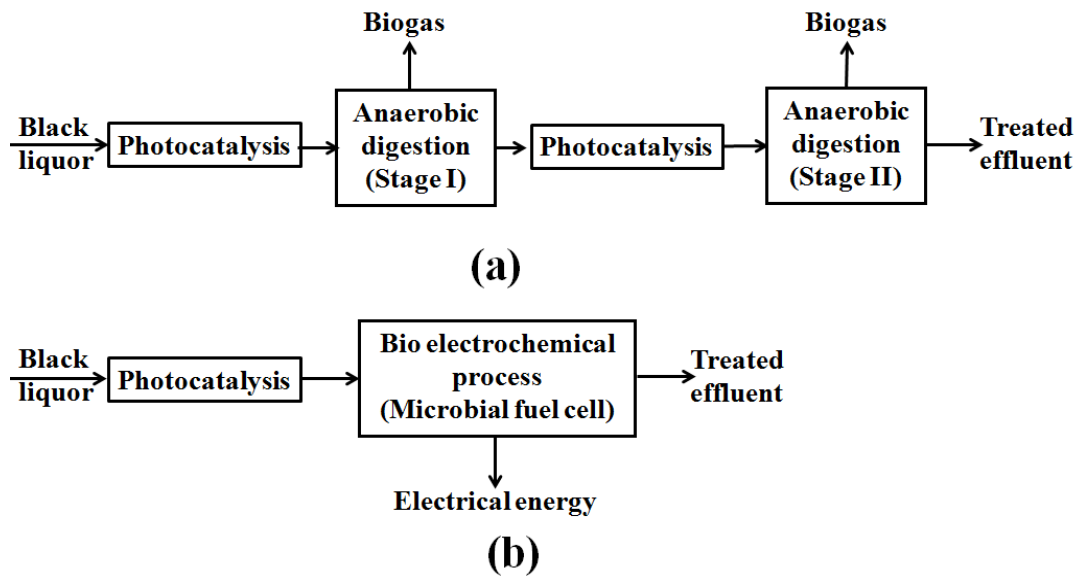
Figure 7.1 Process flow diagram show a) photocatalysis plus AD and b) photocatalysis plus MFC processes under consideration.

7.2.1 Mixed anaerobic cultures source

7.2.1.1 Anaerobic reactor culture source

The mixed culture inoculum used in the anaerobic reactors was obtained from anaerobic digesters located at a municipal wastewater treatment facility (Chatham, ON). The inoculum pH and volatile suspended solids (VSS) were approximately 6.62 and 18,200±400 mg L^{-1}. The reactors were operated at 37±1°C.

7.2.1.2 MFC microbial culture source

Microbial cultures for the SCMFCs were taken from two chamber MFCs which were used in studies reported by Shewa (2016). Mixed anaerobic cultures for the two chamber MFCs were obtained from anaerobic digesters located at a municipal wastewater treatment facility (Chatham, ON). The SCMFCs were operated at 37±1°C.

7.2.1.3 Biological oxygen demand (BOD) test inocula

The BOD test seed culture was obtained from raw domestic wastewater sampled from a municipal wastewater treatment facility (Windsor, ON). The wastewater sample was stored at 4°C prior to conducting the test.

7.2.2 Medium and chemicals

7.2.2.1 Feed to anaerobic digester

The basal medium added (mg L^{-1} of deionized water) to the anaerobic reactors contained the following: $NaHCO_3$, 6000; NH_4HCO_3, 70; KCl, 10; K_2HPO_4, 12.5; $(NH_4)_2SO_4$, 10; yeast extract, 10; $MgCl_2 \cdot 4H_2O$, 9; $FeCl_2 \cdot 4H_2O$, 2; resazurin, 1; EDTA, 1; $MnCl_2 \cdot 4H_2O$, 0.5; $CoCl_2 \cdot 6H_2O$, 0.15; Na_2SeO_3, 0.1; $(NH_4)_6MoO_7 \cdot 4H_2O$, 0.09; $ZnCl_2$,

0.05; H_3BO_3, 0.05; $NiCl_2 \cdot 6H_2O$, 0.05; and $CuCl_2 \cdot 2H_2O$, 0.03. [Adapted from Wiegant and Lettinga, 1985]. All the chemicals were 99% purity and purchased from Spectrum Chemicals (CA).

7.2.2.2 Feeds to microbial fuel cell

The basal medium added to the SCMFCs contained the following: 310 mg L^{-1} NH_4Cl, 130 mg L^{-1} KCl, 4225 mg L^{-1} $NaH_2PO_4.H_2O$, 7400 mg L^{-1} $Na_2HPO_4.12H_2O$, 10 mg L^{-1} yeast extract plus 1 mL L^{-1} of a mineral solution. The mineral solution was prepared in accordance with the procedure described by Wiegant and Lettinga (1985) and contained the following (Spectrum Chemicals, CA): (mg per L of distilled water): $MgCl_2 \cdot 4H_2O$, 9; $FeCl_2 \cdot 4H2O$, 2; resazurin, 1; EDTA, 1; $MnCl_2 \cdot 4H_2O$, 0.5; $CoCl_2 \cdot 6H_2O$, 0.15; Na_2SeO_3, 0.1; $(NH_4)_6MoO_7 \cdot 4H_2O$, 0.09; $ZnCl_2$, 0.05; H_3BO_3, 0.05; $NiCl_2 \cdot 6H_2O$, 0.05; and $CuCl_2 \cdot 2H_2O$, 0.03.

7.2.3 Photocatalysis

The black liquor (Table 7.1, Figure C1) was obtained from a pulp and paper mill (Lakehead, Ontario, Canada) and stored at 4^oC. Photocatalysis of the diluted black liquor was performed using TiO_2 anatase nanoparticles (10 nm) (Alfa Aesar, Ward Hill, MA, USA). The COD concentration of the diluted black liquor was 962 mg L^{-1}. The characteristics of the TiO_2 nano particles were previously described in Choquette-Labbé et al. (2014). The operating conditions for the pretreatment of diluted black liquor were selected based on a prior optimization study conducted on the photodegradation of a model lignin compound by Shewa et al. (2014b).

Table 7.1 Raw black liquor characteristics

Property	Unit	Value
pH		13.40
Density	g L^{-1}	1090±10
COD	mg L^{-1}	208900±1160
Total solids	mg L^{-1}	225±5
Ash	%	13.0±0.5
Acid soluble lignin	mg g^{-1}	140±45
Acid insoluble lignin	mg g^{-1}	240±35
Total lignin	%	37.9±7.5
Total carbohydrate	%	2.95±0.50

A stock suspension of the TiO_2 nanoparticles (in aqueous) was prepared and stored at 21°C in sealed 150 ml conical flasks. The stock solutions of TiO_2 were sonicated in an ultrasonic bath (VWR, Mississauga, ON) for approximately 10–15 min to ensure homogeneous mixing prior to reaction solution preparation.

Photocatalytic reactions were performed in a modified Rayonet RPR−100 UV photocatalytic chamber (The Southern New England Ultraviolet Company, CT, USA). Configuration of the reactor and procedures followed during the photocatalytic degradation experiment were reported by Shewa and Lalman (2014).

The photocatalytic degradation experiments were conducted at an initial pH of 7. The pH of the black liquor solution was adjusted to pH 7 before the reaction using 1 M HCl. The pH was not controlled during the reaction. The pH was determined using a pH meter (Symphony, VWR, Mississauga, ON, Canada). All the solutions were prepared using Milli-Q® water.

The effluent from the photo-chemical reactor was centrifuged (Marathon 3200R centrifuge, Fisher-Scientific, Blaine, MN) at 3000 rpm for 20 minutes to separate the TiO_2 particles from the solution. The clear centrate, pretreated black liquor (PrBL), was removed and stored at 4^oC prior to feeding to the anaerobic reactors and SCMFCs.

After the first stage anaerobic digestion, photocatalysis was performed on the effluent for 2 hours using a TiO_2 concentration of 1000 mg L^{-1} and 10 RPM. Next, the effluent from the photocatalytic reactor was centrifuged at 3000 rpm for 20 minutes to obtain a clear centrate prior to feeding to the 2nd stage AD.

7.2.4 Anaerobic reactor set-up and operation

Before adding the photocatalytic reaction mixture, the anaerobic reactors (160 mL Serum bottles) were wrapped in aluminum foil to prevent light penetration. Next, the bottles were filled with 50 mL of the PrBL, basal media and mixed anaerobic culture (2000 mg VSS L^{-1}) under a 70% N_2/30% CO_2 (Praxair Inc., ON) atmosphere. Finally, the bottles were sealed with Teflon$^®$-lined silicone rubber septa (Cobert Assoc., St. Louis, MO) and aluminum crimp caps (Cobert Assoc., St. Louis, MO). The bottles were agitated using an orbital shaker (Lab Line Instruments Model 3520, IA) at 200 rpm and maintained at $37\pm1°C$ throughout the duration of the study. The study was conducted for 4 days. The photocatalysis procedure used for the 1st stage AD was repeated again using the effluent from 1st stage AD. The treated 1st stage AD photocatalytic effluent was fed to the 2nd stage AD.

7.2.5 Microbial fuel cell set-up and operation

The MFC (working volume 130 mL) and the air-cathode were constructed as previously described by Shewa and Lalman (2014) (Figure 7.2). The carbon brush anodes (9 cm long and 9 cm in outer diameter) (Mill-Rose Co., Mentor, OH) were constructed with a Panex 35 carbon fiber fill (400,000 tips per inch) and fixed to a titanium stem wire (12.5 cm long and 0.135 cm diameter).
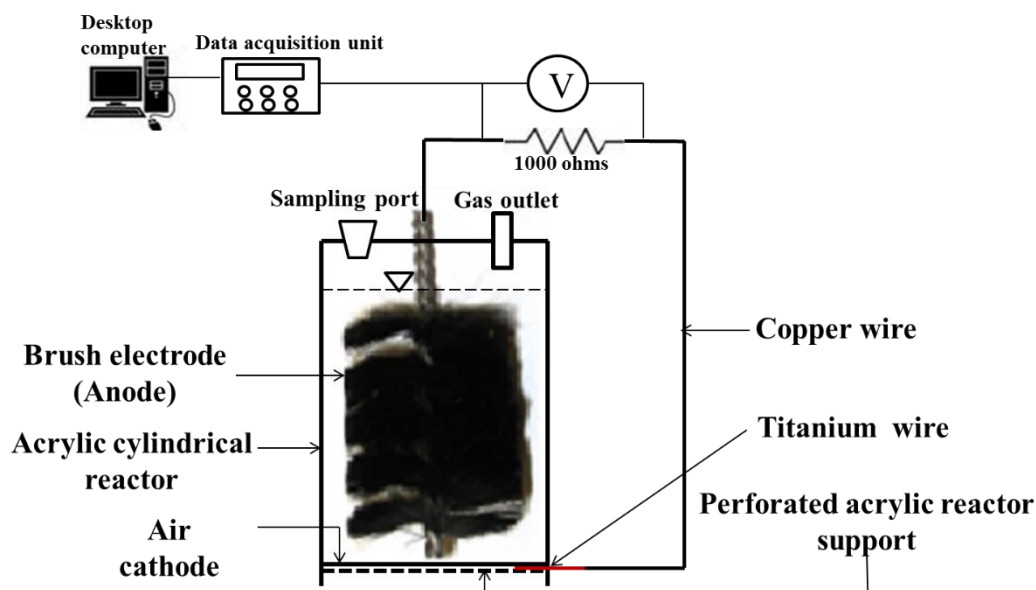
Figure 7.2 Schematic of the single-chamber microbial fuel cell.

All the SCMFCs were operated in batch mode at 37±1 ∘C. The SCMFCs were fed repeatedly with fresh solution until the voltage decreased to within the range 20 to 50 mV. The time for the voltage to decrease within 20 to 50 mV was designated as one feeding cycle.

7.2.6 Analytical methods

7.2.6.1 Gas analysis

Headspace gas samples (25 µl) were removed from the anaerobic reactor every 24 hr and analyzed using a Varian-3600 (Varian, Palo Alto, CA) gas chromatograph (GC) configured with a thermal conductivity detector (TCD). A 2 m long X 2 mm I.D. Carbon Shin column (Alltech, Deerfield, IL) was used for conducting the analysis. The GC injector, detector, and oven temperatures were set at 100°C, 200°C, and 200°C, respectively. The nitrogen carrier gas flow rate was set at 10 mL min^{-1}. The detection limit for methane was 0.0064 kPa [5µL/ bottle (160 mL)].

7.2.6.2 Electrochemical and biochemical analysis

Measurement of the voltage, electrochemical analysis (cyclic voltammetry (CV)) and linear swipe voltammetry (LCV)) were performed according to the procedures and methods described in Shewa et al. (2014a). The coulombic efficiencies (C_E) for SCMFCs were calculated using Equation 7.1 (Logan, 2008).

$$C_E = \frac{M \int_0^{t_b} Idt}{Fb\,v_{An}\,\Delta COD}$$

(7.1)

where M is the molecular weight of oxygen (32), t_b is time for one feeding cycle, I is the current, F is Faraday's constant, b is the number of electrons exchanged per mole of oxygen (4), v_{An} is the volume of liquid in the anode compartment and ΔCOD is the change in the chemical oxygen demand (COD) over a feeding cycle.

The energy conversion efficiency (ECE) was obtained by multiplying coulombic efficiency and potential efficiency (PE) where PE is the ratio between actual cell voltage and open circuit voltage (OCV) (Lee et al., 2008).

COD and BOD of liquid samples were determined in accordance with *Standard Methods* (APHA et al., 2005). Liquid samples were filtered through a 0.2 µm filter paper prior to the COD and BOD analyses.

7.3 Results and discussion

7.3.1 Photocatalytic degradation

Biological treatment of wastes containing recalcitrant chemicals is challenging because of concerns related to toxicity and biodegradation. In some cases, researchers have utilized model chemicals to assess toxicity and biodegradability before conducting studies with effluents containing chemicals containing complex structures. According to Oller et al. (2011), a systematic procedure of utilizing model chemicals with simultaneous evaluation of toxicity and biodegradability is a usually approach together with employing pilot-plant scale studies using industrial effluents. The approach suggested by Oller et al. (2011) has been adopted in studies conducted by Shewa et al. (2014b). Shewa et al. (2014b) evaluated the photocatalytic degradation of a model lignin compound before assessing the photo degradation of black liquor. The optimization and the modeling of the photocatalytic degradation of the model lignin compound (LS) was performed using the Box-Behnken design (BBD) indicated that the factor values for maximum BOD_5/COD ratio were at an 569 mg COD L^{-1} LS concentration, 944 mg L^{-1}

TiO$_2$ and 9 RPM (Shewa et al., 2014b). The operational conduction used by Shewa et al. (2014b) were an irradiation time of 4 hr and an initial pH of 7.

The selected operating conditions for black liquor photocatalytic pretreatment were 5000 mg L^{-1} black liquor (962 mg COD L^{-1}), 1000 mg L^{-1} TiO$_2$ concentration and 10 RPM. The BOD$_5$ and COD of the effluent from the photocatalytic degradation of the black liquor were 248 mg L^{-1} and 620 mg L^{-1}, respectively with a BOD$_5$ to COD ratio of 0.4.

7.3.2 Two-stage anaerobic digestion

The COD of the diluted black liquor fed to the photo-reactor was 962 mg L^{-1}. Pretreatment using photocatalysis improved the biodegradability of the diluted black liquor feed and at the same time removed 35.5±3.6% of the COD. Approximately 64.4% of the COD (620 g L^{-1}) was available for biogas production. The quantity of biogas produced from the 2-stage AD process is shown in Table 7.2.

Table 7.2 Total biogas production.

CH$_4$ (mL per g COD$_{added}$)		Total CH$_4$ production from PrBL (mL per g COD$_{added}$)	Total CH$_4$ production from diluted BL (mL per g COD$_{added}$)
Stage I	**Stage II**		
160±25	35±3	195±30	130±20

The gas yield from the 1st-stage AD process reached 161 mL CH$_4$ per g COD$_{added}$ (Table 7.2). Approximately 34 mL CH$_4$ per g COD$_{added}$ was produced during the 2nd-stage AD process (Table 7.2). This represents an increase in the CH$_4$ gas yield of approximately 21%. The total amount of CH$_4$ produced based on 1 L or 1.086 kg of black liquor was 23.4 L. Note that the percent solids content of the raw black liquor was

approximately 20.6%. The CH$_4$ gas production was approximately 0.022 m^3 per kg of liquid black liquor. The total CH$_4$ yield (195±30 mL CH$_4$ per g COD$_{added}$) achieved from this study demonstrates the capability of 2-stage AD process to recover energy from black liquor. The data indicate photocatalytic degradation resulted in substrates which were degraded by anaerobic microorganisms (Liu et al., 2002).

The CH$_4$ yield from AD of readily biodegradable substrates is variable and typically range from 50 to 80% of the theoretical CH$_4$ yield assuming 1 mol glucose produces 3 mol CH$_4$ (Rabaey et al., 2005). In this study, the CH$_4$ yield from PrBL AD was 56±8% of the theoretical CH$_4$ yield. The reason for not attaining the maximum biogas production might be attributed to the oxidative nature of the photocatalysis process which resulted in loss of reduced carbon chemicals for AD (Carlsson et al., 2012). An additional reason is the possible presence of residual lignin in the pretreated black liquor. In addition, increasing biogas production can be expected if the retention time is extended to greater than 4 days.

7.3.3 Microbial fuel cell performance

Shewa and Lalman (2014) recently reported electricity production from a feed containing a model lignin compound. Evaluating the performance of the SCMFCs was based on voltage generation, power density, potential efficiency, columbic efficiency and COD removal. In this case, we tested different feeds that included 1) diluted black liquor, and 2) pretreated black liquor (PrBL).

7.3.3.1 Electricity generation

The feasibility of utilizing PrBL as a feedstock for electricity generation was evaluated and compared with glucose. The SCMFCs were fed repeatedly with glucose and until a repeatable voltage was achieved and thereafter, the reactors were fed with PrBL plus glucose in an incremental fashion (Table 7.3). The glucose level in the fed was reduced while incrementally increasing the PrBL concentration. The results show that the biofilm adapted to PrBL after three feeding cycles. Similar studies conducted by Chae et al. (2009) indicated that an anode biofilm enriched for a specific substrate has the potential to acclimate to other substrates within a short time depending on the substrate type. The phylum-level relative abundance of dominant bacterial in PrBL fed SCMFCs is shown in Appendix F (Figure F1).

The maximum voltage produced from SCMFCs fed with PrBL at different proportions is shown in Table 7.3. The COD content of the feeds at each phase was constant in order to compare the electricity generation capacity. The maximum voltage of 524±93 mV which was achieved for PrBL fed SCMFCs was approximately 82% of the maximum achieved from glucose fed SCMFCs. The voltage production data clearly indicate the electricity producing potential of SCMFCs feed with PrBL (Figure 7.3).

Table 7.3 Maximum voltages obtained with glucose, glucose plus PrBL mixtures and PrBL

Substrate	Maximum Voltage (V)
Glucose (GL)	0.640±0.010
GL(2/3) plus PrBL(1/3)	0.590±0.045
GL(1/3) plus PrBL(2/3)	0.600±0.040
PrBL only	0.525±0.095

Note: COD content of the feeds at each phase = 620±25 mg/L;
    GL = Glucose; PrBL = Pretreated black liquor.
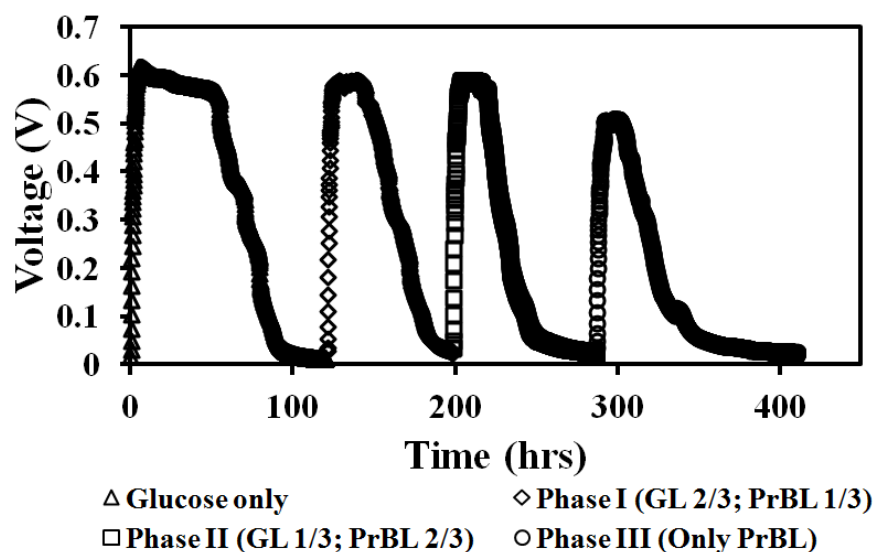
Figure 7.3 Voltage generation from GL (glucose) and PrBL (pretreated black liquor) at mesophilic temperature for one feeding cycle after obtaining a stable and repeatable voltage.

The SCMFCs controls were operated with the feed containing media plus nutrients and without PrBL to demonstrate that PrBL is the source of electron equivalents for electricity production. The controls show that in the absence of PrBL, the electricity generation capacity was low (Figure 7.4). A comparison of the voltage produced in the presence of PrBL (Figure 7.3) and in the absence of PrBL (Figure 7.4) clearly indicates that PrBL and its precursors were substrates which were utilized for electricity generation by electrogenic bacteria. To the best of our knowledge, this is the first study to demonstrate electricity production from byproducts produced from diluted photocatalyzed black liquor.
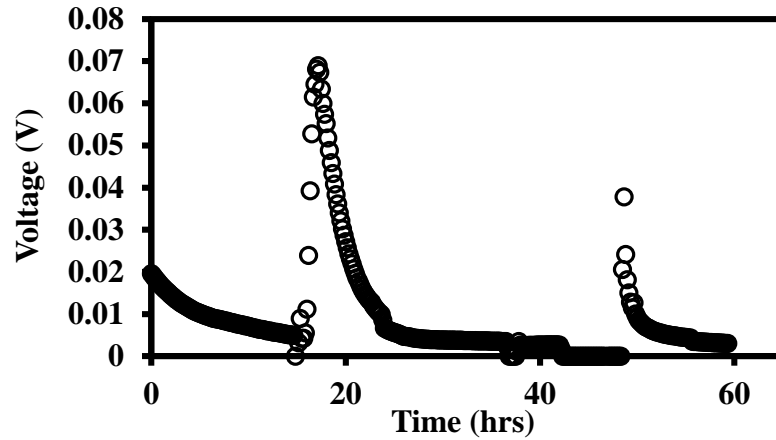
Figure 7.4 Back ground experiment without substrate (control).
(Initial COD = 0 mg L^{-1}; Initial pH = 7±1)

7.3.3.2 Effect of pretreatment

To examine the impact of black liquor pretreatment on electricity generation, SCMFCs fed black liquor were compared with those fed glucose and glucose plus PrBL mixtures (Figures 7.3 and 7.5). The diluted black liquor and PrBL fed reactors generated electricity with maximum voltages of 565±20 mV and 525±95 mV, respectively. Notice the voltage data (Figures 7.3 and 7.5) indicate substrates depletion after 50 hr for the black liquor fed cultures compared to more than 96 hrs for the PrBL fed SCMFCs. This voltage data indicate the diluted black liquor has limited quantity of biodegradable substrate for electricity production compared to PrBL irrespective of the greater COD level in the diluted black liquor (1000 mg L^{-1}) when compared to PrBL (620 mg L^{-1}). In addition, the diluted black liquor has a lower BOD$_5$ to COD ratio of 0.08 compared to that of PrBL (BOD$_5$/COD = 0.40).
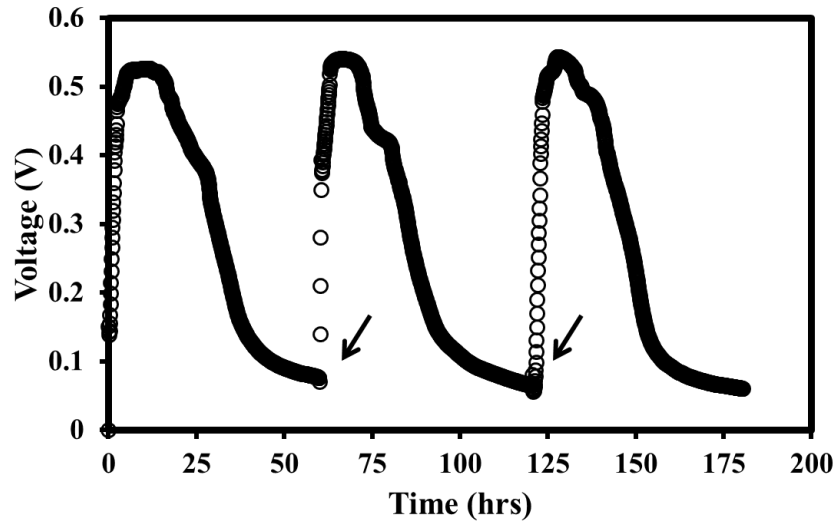
Figure 7.5 Voltage generation from diluted black liquor (Initial COD = 1000 mg L^{-1}; Initial pH = 7±1). Arrows indicate addition of fresh feed.

Based on the difference in the voltages, pretreating the diluted black liquor resulted in producing a larger and a steady voltage for a longer time when compared to untreated diluted black liquor. The data indicate that employing photocataysis pretreatment is a feasible method of improving biodegradability of diluted black liquor and converting it into a feed containing biodegradable chemicals which can be utilized for producing electricity (Ren et al., 2007; Pant et al., 2010). The photacatalyic degradation process of the diluted black liquor could result in the formation of short chain carbon chemicals as well as phenolics which were degraded by the electrogenic microbial community. Bermek et al. (2014) claimed that phenolic compounds appeared to be degraded successfully by the bacterial community in MFCs. They also reported 50% total phenolic removal efficiency in MFC treating olive oil mill wastewater.

7.3.3.3 Power density

According to Pant et al. (2010), the current and power density, C_E and substrate removal efficiencies differences between various reported studies is due to the experimental conditions under examination. These conditions include initial wastewater composition, concentration and MFC operating conditions. The power produced from the SCMFCs fed with PrBL was monitored under similar conditions in comparison to those fed glucose. The COD level in the feed containing either glucose or PrBL was maintained at 620 mg COD L^{-1} to aid in comparison of the data set. The PrBL fed SCMFCs generated maximum current and power densities of 8,045 mA m^{-3} and 2,815 mW m^{-3}, respectively. The corresponding maximum current and power densities normalized to the cathode area were 1,065 mA m^{-2} and 373 mW m^{-2}, respectively.

Even though the initial PrBL and the initial glucose fed levels in SCMFCs were maintained at a constant COD concentration (620 mg L^{-1}), the amount of electricity produced was not the same (Table 7.4). Several studies conducted with different substrates reported less power production than that achieved with acetate and glucose (Logan, 2008). The lower power production could be because of low biodegradability of the substrates and difference in biofilm kinetics (Logan and Rabaey, 2012). SCMFCs fed with PrBL generated less electricity when compared to those fed glucose (Figures 7. 6 and 7.7). The internal resistance (R_{in}) of the SCMFCs fed glucose (202 ohms) was greater than that of PrLS fed SCMFCs (335 ohms). A possible explanation for less power generation and higher R_{in} for PrBL fed SCMFCs is the presence of compounds which are not be easily oxidized by electrogenic bacteria. These compounds may include complex organic chemicals derived from pretreating wood chips (Cardoso et al., 2009).

Numerous studies have indicated that the power generation capacity and performance of MFCs strongly depends on the type of substrate fed to the MFCs (Catal et al., 2008, Lee et al., 2008; Chae et al., 2009; Pant et al., 2010, Sharma and Li, 2010).

Table 7.4 Electrochemical properties of SCMFCs fed with GL and PrBL.

Substrate	Current density		Power density		$R_{in}(\Omega)$
	mA m^{-3}	mA m^{-2}	mW m^{-3}	mW m^{-2}	
Glucose	15630	2070	6425	850	200
PrBL	8045	1065	2815	375	335

Note: R_{in} = Internal resistance.
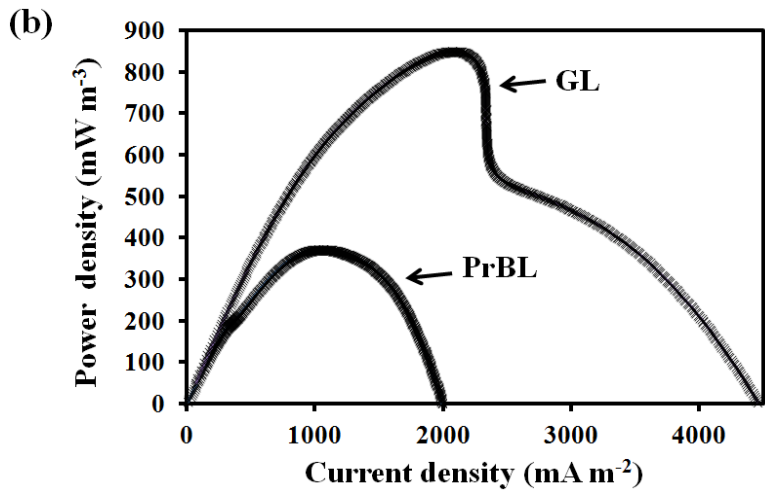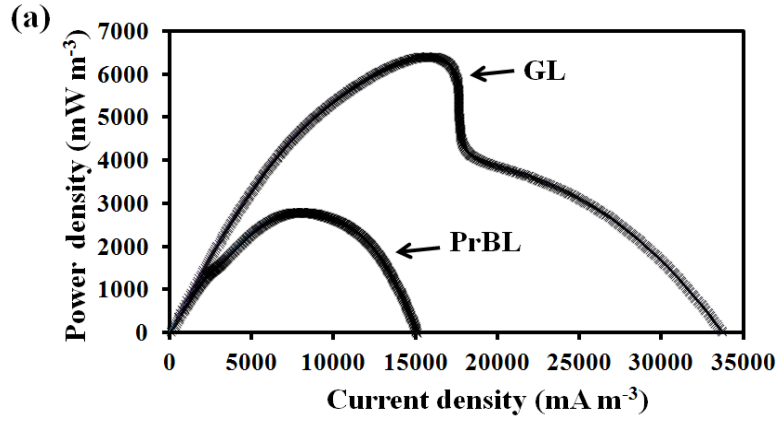
Figure 7.6 Power density curves normalized to (a) working volume and (b) cathode surface area.
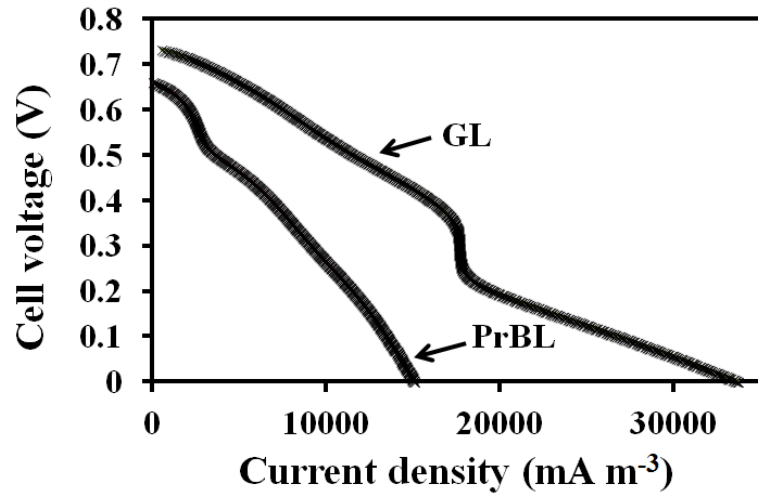
Figure 7.7 Polarization curves of SCMFCs fed GL (glucose) and PrBL (pretreated black liquor).

7.3.3.4 Coulombic efficiency and COD removal

The coulombic efficiency is an indicator of the fraction of organic matter diverted to electricity production (Lefebvre et al., 2008). The C_E obtained from the PrBL fed SCMFCs was 7.8±0.6% (Table 7.5). Similar studies by Ozkaya et al. (2013) using leacheate as a fed to MFCs reported a C_E value of 8%. However, the COD removal reported by Ozakaya et al. (2013) was 45% while in this study the COD removed reached approximately 89%. Work by Min et al. (2005) has reported a C_E of 8% from single chamber MFC treating swine wastewater.

Table 7.5 Efficiencies of SCMFCs fed with GL and PrBL

Substrate	V_{max} (mV)	OCV_{max} (mV)	PE (%)	C_E (%)	ECE (%)	η_{COD} (%)
Glucose	642	829	77.4	20.3	15.7	76.1
PrBL	525	797	65.7	7.8	5.1	89.3

Note: V_{max} = Maximum voltage; OCV = Open circuit voltage; PE = Potential efficiency; C_E = Coulombic efficiency; ECE = Energy conversion efficiency; η_{COD} = COD removal efficiency

The low C_E (7.8±0.6%) achieved from PrBL might be attributed to the presence of methanogens which compete with electrochemically active microorganisms and convert organic material to methane (Oliveira et al., 2013). This is a major drawback of MFCs since, methane production can considerably lower the amount of electricity that can be potentially harvested (Lefebvre et al., 2008). However, when considering wastewater treatment, this could be acceptable since other processes can be seen as co-treatment which results in improving the overall treatment efficiency (Lefebvre et al., 2008).

In comparison to PrBL, the higher C_E value (20.3%) for glucose fed SCMFCs is consistent with previous studies conducted on glucose fed MFCs. The C_E reported in this study is comparable with values reported by Cheng et al. (2006). Using similar graphite

brush anode electrodes and air-cathode, Cheng et al. (2006) reported a C_E of 23%. The higher C_E values observed for SCMFCs fed glucose is attributed to the biodegradability of glucose and its byproducts when compared to PrBL. Work by Chae et al. (2009) has shown a 72.3% C_E for acetate-fed MFC while the C_E for butyrate, propionate and glucose were 43.0%, 36.0% and 15.0%, respectively. Catal et al. (2008) also compared C_Es of twelve monosaccharides and reported a range from 21 to 37%.

The potential efficiency for the glucose fed SCMFCs of approximately 77.4% is comparable to the potential efficiency (65.7 %) for PrBL. The COD removal efficiencies were 76.1% and 89.3% for the glucose fed and PrBL fed SCMFCs, respectively. Therefore, the comparable COD removal and potential efficiency achieved when using glucose and PrBL as a feed to SCMFCs confirm that microbial fuel cells are a promising technology for recovering energy from black liquor pretreated with photocatalysis.

7.3.4 Comparison of energy production

Based on the calorific content of glucose, a MFC can theoretically (at 100% efficiency during fermentation) deliver 3 kWh for every kg of organic matter (dry weight) in one single fermentative step (instead of 1 kWh of electricity and 2 kWh of heat per kg in hydrogen and biogas production by employing several process steps) (Rabaey et al., 2005). To aid the comparison of energy production for the two technologies, the energy was calculated based on Joules/COD_{added}. The energy production was 7143 and 874 J/g COD_{added} for the two stage anaerobic digestion and SCMFC, respectively. The corresponding energy generated from the 2 stage AD and SCMFC are 1.98 and 0.24 kWh per kg COD_{added}, respectively. Despite the fact that energy conversion efficiencies are higher for MFCs compared to other biofuel production processes, the results from this

study indicate that the energy recovered by the SCMFC is less than that of the 2-stage AD. The lower generation of electricity by MFCs, which is less than the theoretical expected generation, can be attributed to physical, chemical and biochemical factors that include (1) the microbial activity to oxidize the PrBL, (2) electron transfer rate to the electrode from the microbes, (3) circuit resistance, (4) proton transfer from the anode compartment to the air-cathode, (5) oxygen supply and reduction at the cathode, and (6) oxygen diffusion into the anode compartment (Kim et al., 2006). According to studies conducted by Liu et al. (2005), factors that are responsible for low electron and energy recoveries in MFCs could be attributed to oxygen transfer into the anode chamber, substrate loss due to methanogenesis, use of substrate for bacterial growth and production of biomass, presence of alternate electron acceptors, such as sulfate present in the medium. It should be noted that in the energy production calculation for the SCMFCs, the methane produced from the SCMFCs was not taken into account.

Even though the assessment of energy production for the two technologies revealed a higher energy production from 2-stage AD, several potential benefits from using MFCs include energy, environmental, operational and economic sustainability (Li et al., 2014). Direct electricity generation in MFCs is also an obvious advantage over the 2-stage AD which require biogas collection, and the conversion of methane into useful energy carrier (He et al. 2005; He, 2013). The 2 stage AD process which is configured with two photocatalytic degradation stages and 2 AD stages is operationally complex when compared to SCMFC for energy generation from black liquor (Figure 7.1). In addition, in the 2-stage AD process, biogas storage is complicated, the quality of the biogas produced is often suboptimal, and in biogas containing H_2S, the removal is costly (Pham

169

et al., 2006). It should be noted that biogas is usually used in combined heat and power (CHP) stations and the electric efficiency acieved in such systems is only up to 43% (Weiland, 2010). According to Weiland (2010), the other alternatives to the common motor CHP stations, such as microgas turbines result in a much lower electric efficiency of 25 to 31%.

7.4 Conclusions

This study demonstrated the feasibility of using a 2-stage AD or electro-biochemical processes for treating and recovering energy from diluted black liquor. The energy produced from both systems was analyzed and quantified. This is the first study to demonstrate the possibility and potential of producing electricity from diluted black liquor using MFCs. The conclusions from this study are as follows:

- The UV/TiO$_2$ photocatalytic degradation process enhanced the biodegradablility of black liquor.

- A total biogas production of 195±30 mL CH$_4$ per g COD$_{added}$ was obtained from a two-stage anaerobic digestion of PrBL.

- The PrBL feed SCMFCs, operating at 37°C, generated maximum current and power densities of 8045±340 mA m^{-3} and 2815±120 mW m^{-3}, respectively. The corresponding maximum current and power densities normalized to the cathode area were 1065±45 mA m^{-2} and 375±15 mW m^{-2}, respectively. The SCMFCs removed 89.3±0.8% of the COD of PrBL and achieved a coulombic and potential efficiencies of 7.8±0.6% and 65.7%, respectively.

- The low current and power densities for SCMFCs fed PrBL compared to those fed glucose is likely due to the inability of electrogenic bacteria to oxidize complex organic compounds.

- The 2 stage AD produced higher amount of energy (1.98±0.30 kWh per kg CODadded) from PrBL compared to the energy recovered by SCMFC (0.24±0.02 kWh per kg CODadded).

7.5 References

Abbasi, T., Tauseef, S.M., and Abbasi, S.A. (2012) Biogas and biogas energy: an introduction. In *Biogas Energy*. New York, NY: Springer, pp. 1–10.

Abu-Orf, M., and Goss, T. (2013) Close-coupled gasification: where does it fit economically in processing residuals? *Proceedings of the Water Environment Federation*, 2013(16): 2169–2178.

APHA, AWWA, and WPCF. (2005) Standard methods for the examination of water and wastewater, 21st edn. Washington, D.C: American Public Health Association.

Angelidaki, I., and Sanders, W. (2004) Assessment of the anaerobic biodegradability of macropollutants. *Rev. Environ. Sci. Biotechnol.* **3**(2): 117–129.

Angenent, L.T., Karim, K., Al-Dahhan, M.H., Wrenn, B.A., and Domíguez-Espinosa, R. (2004) Production of bioenergy and biochemicals from industrial and agricultural wastewater. *Trends Biotechnol.* **22**(9): 477–485.

Bajpai, P. (2012) Brief description of the pulp and paper making process. In *Biotechnology for pulp and paper processing*. New York, NY: Springer, pp. 7–14.

Bermek, H., Catal, T., Akan, S.S., Ulutaş, M.S., Kumru, M., Özgüven, M., et al. (2014) Olive mill wastewater treatment in single-chamber air-cathode microbial fuel cells. *World J. Microbiol. Biotechnol.* **30**(4): 1177–85.

Cardoso, M., de Oliveira, É.D., and Passos, M.L. (2009) Chemical composition and physical properties of black liquors and their effects on liquor recovery operation in Brazilian pulp mills. *Fuel* **88**(4): 756–763.

Carlsson, M., Lagerkvist, A., and Morgan-Sagastume, F. (2012) The effects of substrate pre-treatment on anaerobic digestion systems: A review. *Waste Manag.* **32**(9): 1634–1650.

Catal, T., Li, K., Bermek, H., and Liu, H. (2008) Electricity production from twelve monosaccharides using microbial fuel cells. *J. Power Sources* **175**(1): 196–200.

Chae, K.-J., Choi, M.-J., Lee, J.-W., Kim, K.-Y., and Kim, I.S. (2009) Effect of different substrates on the performance, bacterial diversity, and bacterial viability in microbial fuel cells. *Bioresour. Technol.* **100**(14): 3518–3525.

Chang, I.S., Moon, H.., Bretschger, O., Jang, J.K., Park, H.I., Nealson, K. H., and Kim, B.H. (2006) Electrochemically active bacteria (EAB) and mediator-less microbial fuel cells. *J. Microbiol. Biotechnol.* **16**(2): 163–177.

Cheng, S., Liu, H., and Logan, B.E. (2006) Increased performance of single-chamber microbial fuel cells using an improved cathode structure. *Electrochem. Commun.* **8**(3): 489–494.

Chynoweth, D.P., Owens, J.M., and Legrand, R. (2000) Renewable methane from anaerobic digestion of biomass. *Renew. Energy* **22**(1): 1–8.

Fongsatitkul, P., Elefsiniotis, P., and Wareham, D.G. (2012) Two-phase anaerobic digestion of the organic fraction of municipal solid waste: estimation of methane production. *Waste Manag. Res.* **30**(7): 720–6.

Font, X., Caminal, G., Gabarrell, X., Romero, S., and Vicent, M.T. (2003) Black liquor detoxification by laccase of Trametes versicolor pellets. *J. Chem. Technol. Biotechnol.* **78**(5): 548–554.

Francis, A.C., and Chungpaibulpatana, S. (2014) Waste heat recovery for power generation using organic rankine cycle in a pulp and paper mill. In *Green Energy for Sustainable Development (ICUE)*, 2014 International Conference and Utility Exhibition. Pattaya: IEEE, pp. 1–6.

He, Z. (2013) Microbial fuel cells: Now let us talk about energy. *Environ. Sci. Technol.* **47**(1): 332–333.

He, Z., Minteer, S.D., and Angenent, L.T. (2005) Electricity generation from artificial wastewater using an upflow microbial fuel cell. *Environ. Sci. Technol.* **39**(14): 5262–5267.

Kim, B.H., Chang, I.S., and Moon, H. (2006) Microbial fuel cell-type biochemical oxygen demand sensor. *Encycl. Sensors* **10**: 1–12.

Kortekaas, S., Vidal, G., Yan-Ling, H., Lettinga, G., and Field, J. A. (1998) Anaerobic-aerobic treatment of toxic pulping black liquor with upfront effluent recirculation. *J. Ferment. Bioeng.* **86**: 97–110.

Kyazze, G., Dinsdale, R., Guwy, A.J., Hawkes, F.R., Premier, G.C., and Hawkes, D.L. (2007) Performance characteristics of a two-stage dark fermentative system producing hydrogen and methane continuously. *Biotechnol. Bioeng.* **97**(4): 759–770.

Lara, M.A., Rodríguez-Malaver, A.J., Rojas, O.J., Holmquist, O., González, A.M., Bullón, J., et al. (2003) Black liquor lignin biodegradation by Trametes elegans. *Int. Biodeterior. Biodegrad.* **52**(3): 167–173.

Leach, J.M., and Thakore, A.N. (1976) Toxic constituents of mechanical pulping effluents. *TAPPI J.* **59**: 129–132.

Lee, H.S., Parameswaran, P., Kato-Marcus, A., Torres, C.I., and Rittmann, B.E. (2008) Evaluation of energy-conversion efficiencies in microbial fuel cells (MFCs) utilizing fermentable and non-fermentable substrates. *Water Res.* **42**(6): 1501–1510.

Lefebvre, O., Al-Mamun, A., Ooi, W.K., Tang, Z., Chua, D.H.C., and Ng, H.Y. (2008) An insight into cathode options for microbial fuel cells. *Water Sci. Technol.* **57**(12): 2031–2037.

Li, W.W., Yu, H.Q., and He, Z. (2014) Towards sustainable wastewater treatment by using microbial fuel cells-centered technologies. *Energy Environ. Sci.* **7**(3): 911-924.

Liu, D., Liu, D., Zeng, R.J., and Angelidaki, I. (2006) Hydrogen and methane production from household solid waste in the two-stage fermentation process. *Water Res.* **40**(11): 2230–2236.

Liu, H., Cheng, S., and Logan, B.E. (2005) Production of electricity from acetate or butyrate using a single-chamber microbial fuel cell. *Environ. Sci. Technol.* **39**(2): 658–662.

Logan, B.E. (2008) Microbial fuel cells. New York, NY: John Wiley and Sons.

Logan, B.E. (2009) Exoelectrogenic bacteria that power microbial fuel cells. *Nat. Rev. Microbiol.* **7**(5): 375–381.

Logan, B.E., and Rabaey, K. (2012) Conversion of wastes into bioelectricity and chemicals by using microbial electrochemical technologies. *Science* **337**(6095): 686–690.

Min, B., Kim, J., Oh, S., Regan, J.M., and Logan, B.E. (2005) Electricity generation from swine wastewater using microbial fuel cells. *Water Res.* **39**(20): 4961–4968.

Oliveira, V.B., Simões, M., Melo, L.F., and Pinto, A.M.F.R. (2013) Overview on the developments of microbial fuel cells. *Biochem. Eng. J.* **73**: 53–64.

Oller, I., Malato, S., and Sánchez-Pérez, J. A. (2011) Combination of Advanced Oxidation Processes and biological treatments for wastewater decontamination-A review. *Sci. Total Environ.* **409**(20): 4141–4166.

Ozkaya, B., Cetinkaya, A.Y., Cakmakci, M., Karadağ, D., and Sahinkaya, E. (2013) Electricity generation from young landfill leachate in a microbial fuel cell with a new electrode material. *Bioprocess Biosyst. Eng.* **36**(4): 399–405.

Pant, D., Van Bogaert, G., Diels, L., and Vanbroekhoven, K. (2010) A review of the substrates used in microbial fuel cells (MFCs) for sustainable energy production. *Bioresour. Technol.* **101**(6): 1533–1543.

Pham, T.H., Rabaey, K., Aelterman, P., Clauwaert, P., De Schamphelaire, L., Boon, N., and Verstraete, W. (2006) Microbial fuel cells in relation to conventional anaerobic digestion technology. *Eng. Life Sci.* **6**(3): 285–292.

Poggi-Varaldo, H.M., Munoz-Paez, K.M., Escamilla-Alvarado, C., Robledo-Narváez, P.N., Ponce-Noyola, M.T., Calva-Calva, G., Ríos-Leal, E., Galíndez-Mayer, J., Estrada-Vázquez, C., Ortega-Clemente, A., and Rinderknecht-Seijas, N.F. (2014) Biohydrogen, biomethane and bioelectricity as crucial components of biorefinery of organic wastes: a review. *Waste Manag. Res.* **32**(5): 353–65.

Pokhrel, D., and Viraraghavan, T. (2004) Treatment of pulp and paper mill wastewater - A review. *Sci. Total Environ.* **333**(1): 37–58.

Rabaey, K., Lissens, G., and Verstraete, W. (2005) Microbial fuel cells: performances and perspectives. In *Biofuels for fuel cells: Renewable energy from biomass fermentation*. Lens, P., Westermann, P., Haberbauer, M., and Moreno, A. eds. IWA Publishing, London, pp. 377–399.

Reid, I.D. (1995) Biodegradation of lignin. *Can. J. Bot.* **73**(S1): 1011–1018.

Ren, Z., Ward, T.E., and Regan, J.M. (2007) Electricity production from cellulose in a microbial fuel cell using a defined binary culture. *Environ. Sci. Technol.* **41**(13): 4781–4786.

Schievano, A., Tenca, A., Lonati, S., Manzini, E., and Adani, F. (2014) Can two-stage instead of one-stage anaerobic digestion really increase energy recovery from biomass? *Appl. Energy* **124**: 335–342.

Sharma, Y., and Li, B. (2010) The variation of power generation with organic substrates in single-chamber microbial fuel cells (SCMFCs). *Bioresour. Technol.* **101**(6): 1844–1850.

Shewa, W.A. (2016) Converting low value lignocellulosic residues into valuable products using photo-and bioelectrochemical catalysis. PhD Thesis. University of Windsor, Windsor, Ontario, Canada.

Shewa, W.A., and Lalman, J.A (2014) Producing electricity using a microbial fuel cell fed with feedstock chemicals produced from the photocatalysis of a lignin model chemical. In: Proceedings of the 87th Annual Water and Environment Federation Technical Exhibition and Conference, 27 September–01 October 2014, New Orleans, LA, USA, pp. 2484–2503.

Shewa, W.A., Chaganti, S.R., and Lalman, J.A. (2014a) Electricity generation and biofilm formation in microbial fuel cells using plate anodes constructed from various grades of graphite. *J. Green Eng*, **4**(1): 13–32.

Shewa, W.A., Chaganti, S.R., and Lalman, J.A. (2014b) Optimizing the photocatalytic degradation of a model lignin chemical using a Box-Behnken design and converting the degradation byproducts into electricity *(Unpublished).*

Sierra-Alvarez, R., and Lettinga, G. (1990) The methanogenic toxicity of wood resin constituents. *Biol. Wastes* **33**: 211–226.

Tran, H., and Vakkilainen, E.K. (2007) Advances in the Kraft chemical recovery process. In *Source 3rd ICEP international colloquium on eucalyptus pulp*. Belo Horizonte, Brazil, pp. 4–7.

Ueno, Y., Fukui, H., and Goto, M. (2007) Operation of a two-stage fermentation process producing hydrogen and methane from organic waste. *Environ. Sci. Technol.* **41**(4): 1413–1419.

Weiland, P. (2010) Biogas production: current state and perspectives. *Appl Microbiol Biotechnol* **85**(4): 849–860.

Yadvika, S., Sreekrishnan, T.R., Kohli, S., and Rana, V. (2004) Enhancement of biogas production from solid substrates using different techniques- A review. *Bioresour. Technol.* **95**(1): 1–10.

CHAPTER 8

CONCLUSIONS AND RECOMENDATIONS

This work in this thesis investigated the importance of photocatalytic degradation as a pretreatment method to reduce the toxicity and improve biodegradability of lignin rich wastewaters. The work further demonstrated the possibility of producing electricity from the pretreated wastewater using MFCs. MFCs are bioelectrochemical systems that use electrochemically active bacteria to generate electricity from organic compounds. In addition to the electricity generation, this research has also given an account of the treatment capacity of the photocatalytic degradation and bioelectrochemical processes in terms of COD removal efficiency. Chapters 3 and 4 focused on the evaluation and selection of best performing anode electrode for the MFC set up. The work in Chapters 5 and 6 present several key findings on the photocatalytic degradation and MFC performances using a model lignin chemical as a substrate. The work in Chapter 7 is focused on electricity generation from black liquor using MFC and comparing energy production with that of a 2-stage AD process.

Configuration and selection of electrode material play important role in electricity generation from MFCs. In this study an air-cathode single chamber MFC (SCMFC) was selected because it has low internal resistance and increased mass transfer from the anode to cathode (Liu et al., 2005). SCMFCs are the most likely configuration to be scaled up for wastewater treatment due to their high power output, simple structure, and relatively low cost (Kim et al., 2007; Cheng and Logan, 2011). The anode electrode performance evaluation study conducted in Chapters 3 and 4 indicated that graphite brush electrode is

the preferred option and the trend for increasing electricity generation was as follows: Brush > POCO3 > G347 > Felt > HK06.

Chapters 5 and 6 have shown the process for the controlled or partial photocatalysis of a model lignin compound, sodium lignosulfonate (LS), and more particularly the production of feedstock chemicals by photocatalysis for use in MFCs. The optimization and modeling of the photocatalytic degradation process, performed using the Box-Behnken design method, indicated that a maximum BOD_5/COD ratio (0.3859) was obtained under optimum conditions of an initial LS concentration of 569 mg COD L^{-1}, TiO_2 concentration of 944 mg L^{-1} and 9 RPM. The liquid chromatography–mass spectrometry (LC-MS) analysis indicated the presence of several biodegradable compounds in the photocatalytic degradation byproducts (PrLS). The PrLS (390 mg COD L^{-1}) was used to produce electricity in single chamber microbial fuel cells (SCMFCs) and the results from this study indicate that the PrLS fed SCMFCs, operated at 37 ± 1^oC, generated maximum current and power densities of $6,555\pm360$ mA m^{-3} and $1,880\pm105$mW m^{-3}, respectively. The corresponding maximum current and power densities normalized to the cathode area were 870 ± 50 mA m^{-2} and 250 ± 15 mW m^{-2}, respectively. The SCMFCs removed $77.6\pm2.3\%$ of the COD of the PrLS and achieved a coulombic efficiency of $17.7\pm1.2\%$.

The most obvious finding to emerge from Chapter 7 is the possibility and potential of generating electricity from black liquor, a lignin rich waste from pulp and paper mills, using MFCs. The black liquor was pretreated with UV/TiO_2 photocatalysis. The effluent (PrBL) from the photocatalytic degradation process was fed to SCMFCs and generated maximum current and power densities of 8045 ± 340 mA m^{-3} and 2815 ± 120 mW m^{-3}

respectively. The SCMFCs removed 89.3% of the COD of PrBL and achieved coulombic and potential efficiencies of 7.8% and 65.7%, respectively. This study demonstrated that combining photocatalysis together with a bioelectrochemical process was useful for recovering energy from black liquor.

In Chapter 7, the energy production from PrBL using a 2-stage anaerobic digestion (AD) was assessed and compared with that of SCMFCs. The comparison study revealed energy production were 7145 ± 1060 and 875 ± 70 J/g COD_{added} for the 2-stage AD and SCMFC, respectively. Evidence from this study suggests the potential losses in the SCMFCs and the chemicals found in PrBLwhich were not converted to electricity might be the main reasons for the lower energy yield. Therefore, further work is required to reduce the potential losses and explore the possibility of collecting methane from the MFCs.

Further studies on TiO_2 recovery and reuse are recommended as this will aid in lowering the cost of the photocatalytic degradation process. Techniques to immobilize TiO_2 could be adopted to avoid post-treatment processes such as filtration (Ray, 2010; Mukherjee et al., 2013).

Visible light instead of UV light could also be considered for the photocatalysis process which could be conducted by modifying TiO_2 using methods such as coupling with a narrow band gap semiconductor, metal ion/non-metal ion doping, codoping with two or more foreign ions, surface sensitization by organic dyes or metal complexes and noble metal deposition (Kumar and Devi, 2012). Note that in spite of extensive research efforts, the photocatalytic research efforts in the visible region have remained relatively low (Kamat, 2012).

Studies on the continuously operating SCMFCs based on the results obtained in this study are also needed to provide design and operation data for practical implementation and scaling-up. Research and design considerations will be required to improve the performance of MFCs, generate higher electrical energy, and increase the efficiency for scaling up the technology. The improvements could include optimization of MFC operating conditions, increasing the air-cathode surface area (Cheng and Logan, 2011), modification of MFC designs (Janicek et al., 2014) and treatment of electrodes (Feng et al., 2010). Note that the manufacturing capacity to produce air-cathodes is the main obstacle for commercial production of MFCs which represents both a business opportunity and a production challenge (Logan et al., 2015).

References

Cheng, S., and Logan, B.E. (2011) Increasing power generation for scaling up single-chamber air-cathode microbial fuel cells. *Bioresour. Technol.* **102**(6): 4468–4473.

Feng, Y., Yang, Q., Wang, X., and Logan, B.E. (2010) Treatment of carbon fiber brush anodes for improving power generation in air-cathode microbial fuel cells. *J. Power Sources* **195**(7): 1841–1844.

Janicek, A., Fan, Y., and Liu, H. (2014) Design of microbial fuel cells for practical application: a review and analysis of scale-up studies. *Biofuels* **5**(1): 79–92.

Kamat, P. V. (2012) TiO_2 nanostructures: Recent physical chemistry advances. *J. Phys. Chem. C* **116**(22): 11849–11851.

Kim, J.R., Jung, S.H., Regan, J.M., and Logan, B.E. (2007) Electricity generation and microbial community analysis of alcohol powered microbial fuel cells. *Bioresour. Technol.* **98**(13): 2568–2577.

Kumar, S.G., and Devi, L.G. (2011) Review on modified TiO_2 photocatalysis under UV / visible light : selected results and related mechanisms on interfacial charge carrier transfer dynamics. *J. Phys. Chem. A* **115**: 13211–13241.

Liu, H., Cheng, S., and Logan, B.E. (2005) Production of electricity from acetate or butyrate using a single-chamber microbial fuel cell. *Environ. Sci. Technol.* **39**(2): 658–662.

Logan, B.E., Wallack, M.J., Kim, K.-Y., He, W., Feng, Y., and Saikaly, P.E. (2015) Assessment of microbial fuel cell configurations and power densities. *Environ. Sci. Technol. Lett.* DOI: 10.1021/acs.estlett.5b00180.

Mukherjee, D., Barghi, S., and Ray, A. (2013) Preparation and characterization of the TiO_2 immobilized polymeric photocatalyst for degradation of aspirin under UV and solar light. *Processes* **2**(1): 12–23.

Ray, S. (2010) Developing an efficient nanocatalyst system for enhanced photocatalytic degradation of toxic aqueous contaminants. PhD Thesis. University of Windsor, Windsor, Ontario, Canada.

CHAPTER 9

ENGINEERING SIGNIFICANCE

The use of lignin, representing approximately 30% of the organic carbon in the biosphere, is becoming more attractive in a variety of applications as it is not dependent on the supply and cost of fossil fuel resources. Lignin is a waste product of industrial processes such as pulping that utilize plant material and it is readily available in large quantities. The overall engineering significance of this dissertation lies in the process for the photocatalysis of lignin and more particularly the production of feedstock chemicals by lignin photocatalysis for use in microbial fuel cells (MFCs) and in anaerobic digestion (AD). The results demonstrate that partial/controlled UV/TiO$_2$ photocatalysis of lignin rich wastewater can be used as a pre-treatment method and electricity could be successfully generated using MFCs and AD. Therefore, the findings of this dissertation contribute to the current interest and search for generating energy from renewable resources.

The evaluation of anode electrode graphite materials (Chapters 3 and 4) contributes to the existing knowledge in microbial fuel cell study by providing crucial comparison parameters that include energy generation capacity, material properties, biofilm microbial diversity and cost of electrode. This study provides tools for selecting suitable anode graphite materials and suggests the need to compare and evaluate different carbon electrode materials. The results from Chapter 5 on investigating operating parameters significantly influence the photocatalytic degradation process of lignin and the optimization and modeling study (Chapter 6) of the selected degradation parameters are

useful to ensure efficient photocatalytic degradation processes for practical applications in pilot or large scale operations.

Another important engineering significance of this dissertation as articulated in Chapter 7 is the energy recovery form black liquor, a lignin-rich waste product from pulp and paper industries, using MFCs and AD. This will be an alternative to the currently used methods for recovering energy from black liquor which include recovery boilers and gasification. An implication of the findings from Chapter 7 is the possibility of using the suggested processes (photocatalytic degradation followed bioelectrochemical processes) for the generation of electricity or biogas and the simultaneous treatment of wastewaters from paper and pulp industries and other facilities that generate lignin-rich effluents.

APPENDICES

APPENDIX A: CALIBRATION CURVES
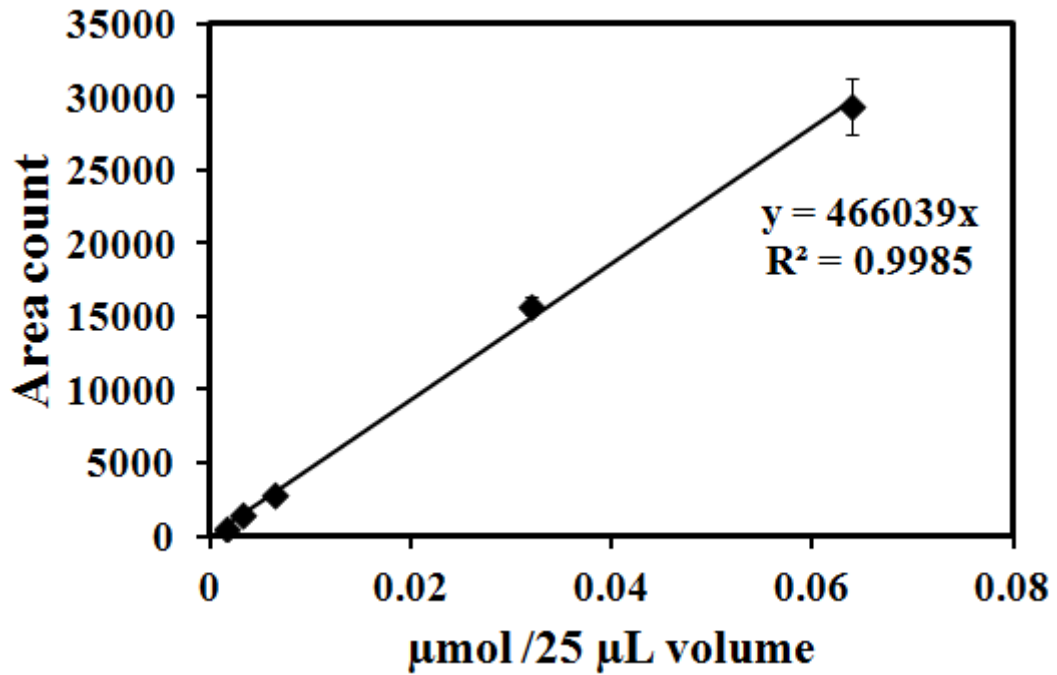
Figure A1 Calibration curve for hydrogen in GC.
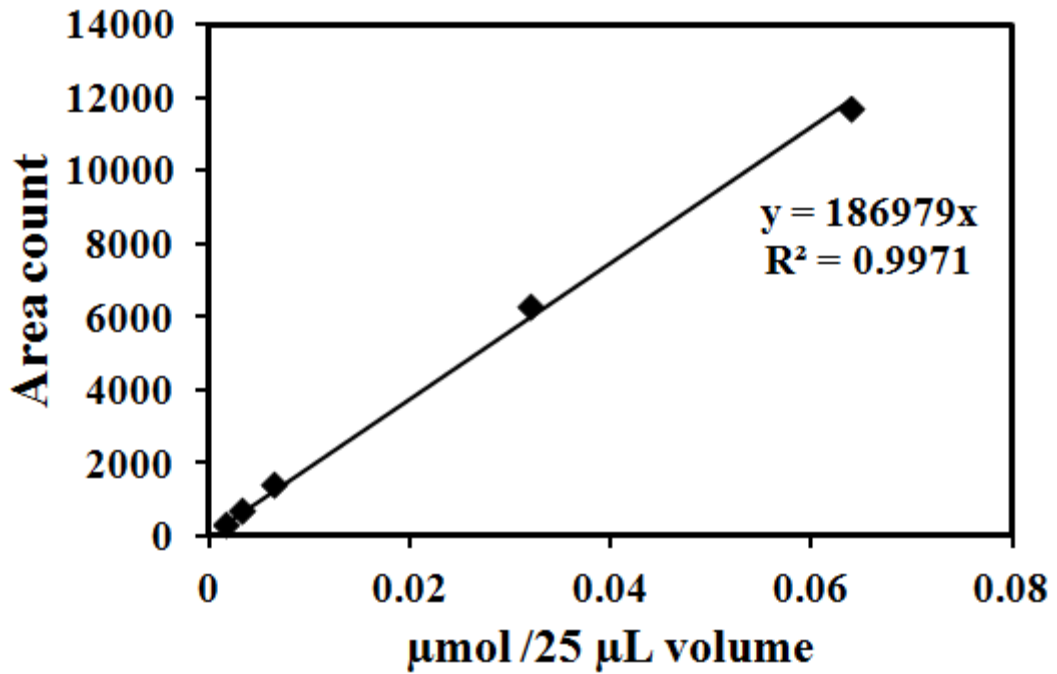
Figure A2 Calibration curve for methane in GC.
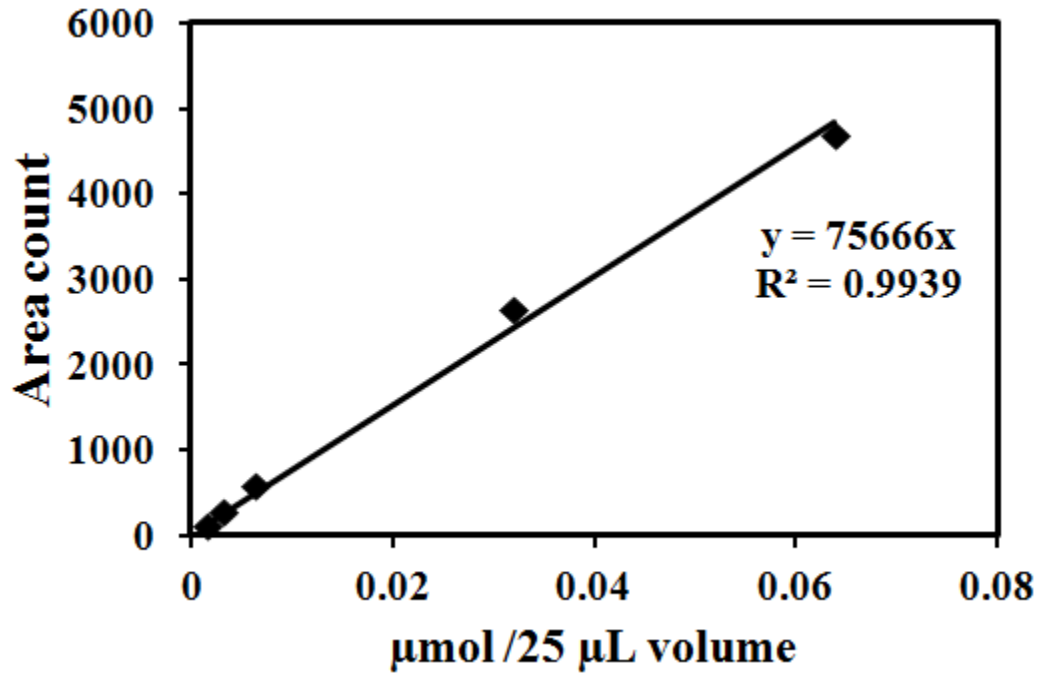
Figure A3 Calibration curve for carbon dioxide in GC.
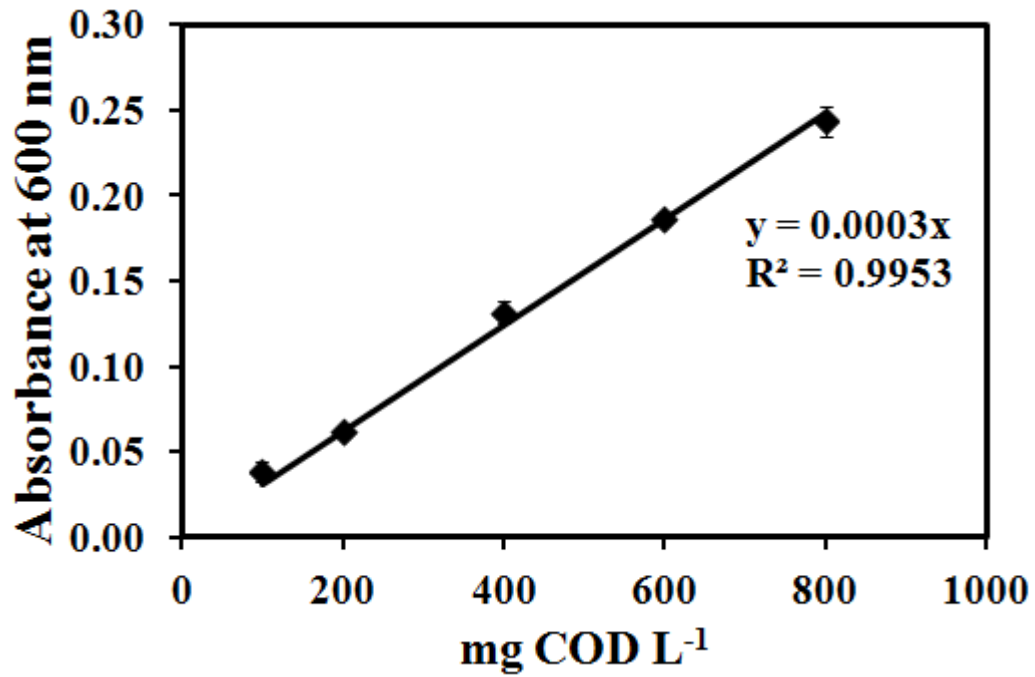
Figure A4 Typical COD calibration curve (higher range).
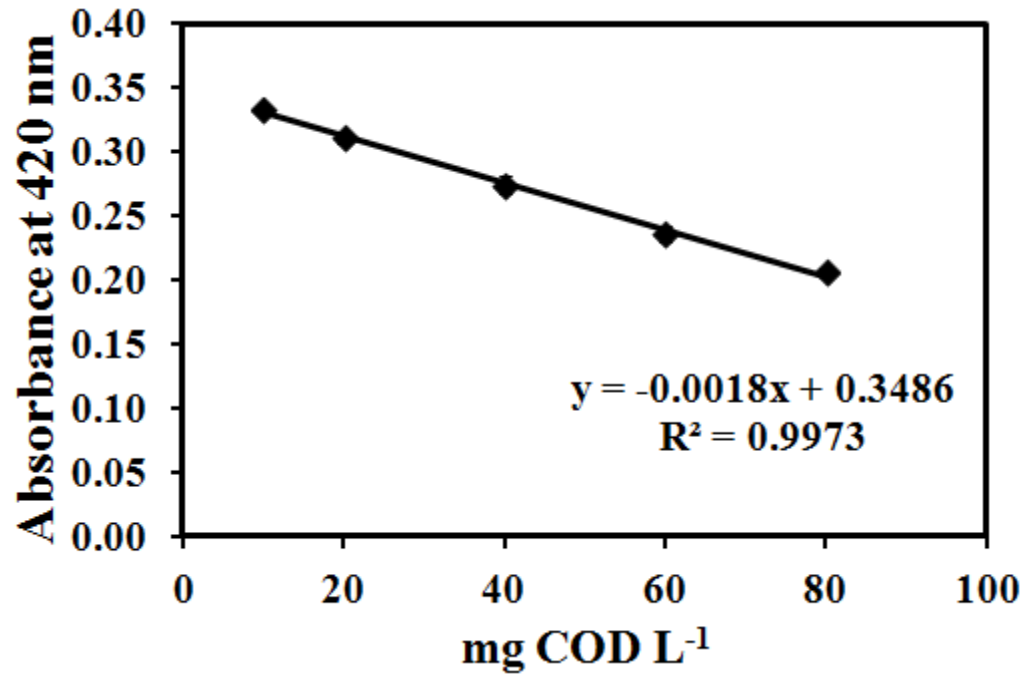
Figure A5 Typical COD calibration curve (lower range).

APPENDIX B: ANALYSIS OF PRODUCTS PRODUCED DURING THE
PHOTOCATALYTIC DEGRADTION OF A MODEL LIGNIN CHEMICAL
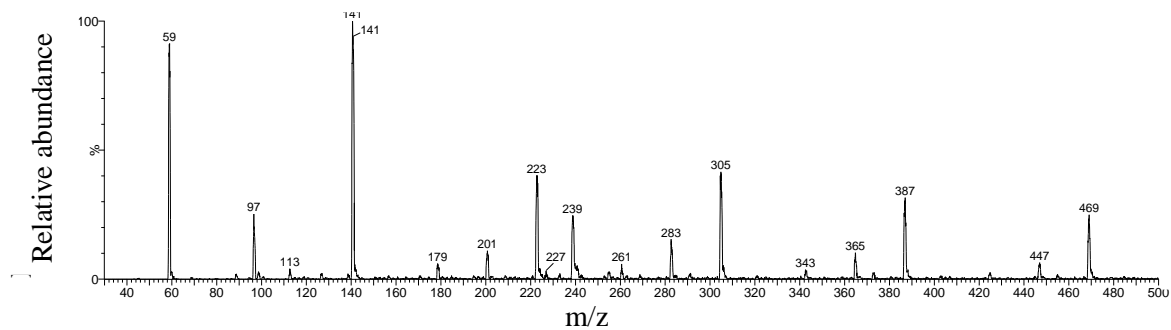
Figure B1 Typical LC-MS spectrum for photocatalysed LS.

APPENDIX C: BLACK LIQUOR CHARACTERIZATION

Figure C1 Digital picture showing the color of 50,000 mg L^{-1} black liquor (5 g black liquor diluted to 100 mL using DI water) a) without pH adjustment (right) b) pH adjusted to 7 (left).

APPENDIX D: PROTOCOL FOR CONSTRUCTING THE AIR-CATHODE

D 1 Material and equipment used for constructing 15 air-cathodes

The air-cathode construction protocol is adopted from (Cheng et al., 2006 and Middaugh et al., 2006). The material used to construct 15 air-cathodes are listed in Table D1. The equipment used to construct the air-cathodes are shown in Figure D1.

Table D1 Material used for constructing 15 air-cathodes.

S.No.	Item Description	Unit	Quantity
1	Carbon cloth	cm^2	540
2	Carbon black powder	mg	850
3	40% PTFE solution	mL	10
4	60% PTFE solution (4 layers)		
5	10% by Weight Platinum on Carbon Powder	mg	1350
6	Nafion® solution	mL	13.5
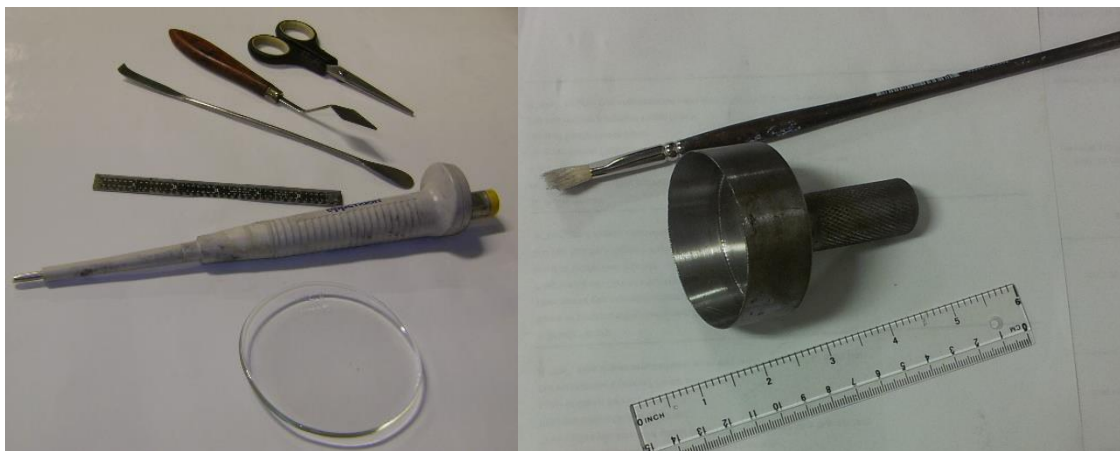
Figure D1 Equipment used for constructing air-cathode.

D2 Applying the Carbon base layer (diffusion layer)

1. Cut 15 pieces of carbon cloth (6 cm X 6 cm) each.

2. Measure 2.5 mg of carbon black for every 1 cm^2 of cathode surface area.

3. Measure 12 µL of 30% PTFE solution for every 1 mg of carbon black.

4. Mix the carbon black with the PTFE solution.

5. Spread the paste-like mixture on one the piece of carbon cloth.

6. Allow the coating to air-dry (Figure D2).

7. Place the piece of carbon cloth in a pre-heated furnace at 370℃ for about 30 minutes.

8. Cool to room temperature.

Figure D2 Digital picture showing carbon cloth pasted with a carbon base layer.

D3: Applying the diffusion layer

1. Apply one coat of 60% PTFE solution the coated side of the carbon cloth.

2. Allow the PTFE coating to air-dry for at least 10 minutes.

3. Place in a pre-heated furnace at 370℃ for 15 minutes.

4. Cool to room temperature.

5. Repeat steps 1 to 2 above three more times to add a total of 4 PTFE coatings.

D4: Applying the Catalyst layer

1. Measure the amount of 10% Pt/C corresponding to 2.5 mg of Pt/C for every 1 cm^2 of cathode surface.

2. Add about 0.83 µL of DI water for every 1 mg of Pt/C in a dropwise fashion to the 10% Pt/C.

3. Measure 10 µL of Nafion solution for every 1 mg of Pt/C using the micropipettor.

4. Mix the "water-treated" Pt/C with the Nafion solution.

5. Spread the paste-like mixture on the side opposite the diffusion layer.

6. Allow the coating to air-dry for at least 24 hours.

7. Punch out the circular air-cathode using 6 cm diameter circular puncher.

References

Cheng, S., Liu, H., and Logan, B.E. (2006) Increased performance of single-chamber microbial fuel cells using an improved cathode structure. *Electrochem. Commun.* **8**(3): 489–494.

Middaugh, J., Cheng, S., Liu, W., and Wagner, R. (2006) How to make cathodes with a diffusion layer for single-chamber microbial fuel cells. [WWW document]. URL http://www.engr.psu.edu/ce/enve/logan/bioenergy/pdf/Cathode_093008.pdf.

APPENDIX E: OPTIMIZATION STUDY AND PRINCIPAL COMPONENT ANALYSIS

E1 Optimization study

There are several design experimental methods available for optimization of experimental factors of a process. In this thesis one-at-a-time method of experimental design was used in some occasions for parameter study and Box-Behnken design (BBD) (Box and Behnken, 1960) was used for the optimization study.

Though there is a role for one-at-a-time plans that they are more effective than orthogonal arrays under certain conditions, the one-at-a-time plans have the following draw backs (Frey et al., 2003):

- More runs are required for the same precision in effect estimation.

- Some interactions between variables cannot be captured.

- The conclusions from the analysis are not general (i.e. only conditional main effects are revealed).

- Optimal settings of factors can be missed and

- One-at-a-time plans essentially rule out the possibility of randomization and can be susceptible to bias due to time trends.

Box-Behnken designs are a class of rotatable or nearly rotatable second-order designs based on three-level incomplete factorial designs (Ferreira et al., 2007). For three factors its graphical representation can be seen in two forms (Ferreira et al., 2007): 1) A cube that consists of the central point and the middle points of the edges, as can be

observed in Figure E-a and a figure of three interlocking 2^2 factorial designs and a central point, as shown in Figure E-b.
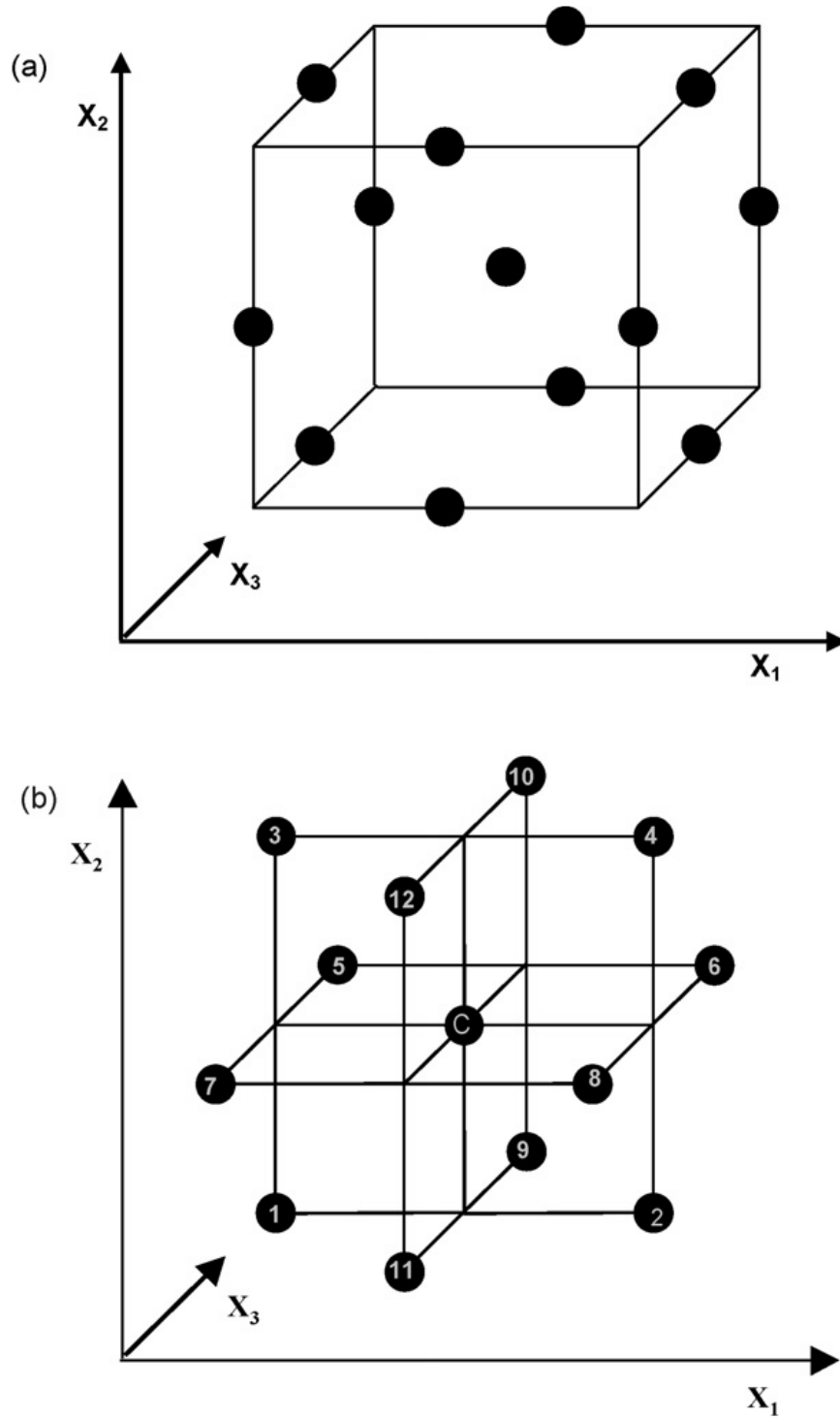

Figure E1 Graphical representation of BBD.

Response surface methodology (RSM) was used to optimize the experiments designed using BBD. The second-order model (Equations E1 and E2) was employed in the response surface methodology used in this thesis for several reasons (Myers et al., 2009). Among these are the following:

1. The second-order model is very flexible. It can take on a wide variety of functional forms, so it will often work well as an approximation to the true response surface.

2. It is easy to estimate the parameters (the β's) in the second-order model.

3. There is considerable practical experience indicating that second-order models work well in solving real response surface problems.

$$y = \beta_0 + \beta_1 x_1 + \beta_2 x_2 + \cdots + \beta_k x_k + \beta_{11} x_1{}^2 + \ldots + \beta_{kk} x_{k1}{}^2 + \beta_{12} x_1 x_2 + \beta_{13} x_1 x_3 +$$
$$\ldots + \beta_{k-1.k} x_{k-1} x_k + \varepsilon \tag{E1}$$

$$y = \beta_0 + \sum_{i=1}^{k} \beta_i x_i + \sum_{i=1}^{k} \beta_{ii} x_i{}^2 + \sum . \sum_{i<j=2}^{k} \beta_{ij} x_i x_j + \varepsilon \tag{E2}$$

where y is the response variable (yield); x1, x2, …, xk are predictor variables; β_o is a constant; β_i is the linear coefficient; β_{ii} is the squared coefficient; β_{ij} is the cross-product coefficient; i and j are the index numbers; and ε is the "error" in the system that include effects such as measurement error on the response, other sources of variation that are inherent in the process or system, the effect of other (possibly unknown) variables, and so on.

194

E2 Principal Component Analysis (PCA)

Principal component analysis (PCA) is a statistical technique used to identify patterns in data, and express the data in such a way as to highlight their similarities and differences (Smith, 2002). A PCA of a set of p original variables generates p new variables, the *principal components*, PC_1, PC_2,.... PC_p, with each principal component being a linear combination of the subjects' scores on the original variables (Harris, 2001), that is,

$$PC_1 = b_{1,1}X_1 + b_{1,2}X_2 + \cdots + b_{1,m}X_m$$
$$PC_2 = b_{2,1}X_1 + b_{2,2}X_2 + \cdots + b_{2,m}X_m$$
$$\vdots \qquad\qquad\qquad\qquad (E3)$$
$$PC_m = b_{m,1}X_1 + b_{m,2}X_2 + \cdots + b_{m,m}X_m$$

The coefficients for PC_1 are chosen so as to make its variance as large as possible. The coefficients for PC_2 are chosen so as to make the variance of this combined variable as large as possible, subject to the restriction that scores on PC_2 and PC_1 (whose variance has already been maximized) be uncorrelated. In general, the coefficients for PC_m are chosen so as to make its variance as large as possible subject to the restrictions that it be uncorrelated with scores on PC_1 through PC_{m-1}.

References

Box, G.E.P., and Behnken, D.W. (1960) Some new three level designs for the study of variables quantitative. *Technometrics* **2**(4): 455–475.

Ferreira, S.C., Bruns, R.E., Ferreira, H.S., Matos, G.D., David, J.M., Brandao, G.C., da Silva, E.G.P., Portugal, L.A., dos Reis, P.S., Souza, A.S., and Dos Santos, W.N.L. (2007) Box-Behnken design: An alternative for the optimization of analytical methods. *Anal. Chim. Acta* **597**(2): 179-186.

Frey, D.D., Engelhardt, F., and Greitzer, E.M. (2003) A role for "' one-factor-at-a-time '" experimentation in parameter design. *Res. Eng. Des.* **14**(2): 65–74.

Harris, R. J. (2001) A primer of multivariate statistics, 3rd edn. Mahwah, NJ: Lawrence Erlbaum Associates, publishers.

Myers, R. H., Montgomery, D. C., and Anderson-Cook, C. M. (2009) Response surface methodology: process and product optimization using designed experiments, 3rd edn. Hoboken, NJ: John Wiley and Sons.

Smith, L.I. (2002) A tutorial on principal components analysis introduction, Volume 51. Dublin: SEAL-BER Statistics.

Table F1 Diversity and abundance of microbial communities in glucose fed SCMFC.

Domain	Phylum	Class	Genus	Species	Abundance (%)
Archaea	Euryarchaeota	Methanobacteria	*Methanobacterium*	*Methanobacterium subterraneum*	3.330
			Methanoregula	*Methanoregula boonei*	3.333
			Methanosaeta	*Methanosaeta concilii*	16.667
				Methanosaeta harundinacea	16.667
		unclassified (derived from Euryarchaeota)	*unclassified (derived from Euryarchaeota)*	*uncultured euryarchaeote*	56.667
	unclassified (derived from Archaea)	unclassified (derived from Archaea)	*unclassified (derived from Archaea)*	*uncultured archaeon*	3.333
Bacteria	Actinobacteria	Actinobacteria (class)	*Streptomyces*	*Streptomyces sclerotialus*	20.000
	Bacteroidetes	Bacteroidia	*Parabacteroides*	*Parabacteroides goldsteinii*	4.000
			Porphyromonas	*Porphyromonas catoniae*	2.286
		Flavobacteriia	*Capnocytophaga*	*Capnocytophaga sputigena*	6.857
			Flavobacterium	*Flavobacterium branchiophilum*	14.286
				Flavobacterium columnare	4.000
				Flavobacterium johnsoniae	1.714
			Tenacibaculum	*Tenacibaculum mesophilum*	0.571
		Sphingobacteriia	*Terrimonas*	*Terrimonas ferruginea*	2.286
	Deinococcus-Thermus	Deinococci	*Thermus*	*Thermus scotoductus*	0.571
	Firmicutes	Clostridia	*Pelotomaculum*	*Pelotomaculum propionicicum*	0.571
			Coprothermobacter	*Coprothermobacter proteolyticus*	0.571
	Planctomycetes	Planctomycetia	*Pirellula*	*Pirellula staleyi*	2.857
			Planctomyces	*Planctomyces limnophilus*	0.571
	Proteobacteria	Betaproteobacteria	*Achromobacter*	*uncultured Achromobacter sp.*	1.143
			Comamonas	*Comamonas aquatica*	28.571
			unclassified (derived from Betaproteobacteria)	*uncultured beta proteobacterium*	0.571

Domain	Phylum	Class	Genus	Species	Abundance (%)
		Deltaproteobacteria	*unclassified (derived from Deltaproteobacteria)*	*uncultured delta proteobacterium*	0.571
		Gammaproteobacteria	*unclassified (derived from Gammaproteobacteria)*	*uncultured gamma proteobacterium*	1.714
	Spirochaetes	Spirochaetia	*Leptospira*	*Leptospira interrogans*	1.714
	unclassified (derived from Bacteria)	unclassified (derived from Bacteria)	*unclassified (derived from Bacteria)*	*uncultured bacterium*	3.429
unclassified sequences	unclassified (derived from unclassified sequences)	unclassified (derived from unclassified sequences)	*unclassified (derived from unclassified sequences)*	*uncultured organism*	1.143

Table F2 Diversity and abundance of microbial communities in PrLS fed SCMFC.

Domain	Phylum	Class	Genus	Species	Abundance (%)
Archaea	Euryarchaeota	Methanomicrobia	*Methanoculleus*	*Methanoculleus palmolei*	30.343
			unclassified (derived from Methanomicrobiaceae)	*uncultured Methanomicrobiaceae archaeon*	0.003
			Methanolinea	*Methanolinea tarda*	8.072
			Methanoregula	*Methanoregula boonei*	0.466
			Methanosaeta	*Methanosaeta concilii*	4.060
				Methanosaeta harundinacea	21.260
			Methanococcoides	*Methanococcoides alaskense*	0.003
			Methanosalsum	*Methanosalsum zhilinae*	0.107
		unclassified (derived from Euryarchaeota)	*unclassified (derived from Euryarchaeota)*	*uncultured euryarchaeote*	19.751
	unclassified (derived from Archaea)	unclassified (derived from Archaea)	*unclassified (derived from Archaea)*	*uncultured archaeon*	15.935
Bacteria	Actinobacteria	Actinobacteria (class)	*Streptomyces*	*Streptomyces sclerotialus*	0.015
	Bacteroidetes	Bacteroidia	*Bacteroides*	*Bacteroides vulgatus*	0.687
			Porphyromonas	*Porphyromonas catoniae*	0.120
			Rikenella	*Rikenella microfusus*	0.008
		Cytophagia	*Cytophaga*	*Cytophaga sp. I-1858*	1.177
				Cytophaga sp. MBIC04667	0.216
		Flavobacteriia	*Blattabacterium*	*Blattabacterium sp. (Blattella germanica)*	0.127
			Arenibacter	*Arenibacter latericius*	0.434
			Capnocytophaga	*Capnocytophaga canimorsus*	0.002
				Capnocytophaga ochracea	0.009
				Capnocytophaga sputigena	3.475
			Chryseobacterium	*Chryseobacterium soldanellicola*	0.162
			Coenonia	*Coenonia anatina*	0.042

Domain	Phylum	Class	Genus	Species	Abundance (%)
			Dokdonia	*Dokdonia donghaensis*	0.005
			Flavobacterium	*Flavobacterium branchiophilum*	2.048
				Flavobacterium columnare	4.071
				Flavobacterium johnsoniae	10.474
				Flavobacterium sp. SOC A4(12)	2.984
			Myroides	*Myroides odoratimimus*	0.009
				Myroides profundi	0.001
			Riemerella	*Riemerella anatipestifer*	0.001
			Tenacibaculum	*Tenacibaculum mesophilum*	0.001
		Sphingobacteriia	*Terrimonas*	*Terrimonas ferruginea*	3.158
		unclassified (derived from Bacteroidetes)	*unclassified (derived from Bacteroidetes)*	*marine CFB-group bacterium MBIC01599*	0.777
	Deinococcus-Thermus	Deinococci	*Deinococcus*	*Deinococcus ficus*	0.124
		Clostridia	*Tissierella*	*Tissierella sp. LBN 292*	0.165
			Fusibacter	*Fusibacter paucivorans*	0.387
			Acetobacterium	*Acetobacterium psammolithicum*	0.036
			Desulfosporosinus	*Desulfosporosinus sp. DB*	0.014
	Firmicutes		*Pelotomaculum*	*Pelotomaculum propionicicum*	3.025
			unclassified (derived from Ruminococcaceae)	*Bacteroides cellulosolvens*	0.222
			Coprothermobacter	*Coprothermobacter proteolyticus*	0.001
		Negativicutes	*Sporomusa*	*Sporomusa ovata*	1.099
			Veillonella	*Veillonella atypica*	4.796
				Veillonella ratti	0.304
	Gemmatimonadetes	Gemmatimonadetes (class)	*Gemmatimonas*	*Gemmatimonas aurantiaca*	0.160
			Blastopirellula	*Blastopirellula marina*	0.043
	Planctomycetes	Planctomycetia	*Pirellula*	*Pirellula staleyi*	0.197
			Planctomyces	*Planctomyces limnophilus*	0.574

Domain	Phylum	Class	Genus	Species	Abundance (%)
	Proteobacteria	Betaproteobacteria	*Acidovorax*	*Acidovorax konjaci*	0.504
				Acidovorax temperans	0.315
				uncultured Acidovorax sp.	0.001
			Brachymonas	*Brachymonas petroleovorans*	0.077
			Comamonas	*Comamonas aquatica*	0.056
			Pelomonas	*Pelomonas saccharophila*	0.001
			Variovorax	*Variovorax paradoxus*	0.048
			Verminephrobacter	*Verminephrobacter eiseniae*	0.002
				uncultured Verminephrobacter sp.	0.001
			unclassified (derived from Comamonadaceae)	*uncultured Comamonadaceae bacterium*	0.197
			unclassified (derived from Betaproteobacteria)	*uncultured beta proteobacterium*	0.833
		Deltaproteobacteria	*unclassified (derived from Deltaproteobacteria)*	*uncultured delta proteobacterium*	0.803
		Gammaproteobacteria	*Stenotrophomonas*	*Stenotrophomonas maltophilia*	0.089
			unclassified (derived from Gammaproteobacteria)	*Thiobacillus prosperus*	0.013
				uncultured gamma proteobacterium	1.055
		unclassified (derived from Proteobacteria)	*unclassified (derived from Proteobacteria)*	*uncultured proteobacterium*	0.003
	Tenericutes	Mollicutes	*Acholeplasma*	*Acholeplasma modicum*	1.073
	unclassified (derived from Bacteria)	unclassified (derived from Bacteria)	*unclassified (derived from Bacteria)*	*bacterium enrichment culture clone N47*	0.058
				enrichment culture bacterium	0.022
				uncultured bacterium	46.653
				uncultured soil bacterium	0.317
Eukaryota	Streptophyta	Coniferopsida	*Pinus*	*Pinus taeda*	0.080
	unclassified (derived from	Florideophyceae	*Thorea*	*Thorea violacea*	0.060

Domain	Phylum	Class	Genus	Species	Abundance (%)
	Eukaryota)				
unassigned	unassigned	unassigned	*unassigned*	*unassigned*	6.592
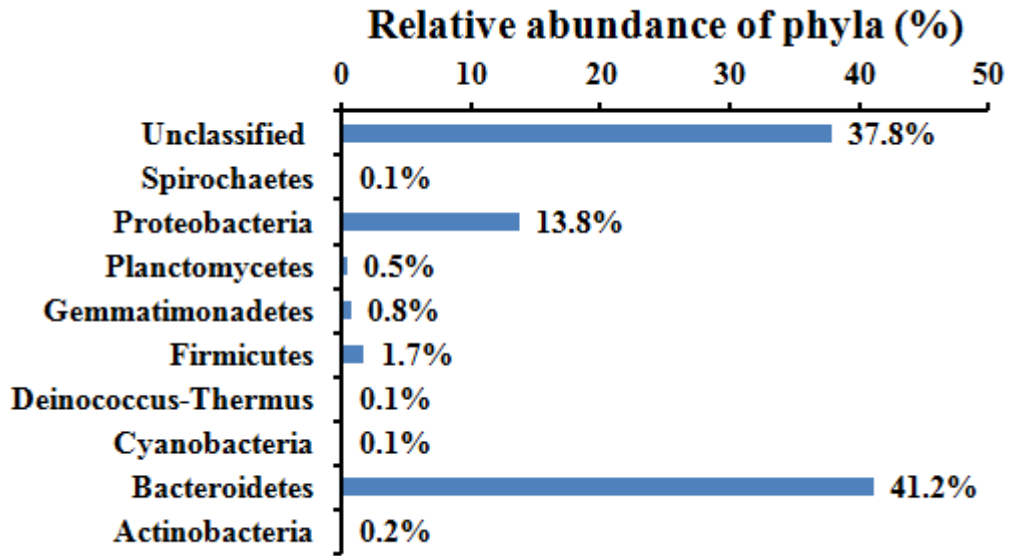
Figure F1 Phylum-level relative abundance of dominant bacterial in PrBL fed
SCMFCs.

VITA AUCTORIS

NAME:	Wudneh Ayele Shewa
PLACE OF BIRTH:	Gamo Gofa, Ethiopia
YEAR OF BIRTH:	1972
EDUCATION:	Sawla Senior Secondary High School, Gamo Gofa Zone, Ethiopia 1985-1989
	Arba Minch University, Arba Minch, Ethiopia Sanitary Engineering (B. Sc.) 1989-1994
	Indian Institute of Technology, Roorkee, India Environmental Engineering (M. Sc.) 1996-1998
	University of Windsor, Windsor, Ontario, Canada Environmental Engineering (PhD) 2011-2015